Biglycan Modulation of Bone Morphogenetic Protein-2 Functions

Patricia A. Miguez

A dissertation submitted to the faculty of the University of North Carolina at Chapel Hill in partial fulfillment of the requirements for the degree of Doctor of Philosophy in the School of Dentistry (Oral Biology).

Chapel Hill

2011

Approved by:

Mitsuo Yamauchi

Eric Everett

Ching-Chang Ko

Yoshiyuki Mochida

Yuji Mishina

Abstract

Patricia A. Miguez

Biglycan Modulation of Bone Morphogenetic Protein-2 Functions
(Under the direction of Professor Mitsuo Yamauchi)

Biglycan (BGN) is a proteoglycan found in high abundance in mineralized tissues. Study of its functions has unveiled roles in collagen organization (i.e. type VI), osteoblast differentiation, matrix mineralization, inflammatory processes, etc. Recently, we have reported that BGN promotion of osteoblast differentiation is due in part to its ability to positively modulate bone morphogenetic protein (BMP) functions. In the studies that follow, we (1) investigated the role of glycosaminoglycans (GAGs) of BGN on BGN-assisted BMP-2 function *in vitro* by utilizing a C2C12 cell system and *in vivo* by using a critical-sized mandible defect model in the Sprague-Dawley rat; (2) characterized by microcomputed tomography and histology the newly formed bone (NFB) in BGN-assisted BMP-2-induced osteogenesis; and (3) investigated which domain of the core protein of BGN is most effective in promoting BMP-2 function *in vitro* and applied it *in vivo*. We found that BGN devoid of GAGs is most effective in assisting BMP function *in vitro* and *in vivo* and that this positive modulation *in vitro* occurs through increased phosphorylation of Smad 1/5/8. In the animal model, rats treated with a low dose of BMP-2 in conjunction with appropriate dose of BGN formed a less porous and more mature type of bone than a high dose of BMP-2 alone. High

dose BMP-2 formed an ectopic type of NFB and presented characteristics of a high turnover bone as per presence of osteoclast-like cells and yellow/orange picrosirius red staining. The BMP-2 and BMP-2 + BGN rats showed strong β-catenin immunoreactivity at 2 weeks post-surgery. The rats that did not form significant amounts of bone did not show this pattern of staining. Finally, the effector domain of the core protein appears to reside between the N terminus and leucine rich repeat (LRR) 6, possibly in the LRR1~3. LRR1~3 was as effective as BGN full core protein in assisting BMP-2-induced osteogenesis *in vivo*. We conclude that the use of BGN or its effective domain combined with low concentrations of BMP-2 may be a more predictable, controllable and cost-effective approach than the use of high dose BMP-2.

To my mom and dad that have so deeply supported my dream of going this far with my education. To my husband and daughter that have sacrificed their time with me for this to happen.

Acknowledgments

I would like to thank up and foremost Dr. Mitsuo Yamauchi for his mentorship. His support and brilliance in extracellular matrix research made this dissertation work possible. My gratitude also goes to my co-mentor Dr. Yoshiyuki Mochida whose extensive knowledge in molecular biology contributed to this research and the committee members Dr. Eric Everett, Dr. Ching-Chang Ko and Dr. Yuji Mishina for their valuable comments and suggestions on the methodology and written dissertation. My sincere appreciation also goes to the current and past Collagen Biochemistry Laboratory colleagues that have contributed directly or indirectly to the data generation: Dr. Marnisa (Ann) Sricholpech, Dr. Hideaki Nagaoka, Dr. Masahiko (Masa) Terajima, Dr. Shizuka Yamada, Dr. Megumi Yokoyama, Dr. Sun Ming Lee and specifically *In memoriam* Dr. Duenpim (Art) Parisuthiman that started the work on biglycan in this laboratory a few years ago. Lastly, I want to thank the invaluable support from Dr. Ching-Chang Ko, Dr. João Ferreira, Dr. Eric Everett, Mr. John Whitley and Ms. Krista Braswell for their help with the *in vivo* studies.

Preface

We know that the formulation of a hypothesis requires extensive reading, studying, and some creativity. In my journey at UNC, I never lacked the energy for those or the experiments that followed. The experiments always resulted in more questions and ideas for future projects and this cycle of events always made me excited about my work. When I decided to pursue a Ph.D. research involving my own interests I had plenty of people discouraging me to take that path and advising me to do research according to my mentor's interests. But I was fortunate and after a few years of struggling, Dr. Yoshiyuki Mochida and Dr. Mitsuo Yamauchi came up with a research idea that was in agreement with my interests and theirs.

Science will never grow if we just repeat the experiments that are already out there. Even worse, science cannot enchant you if you work on something you have little interest in. I went beyond my limits in this dissertation research because my mentor allowed me to do something new and invested in me and my interests. I was very fortunate to work in a project that I was excited about.

After 11 years at UNC, first as a Master's student in Operative Dentistry and since 2004 as a dual-degree Ph.D. candidate for Oral Biology and Certificate in Periodontology, I am finally graduating and excited with my future path in academia. I hope I can be as encouraging to my students in the future as my mentors here have been to me.

People at UNC that have helped me along the way include dear friends in the faculty, staff and student bodies of Operative Dentistry and Periodontology Departments and Oral Biology curriculum. Many have already left UNC. From the ones that have already left, I was particularly strongly and invaluably influenced by Dr. Patricia (Pat) Pereira, Dr. Wagner Duarte, Dr. Ray Williams, Dr. David Paquette and Dr. Mochida Yoshiyuki. All of them are not only close friends but have given me incalculable guidance in growing in my field of study and/or as a person.

For the ones that are here, I want to thank specifically Dr. Mitsuo Yamauchi for his friendship, mentorship, advices for balance in life, kindness and empathy. Dr. Yamauchi was very supportive when I had my baby in 2007 and started to juggle laboratory work and family. I am also thankful for getting to know his family, a true example of companionship, love and endurance over happy or hard times.

Over the years, so many people have stepped out of their comfort zone to be my friend, my coworker and/or a mentor and unfortunately I cannot mention them all. But I want to thank Ann, Hideaki, Masa, Yuki, Ms. Marie Roberts, Ms. Donna Yeager, Pat, Wagner, and many others because you made a great impact. Thank you also to the Oral Biology Curriculum students, course manager Ms. Cindy Blake and course director Dr. Patrick Flood for their support. Thank you so much.

And finally, my husband Rick and daughter Violet for the light they bring to my life. Like my mom and dad, they have given me the love and support I needed to keep my sanity during all these years in graduate school.

Table of Contents

List of Tables

List of Figures

List of Abbreviations and Symbols

ActR	activin receptor
ALK	activin receptor-like kinase
ALP	alkaline phosphatase
AS	anti-sense
ASPN	asporin
ATCC	American type culture collection
BGN	biglycan
BMP	bone morphogenetic protein
BMPR	bone morphogenetic protein receptor
BSP	bone sialoprotein
BV	bone volume
C-ABC	chondroitinase ABC
Cbfa1	core binding factor α1
cDNA	complementary deoxyribonucleic acid

Chsy	chondroitin synthase
CS	chondroitin sulfate
CT	computed tomography
DCN	decorin
DS	dermatan sulfate
ECM	extracellular matrix
ECM2	extracellular matrix protein 2
EGF	epidermal growth factor
FBS	fetal bovine serum
FGF	fibroblast growth factor
Fig	figure
GAG	glycosaminoglycan
Gal	galactose
GalN	galactosamine
GalNAc	N-acetyl galactosamine
Galt	galactosyltransferase

Gat	glucuronosyltransferase
GDF	growth differentiation factor
GlcA	glucuronic acid
GlcN	glucosamine
Gly	glycine
GS	glycine-serine box
GST	glutathione-S-transferase
HAP	hydroxyapatite
HS	heparan sulfate
IACUC	Intitutional Animal Care and Use Committee
IdoA	iduronic acid
IHC	immunohistochemistry
IL	interleukin
IP	immunoprecipitation
IPTG	isopropyl-D-1-thiogalactopyranoside
I-Smad	inhibitory Smad

K_d	dissociation constant
kDa	kilodalton
KS	keratan sulfate
LPS	lipopolysaccharide
LRR	leucine rich repeat
Lys	lysine
MAPK	mitogen activated protein kinase
MC	MC3T3-E1 osteoblastic cell line from calvaria
mRNA	messenger ribonucleic acid
N-	amino
NFB	newly formed bone
OSX	osterix
PBS	phosphate buffer saline
PCR	polymerase chain reaction
PG	proteoglycans
PSR	picrosirius red

R-Smad	receptor Smad
Runx-2	runt-related transcription factor 2
S	sense
Smad	mothers against decapentaplegic
SLRPs	small leucine rich proteoglycans
Ser	serine
TGF	transforming growth factor
Thr	threonine
TLR	toll like receptor
TNF	tumor necrosis factor
Tsg	twisted gastrulation
WB	Western blotting
Xyl	xylose
Xylt	xylosyl transferase
D	aspartic acid
E	glutamic acid

L	leucine
M	methionine
N	asparagine
α	alpha
β	beta
μ	micro
2, 4, 6S	2, 4, 6 sulfate
n	nano

Chapter 1

Review of Literature

1.1. Bone

Bone is characterized as a mineralized connective tissue built to provide support to the body, structure for muscle attachment, calcium and phosphate storage, site for hematopoiesis and generate cells involved in bone homeostasis. Bone is composed of cells, an inorganic matrix of hydroxyapatite (HA) minerals and an organic matrix of collagenous and non-collagenous proteins. The specific cells that are part of bone matrix are the osteoblasts (the bone forming cells on the surface of bone), the osteocytes (the bone cells embedded in bone lacunaes that sense mechanical loading) and the osteoclasts (the bone resorbing cells). The mineral phase of bone and other mineralized tissues like dentin and cementum provides stiffness while the organic phase mainly represented by collagen fibers provide ductility therefore preventing fracture. Type I fibrillar collagen is the major protein of the extracellular matrix (approximately 90%) in bone by weight and it serves as a spatial regulator by defining the space for mineral deposition and growth. Mineral is believed to be deposited initially within the fibrils and later between and around them. The amorphous calcium phosphate later matures into HA ($Ca_{10}(PO_4)_6(OH)_2$)/HAP) [1]. The complete process of biomineralization is highly ordered and tightly regulated by not only collagen deposition and assembly *per se* but by enzymes and other non-collagenous proteins. The non-collagenous proteins in bone account for 10 to 15% of the total bone protein content and

include glycosaminoglycan (GAG)-containing molecules called proteoglycans (PG) (polypeptide chain core with short N-linked oligosaccharides and large O-linked disaccharides), glycoproteins (polypeptide chain core with short N-linked oligosaccharides), phosphoproteins and gama-carboxy glutamic acid-containing molecules [2]. The main non-collagenous proteins in bone are PGs of the small leucine rich family of proteoglycans (SLRPs) [3].

PGs are generally characterized as a collection of macromolecules that surround the cell membrane as well as provide a substrate for them to attach. They are composed of a core

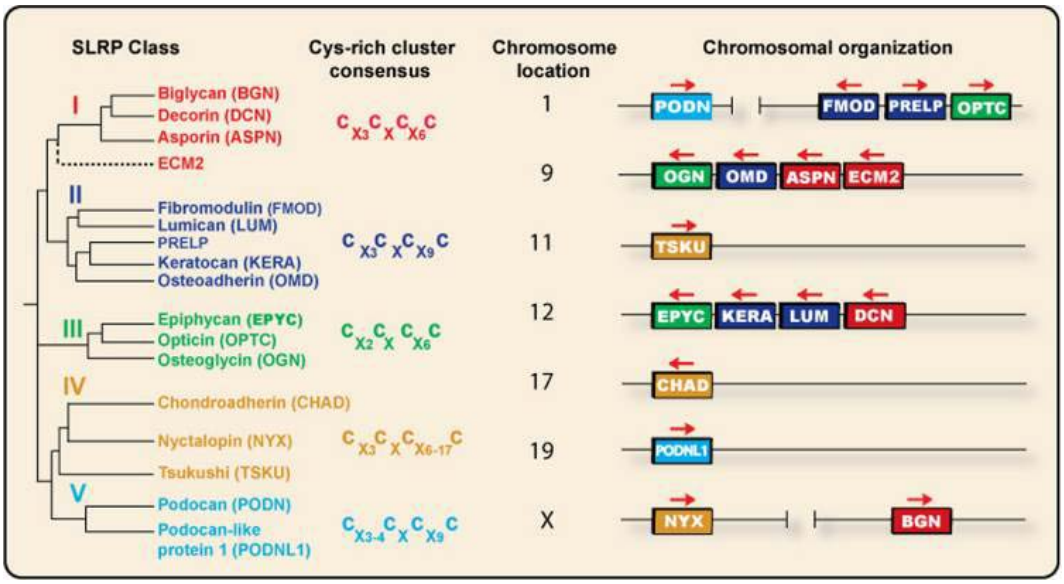

Fig 1.1. Phylogenetic analysis and chromosomal organization of various human SLRP classes. The color-coded dendrogram (*left*) shows the presence of five distinct families of SLRP and related LRR proteins. The consensus for the N-terminal Cys-rich cluster is also shown. The chromosomal arrangement of the various SLRP genes is shown in a telomeric orientation (*right*). Transcriptional direction is shown by the *arrows* above the color-coded boxes. ©*Figure and legend reprinted with permission from American Society for Biochemistry and Molecular Biology. Schaefer L and Iozzo RV. Biological functions of the small leucine-rich proteoglycans: from genetics to signal transduction. Journal of Biological Chemistry 2008 August 1; 283 (31): 21305-21309.*

of polypeptide chains with one or more unbranched covalently bound GAG chains. The large structural diversity of proteoglycans gives rise to a wide variety of biological functions. Both core proteins and GAG chains have been shown to mediate these functions. They have been involved in maintaining the transparency of the eyes, the tensile strength of skin and tendon,

the viscoelasticity of blood vessels, the compressive properties of cartilage and the mineralization of teeth and bones [4].

1.2. Small leucine rich proteoglycans (SLRPs)

SLRPs were first identified as small PGs in bone [5] and the family has expanded considerably from the first two SLPRs in one family (DCN and BGN) to the present

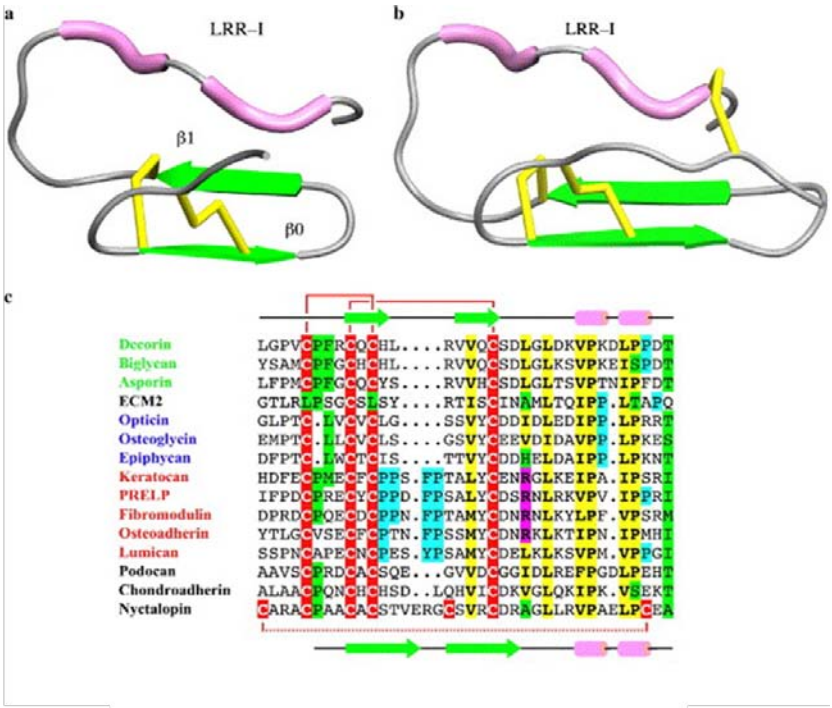

Fig 1.2. Secondary structure, disulfide topology, and sequence conservation in the N-terminal capping motifs of SLRPs: (a) ribbon diagram of the N-terminal cap from the decorin crystal structure: (b) ribbon diagram of the disulfide N-terminal capping for nyctalopin (also a LRR proteoglycan), showing the predicted topology of the three disulfide bonds; (c) structure-based sequence alignment for the N-terminal motifs of all SLRPSs. Yellow, conserved residues; green, partially conserved residues; cyan, partially conserved Pro residues indicative of polyproline II conformation; magenta, polar residues occupying hallmark LRR hydrophobic sites. Cysteine residues are shown in white text over red background and conserved disulfide bonds are shown as red solid lines. Including a predicted additional disulfide bond in nyctalopin that is shown as a red dashed line. *© Figure and legend reprinted with permission from Elsevier. McEwan et al., Structural correlations in the family of small leucine-rich repeat proteins and proteoglycans. Journal of Structural Biology 2006 August; 155(2): 294-305.*

seventeen SLRPs in five families (Fig 1.1). In their structure they have N-terminal cysteine (Cys) clusters with defined spacing, an ear-repeat at the C-terminal [6] and at least one GAG attached [4, 7]. They are usually small, below 150 kDa including their GAGs. The N-

terminal cluster typically contains four Cys and the amino acids that space them have been used as a way to subdivide the SLRP family. The fourth and last Cys of the N-terminal is embedded in the leucine-reach repeat (LRR)-1. Thus, this N-terminal capping is not a separate domain from the LRR-1 (Fig 1.2). Most of the data on SLRPs arise from the extensive research on the Class I SLRP DCN. One study shows the importance of the N-terminal Cys as the lack of binding of DCN to collagen under reducing conditions highlights the hypothesis that the amino terminal of SLRPs is important for its function [6, 8]. It has been speculated that this capping protects the hydrophobic core of the first LRR and therefore LRRs would not fold correctly and would not function properly in the absence of the disulfide bonds. The ear repeat refers to the C-terminal capping involving the last LRR in SLPRs. All class I, II, III and extracellular matrix protein 2 (ECM2) share the same N and C-terminal capping in their LRR domains [9].

In general, the family of SLRPs is organized according to the protein core and genomic homology, chromosome location and Cys regions into 5 subclasses (Fig 1.1). Also their genes (with the exception of BGN) are organized in three chromosomal clusters [10], suggesting close evolutionary relationships as predicted in Fig. 1. 1.

SLRPs are reported to play a role in extra cellular matrix (ECM) development and maintenance as well as regeneration. Mice lacking one or two SLRPs have shown the importance of these PGs on bone formation and maintenance among other physiological development steps [11-15]. The phenotype of these mice is mostly due to affected collagen fibrillogenesis leading to skin fragility (with lack of SLRP DCN)[14] or osteoporosis and spontaneous aortic dissection (with lack of SLRP BGN) [11].

1.2.1. SLRP-ligand binding

Several SLRPs have been shown to interact with different types of collagen, both fibrillar and non-fibrillar, and to recognize different collagen sites [16-18]. DCN and asporin (ASPN) bind to same site of collagen type I and therefore compete. DCN has a negative effect on collagen mineralization and it has been suggested that the polyaspartate acid in ASPN also directly regulates mineralization [19].

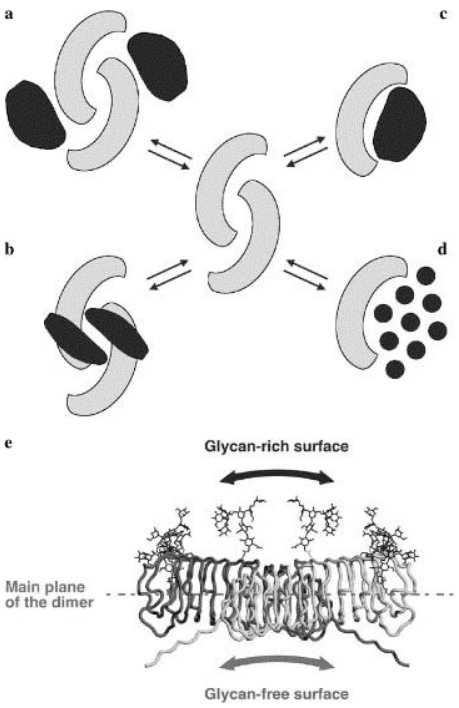

Fig 1.3. Possible ligand-binding scenarios for dimeric SLRPs: dimers may bind two molecules of a ligand as in (a), or one dimeric ligand as in (b); alternatively the dimers might disassemble and use their concave surfaces for binding ligands with 1:1 stoichiometry as in (c), or with more complicated stoichiometries as in (d). The N-linked oligosaccharides accumulate on one side of the decorin dimer (c), leaving the surface on the other side mainly available for possible protein-protein interactions. *© Figure and legend reprinted with permission from Elsevier. McEwan et al., Structural correlations in the family of small leucine-rich repeat proteins and proteoglycans. Journal of Structural Biology 2006 August; 155(2): 294-305.*

More recently, special attention has been given to SLRPs binding to growth factors of the transforming growth factor (TGF)-β family. The binding of DCN and BGN to TGF-β1, 2 and 3 and TGF-β family members bone morphogenetic proteins (BMPs) led to extrapolating the functions of SLRPs not only on ECM assembly but also cell signaling [20]. Binding studies with ASPN also show its specific binding to TGF-β1 and influence on expression of different osteogenic markers highlighting the importance of these Class I SLPRs on ECM osteogenesis and mineralization [20].

Some SLRPs have also been reported to trigger signaling pathways independently of

TGF-β [12, 21-23]. DCN and most recently BGN seem to be very promiscuous molecules, with many reported interactions with various receptors, cell secreted molecules and ECM components [16, 24-30]. Through these interactions, SLRPs influence a variety of signaling pathways including Wnt, mothers against decapentaplegic (Smad) and mitogen-activated protein kinase (MAPK) [29, 31-33].

Despite all the data, especially for DCN, the molecular details and the stoichiometries of the interactions between SLRPs and their ligands remain a mystery. It has been generally assumed that all SLRPs have a horseshoe shape and that the concave side of the horseshoe contains the binding sites. However, it is now known that DCN and other SLRPs form extremely stable dimers in solution and that those dimers assemble through the concave side of the monomers. This warrants rethinking of the assumptions that only the concave area serves as a binding site [6]. In Fig 1.3 several scenarios are illustrated. Dimeric SLRPs may function as units binding ligands with a 2:2 stoichiometry with a twofold symmetry (Fig. 1.3a). Dimerization of SLRPs may facilitate their interaction with other dimmers or oligomers such as TGF-β and epidermal growth factor (EGF) receptor (Fig. 1.3b). Conceivably, dimeric SLRPs might also dissociate to interact with some partners as monomers (Fig. 3c and d).

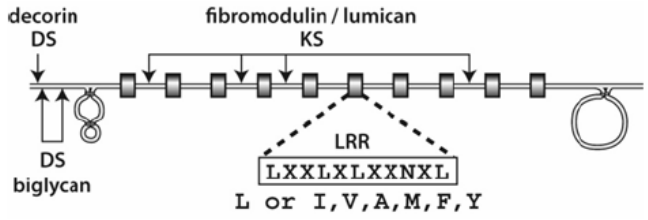

Fig 1.4. The structural domains of SLPRs. The core protein of decorin, biglycan, fibromodulin or lumican is depicted with two disulphide bonded domains flanking ten leucine-rich repeat (LRR) domains. Each LRR domain is composed of the sequence LXXLXLXXNXL, where L is predominantly leucine but may also be I, V, A, M, F or Y, and X may be any amino acid. In the case of decorin or biglycan, one or two chondroitin/dermatan sulphate (DS) chains, respectively, reside in the amino terminal region. In the case of fibromodulin and lumican, one to four keratan sulphate chains (KS) may reside between the LRR. © *Reprinted figure and legend from open access journal of AO foundation. Roughley PJ. The structure and function of cartilage proteoglycans. European Cells and Materials 2006 November 30; 12: 92-101*.

1.3. Biglycan

BGN, a member of class I molecules in the SLRP family, is one of the major non-collagenous proteins in mineralized tissues and was originally identified in the mineral-associated compartment of bone [5]. It consists of about 45 kDa core protein made of 10-12 LRRs that are about 25 amino acids long [34]. BGN has a signal sequence, a propetide, two GAG chains attached to its amino terminus, a Cys loop flanking the N-terminal side of the central LRR region that makes up over 66% of the core protein, and a final Cys loop at the carboxy-terminus [35] (Fig 1.4) . BGN is first synthesized as a pro-form containing 20 residues of N propeptide (human), which will subsequently be removed in most connective tissues. The propeptide containing form is more prevalent in articular cartilage. The function of this propetide is not fully understood but the proteinase responsible for the cleavage has been identified as BMP-1. The sites where BMP-1 processes BGN, M(M/L)N-DEE, are conserved in various species [36]. BGN can undergo further proteolytic cleavage to remove the N-terminal peptide containing GAG chains, resulting also in a non-PG form of the molecule [37].

The *BGN* gene is located on the X chromosome, the Xq28 region in human [38] and at a locus 50-100 kb distal to the DXHSS52 locus in the murine counterpart [39]. Human and murine BGN consist of eight exons and spans over 8 kb for the former and 9.5 kb for the latter. The murine BGN is larger than human due to the intron present between exon 1 and 2. As in other members of the SLRPs its core protein is proposed to have a horseshoe structure which can facilitate protein-protein interaction (Figs 1.3). BGN has been localized to several regions including cartilage, periosteum and skeletal myofibers and keratinocytes [40]. It has been identified in the ECM space, as a nucleator for mineral deposition [41], or at the cell

surface indicating possible regulatory role in cell activities [40]. As a mineral nucleator, BGN and DCN were both found to bind to HAP in a HAP coated affinity column. In addition, DS-DCN and DS-BGN obtained from skin and articular cartilage where analyzed in a gelatin gel diffusion system in which apatite formation occurs in the absence of cells in a 3-5 day period. CS-PGs and DS-BGN promoted the most crystal growth [41]. This data supported the notion that BGN plays a more significant role than DCN in mineralization.

In some instances, BGN has been described as carrying only one GAG chain [37, 42-44]. In a study of mutation of Serine (Ser) residues of BGN, it was shown that the first site Ser 42 is important for the second site Ser 47 to be glycanated. When Ser 42 is mutated, only a small portion of BGN is glycanated. In addition, the authors found that BGN may carry heparan sulfate (HS) GAGs chains as well as sulfated N-linked oligosaccharides [45]. The specific clear functions of DS-, CS- and HS-BGN have not been determined so far.

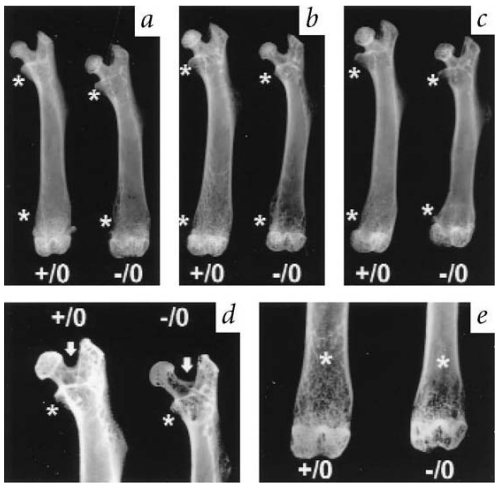

Fig 1.5. Radiological analysis of bones from $Bgn^{+/0}$ and $Bgn^{-/0}$ mice. *a-c*, Radiographs of femora from wild-type (+/0) and mutant (-/0) mice at the age of three (***a***), six (***b***) and nine (***c***) months. Note the progressive decrease in trabecular bone mass (*) with age in the mutant compared with wild-type mice. ***d***,***e***, Details of high resolution microradiographs of six-month-old animals. Note that the trabecular bone is reduced and extends over a shorter distance below the growth plate in the mutant bone (*e*). Also note that the angle between the femoral neck and the great trochanter (arrows) is wider in the mutant bone, a difference in shape that was consistently observed (*d*). © *Figure and legend reprinted with permission from Nature. Xu T, et al. Targeted disruption of the biglycan gene leads to an osteoporosis-like phenotype in mice. Nature Genetics 1998; 20: 78-82.*

1.3.1. Biglycan is a positive modulator of osteoblast function

In order to evaluate the function of full protein BGN in connective tissues, BGN-knockout mice were generated using gene targeting and

homologous recombination [11]. This study and others using the same model have found that BGN deficiency caused decreased bone mass, irregular collagen fibrillogenesis and thin, disorganized dermis [11, 46-48](Fig 1.5). It was proposed that BGN levels can control the level of cell proliferation leading to decreased amount of osteoblast progenitors [46]. It was also proposed that these mice had compromised ability to make new bone because of a reduced response of bone marrow stromal cells to TGF-β [49]. The same group further reported that BGN together with DCN may control the fate of bone marrow stromal cells, thus, the lack of these SLRPs could cause the reduced number of osteoprogenitor cells [13, 50].

When BGN deficient osteoblasts isolated from the neonatal calvaria were determined having less response to BMP-4 stimulation an attempt to restore this response was pursued. The poor response to BMP-4 stimulation was restored when the BGN-deficient cells were infected with BGN-expressing adenovirus. The authors then concluded that osteoblasts lacking BGN displayed a defect in differentiation due to reduced BMP-4 binding, followed by lower BMP-4 sensitivity, resulting in less BMP-4 signal transduction and decreased expression of core binding factor α1 (*Cbfa1*), an essential transcription factor for osteoblast differentiation [49]. This could partially explain the cause of age-dependent osteoporotic phenotype observed in BGN-deficient. The poor responsiveness of the clones to BMP-4 also indicates its potential involvement of BGN in BMP function.

On the other hand, in studies addressing the regulation of BMP-4 signaling pathways during embryonic development, BGN has been shown to bind BMP-4 and accelerate the inhibitory effects of BMP antagonist molecules [chordin and Tsg (Twisted gastrulation)] on BMP-4 activity by increasing the binding of BMP-4 to chordin and improving the efficiency

of chordin-Tsg complexes to inactivate BMP-4 [51]. Later, in *Xenopus* embryos, the microinjection of biglycan mRNA inhibited BMP-4 activity and influenced embryonic development in a chordin-dependent manner. The lack of BGN in bone vs. other tissues (i.e. tendon) promotes different behaviors of cells which could indicate a tissue-specific function of BGN potentially influenced by different players in BMP signaling, *e.g.* competitive binding of BMP-2 and BMP-4 to BGN and other SLRPs.

After the initial characterization of BGN deficient mice and the initial findings of the functional relationship between BGN and BMPs in controlling skeletal differentiation, our

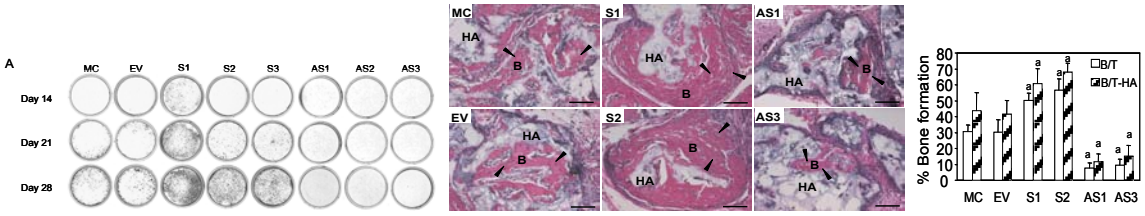

Fig 1.6. *In vitro (A) and in vivo* (B) mineralization assay. (A) Mineralized nodules were formed earlier and to a greater extent in S clones compared to those of controls, while no nodules were observed in AS clones up to day 28. (B) H&E stained sections of transplants show bone-like matrices (B) including osteocytes (arrowheads) (left panel) on the surface of HA/TCP carrier (HA). The percentage of bone-like matrices is shown as B/T+SD and B/T-HA+SD (right panel). The bone-like matrix areas are significantly greater in S clones while they are markedly smaller in AS clones than those of controls. [a] =p< 0.005 vs. controls. Bar=500 μm. © *Figure reprinted with permission from John Wiley and Sons. Parisuthiman D et al. Biglycan modulates osteoblast differentiation and matrix mineralization. JBMR 2005(20): 1878-1886.*

laboratory continued to unveil the mechanism of BGN-assisted BMP function. In Parisuthiman et al., 2005 [52], we reported that in early stages of cell culture the expression of *Cbfa1* and osterix (*Osx*), as well as matrix proteins [i.e. type I collagen, bone sialoprotein (*Bsp*)] were significantly upregulated in pre-osteoblastic MC3T3-E1 cells overexpressing *Bgn* (Sense, S) but downregulated in clones underexpressing (anti-sense, AS) *Bgn*. Mineralization was significantly accelerated in S clones but impaired in AS clones *in vitro* and *in vivo*. These phenotypes of S and AS clones indicate that BGN is a positive modulator of osteoblast differentiation and promoter of mineralization (Fig 1.6). BGN is the first known

agonist of BMP function and has just recently been attributed such function. In comparison to the extensive studies on the BMP-antagonists little is known about the positive matrix modulators of BMPs. A study by Xiao and coworkers has indicated that matrix accumulation is necessary for endogenously or exogenously added BMPs to be fully functional in a MC3T3-E1 cell culture system [53] . The ECM is composed of heterogeneous molecules, including SLRPs thus this may support the idea that those SLRPs (i.e. BGN) in ECM are needed for BMP to function.

Besides the studies with endogenous increase or decrease in BGN production, we further evaluated the effect of exogenous BGN addition on osteoblast differentiation. In Mochida et al., 2006 [28], it was reported that exogenously added recombinant BGN (tagged with glutathione-S-transferase, GST) is able to significantly promote BMP-2 function in C2C12 osteoblasts. GST tag alone was found not to cause any enhancement of BMP function. It was found that recombinant BGN induced earlier and stronger Smad 1/5/8 pathway activation. This activation was also sustained for a longer period of time in BGN + BMP-2 compared to BMP-2 alone. More recently, the underlying pathways of osteoblast differentiation through exogenously added BGN was also studied in MC3T3-E1. BGN was found to activate not only Smad but also ERK signaling pathways in these pre-osteoblasts. In this venue, GAGs were found to play an essential role as deglycanated BGN did not promote ERK signaling in these cells [33].

1.3.2. Biglycan binding partners

BGN has previously been considered as a non fibrillar collagen-binding molecule [54]. However, by employing immunogold labeling technique and immunoprecipitation

(IP)/Western blot (WB) analysis, the binding between recombinant radiolabeled BGN or *in vitro* native BGN and reconstituted type I collagen fibrils has been shown [18]. The binding of the core protein of BGN to collagen is not as strong as of DCN. However, when full protein DCN and BGN (with GAGs) compete, the dissociation constant among them is similar. In other words, BGN with GAGs binds much more strongly to collagen than without them [55, 56].

Besides type I collagen, BGN has also been shown to bind to collagens type II, III, V and VI [17]. In the case of type VI collagen, BGN acts as an organizer for the formation of hexagonal-like network, which resemble tissue structures [57]. Without GAGs BGN is not able to bind collagen type VI or has its binding ability to collagen II significantly reduced [17].

But given the preferential localization of BGN to pericellular space, ECM collagens seem not to be the favored binding partners of BGN. Reports of DCN binding to cell surface and correlating with levels of growth factors was first described in the late eighties [58]. They found a negative regulation of TGF-β levels by DCN. Later, Hildebrand et al., 1994 [20] found that bacteria generated DCN, BGN and fibromodulin bound TGF-β1, -2 and -3 in a dose dependent manner. They also found that removal of GAGs was most beneficial when binding to TGF-β1.

The DS GAGs of SLRPs, like in BGN, have also been reported to bind fibroblast growth factor-2 (FGF-2) during the wound healing process [59]. Speculatively, proteolytic scission may be accompanied by dissociation of the BGN (proposed as a dimer form), leaving a truncated, monomeric PG free to diffuse to its target cells. These latter points are speculative but, as noted by the authors [60], murine enzyme HtrA1 rapidly degrades the

BGN core protein [61]; and the glycanated portion interacts with FGF-2 and its receptor while the chopped part is diffused or stays bound to collagen in ECM [62].

Mochida et al., 2006 [28] have also reported that BGN binds BMP-2, -4 and -6 in a cell culture system by IP-WB analysis. Interestingly, when direct binding assay by GST pull down was performed (BGN was tagged with GST), only BMP-2 showed significant binding to BGN, suggesting that the binding of BGN to BMP-2 is direct not requiring other molecules. In addition, they found that BGN specifically binds to the type I receptor BMP receptor IB (BMPRIB, also called activin-like kinase-6 or ALK-6). The type I receptors primarily determine the BMP signaling pathway and ALK6 is essential for osteoblast differentiation and bone formation. Other receptors like ALK2 and ALK5 and type II receptor BMPRII also showed detectable binding to BGN in cell culture system. In BMP-2 signaling, mainly ALK3 or ALK6 in combination with BMPRII have been described as the oligomerization pattern for BMP-2 function [63].

Aside from growth factor receptors, there is growing evidence that BGN may convey inflammatory processes through pathogen recognizing receptors. Mice lacking BGN survive lipopolisaccharide (LPS) challenges that otherwise would kill them. Addition of LPS induces secretion of interleukin (IL)-1 and -6 equally in cells with and without BGN, but addition of IL-1 to wild type macrophages increases BGN mRNA and protein, increasing TNF-α production. BGN alone also activates the MAP kinase pathways of ERK and p38 in macrophages. These events were found to be likely through toll like receptors (TLR)-4, although there was also BGN binding to TLR-2 which led to increased TNF-α. Interestingly, BGN devoid of GAGs, is not able to cause such response [29, 32]. It is clear that the effect of GAGs of BGN on its functions needs to be further investigated.

1.3.3. Glycosaminoglycans (GAGs) of BGN

The LRRs of the protein cores, which are considered to be particularly relevant for protein-protein interactions, have established SLRPs as important regulators of various biological processes [14, 15, 46, 64-66]. The involvement of GAG chains, however, has not been investigated in greater detail.

GAGs are long unbranched polysaccharides consisting of repeating disaccharide unit. This unit consists of an N-acetyl–hexosamine [e.g. galactosamine (GalN) or glucosamine (GlcN)] and a hexose or hexuronic acid [e.g. galactose (Gal) or glucuronic acid (GlcA) or iduronic acid (IdoA)]. Either or both of each may be sulfated. The combination of the sulfate group and the carboxylate groups gives them a very high density negative charge. BGN was named due to two CS/DS GAGs attached to its N-terminus. In mineralized tissues, BGN has being predominantly substituted with the GAG composed of CS at the N-terminus while in soft tissues, predominantly carry DS [34]. DS is distinguished from CS by the presence of IdoA. CS and DS are attached to the core protein at their reducing end through a tetrasaccharide region consisting of GlcA-Gal-Gal-Xyl with the xylose (Xyl) glycosydically linked to the hydroxyl group of Ser adjacent to a glycine (Gly) residue in the protein core. The first sugar of the GAG chain (linked to the Gal) is always GlcA, but is considered to be part of the linkage oligosaccharide. The biosynthesis of all PG, except the keratan sulfate (KS) portions of cartilage and cornea, consist of: (1) synthesis of the core protein; (2) xylosylation of specific Ser moieties of the core protein; (3) addition of two Gal residues to the Xyl; (4) completion of a common tetrasaccharide linkage region by addition of a GlcA residue; (5) addition of an GalN or GlcN residue to initiate the chondroitin/dermatan or

heparin GAG, respectively; (6) repeat addition of hexosamine residues alternating with GlcA residues to form the large heteropolymer GAG chains; and (7) modification of these GAGs by variable N-deacetylation/N-sulfation, and/or O-sulfation, and variable epimerization of GlcA to IdoA. Each of the GAGs involves several enzymes that have been cloned from vertebrates and other sources as Drosophila, C. elegans and zebra fish. The first steps of the synthesis of GAG chains of CS/DS and HS share a common pathway involving xylosyl transferase (Xylt1, Xylt2), β4-galactosyltransferase (β4galt7), β3-galactosyltransferase (β3galt6), β3-glucuronosyltransferase (β3gat1, β3gat2, β3gat3). CS/DS linkage region biosynthesis and chain extension require two additional enzymes, β4-GalNAc transferase (GalNAct2), and chondroitin synthase (Chsy1, Chsy2, Chsy3-like), which has both β 3GlcAcT and β4GalNAcT activities required to form the repeating disaccharide unit. Lastly, several enzymes are involved in the modification of the CS/DS GAG repeating unit (5 enzymes) that add sulfate to GlcA/IdoA (2S) or GalNAc (4S and/or 6S) [67].

The role of the GAG chains has not been explored in the interaction between BGN and BMPs. Previously, studies on the role of GAGs of PGs that carry HS have proposed that they play an important role in signal transduction through interaction with growth factors and chemokines and that the negative charge of GAGs are responsible for attracting these basic proteins [68]. However, besides charge, the position of those GAGs in the PG may also affect the binding of molecules to the core protein *per se* [69]. From Mochida's study, it is clear that BMP-2 binds to the core protein of BGN [28]. But it is not known what type of effect the GAGs would have on BGN-BMP binding and consequently BMP signaling. We could speculate that the GAG chains may modulate the interaction of BGN with BMP and possibly its receptor.

Despite growing recognition of the importance of GAGs in many physiological processes, a detailed understanding of their structure-function relationship has been lacking. Part of this is because extensive amount of these glycosides are needed to study GAG-protein interaction and generation of GAGs by overexpression of GAG-synthesizing enzymes is difficult due to the involvement of numerous enzymes for their biosynthesis as described above. Despite the difficulties, several studies have been able to prove through affinity chromatography, electrophoretic mobility shift assays and GAG removal by enzymes, i.e. chondroitinase ABC (C-ABC), that GAG components of PGs are coregulators of many growth factors. HS-PGs play crucial roles in regulating key developmental signaling pathways such as the Wnt, Hedgehog, TGF- β and FGF [4, 70]. In these studies, mutations in the enzymes responsible for the biosynthesis of GAG chains have unveiled the importance of PGs in development. But other than HS, the functions of CS/DS PGs have not been well studied in relationship to growth factor interaction. BGN carries most often two CS/DS chains that are linked to Ser 42 and 47 of the core protein. However, there have been reports of ~30% of the core protein being substituted with a single chain only [42, 43]. In addition, proteolytic processing of BGN may generate non-glycanated forms of the molecule [37, 44] as also described earlier for Htra1 [61]. Alterations to PG levels and/or GAGs have been reported in the literature in osteogenesis imperfecta [71, 72] , mucopolysaccharidosis [73], progeroid form of Ehler-Danlos syndrome [74, 75] and aging [72]. BGN has been shown to be decreased and have altered GAG structure in osteogenesis imperfecta and during aging, conditions that show osteopenic phenotype. The double knock out of DCN and BGN mimic a rare disease (OIM#130070) which is characterized by a defect in galactosyltransferase I activity which is responsible for GAG formation and the outcome is production of small PGs

devoid of GAG chains. These data suggest that the GAG chains may have important functions in bone. They also suggest a possible role for the GAGs of BGN in bone formation and maintenance. Considering the physicochemical properties of GAGs and recent studies demonstrating their involvement in PG functions, the GAG component of BGN could also affect the interaction of BGN with BMPs or their receptors consequently the BMP signaling.

The distribution of disaccharides along the polypeptide chains of SLRPs like DCN and BGN have been proposed. The disposition of monomers in the DCN dimer directs the long GAG chains away from the dimer interface [36]. This would allow the simultaneous use of the GAG or O-linked sugar chains and the protein cores for functional interactions. Additionally, the protein core of DCN contains three N-linked oligosaccharides that are all positioned on one side of the DCN dimer (glycan-rich surface), opposite to the ear projections (see Fig. 1.3e)[76]. This glycan-rich surface would not be used in protein–protein interactions. However, depending on the site where growth factors like BMP or its receptors would interact with BGN, GAGs may work as a barrier for growth factor binding.

1.3.4. Biglycan core protein

Besides the determination of the role of GAGs on BGN functions, the determination of the role of the core protein or its domains is of interest. The sequence, folds and turns of the polypeptide chain could presumably influence function. DCN and BGN have very similar secondary and tertiary structures although their sequence homology is quite different. Take for instance the structure of the first LRR that is always connected to the N-terminal sequence by a disulfide bond and said to be important for stability of the LRRs. It is about 68 amino acids long in both proteins but only have two 7 amino acid long sequences that are

identical with other random similar amino acids. The remaining LRRs follow the same pattern, thus with very limited homology. Yet again, the full protein DCN and BGN functions have started to be unveiled and they seem to be quite different and even opposites in some circumstances. The peculiarities in the sequences and/or structures of those proteins should hold the secret to their different functions as in conformation (horseshoe dimmers) they are very similar.

1.4. Bone morphogenetic proteins

BMPs were originally identified from extracts of bone matrix after an orthopedic surgeon and researcher, Urist, found that demineralized bone matrix could induce heterotopic bone formation in a rodent model [77]. Since then, more than 20 related proteins with BMP sequences and activities have been sequenced and cloned [78, 79]. They have been either purified from bone or generated by recombinant DNA technology and shown to induce endochondral or intramembranous bone formation depending on the anatomical site in which they have been administered. BMPs are members of TGF-β superfamily. The superfamily consists of proteins that have a highly conserved seven Cys domain at the carboxy-terminal region. This super family of proteins includes five isoforms of TGF–β (1 through 5), the BMPs, growth differentiation factors (GDF), activins, inhibins and Mullerian inhibiting substance [80]. They are dimeric molecules with two polypeptide chains held together by a single disulfide bond, secreted as precursors, processed to release mature, active proteins which have a molecular weight of 20-30 kDa retaining the critical seven Cys residues [81] (Fig 1.7). The superfamily has impact on a wide array of cellular activities including cell growth and differentiation as well as the synthesis of ECM. BMPs control many key steps in the development of organs (heart, kidney, reproductive organs, the vertebrate nervous system

regulating cell fate, proliferation and differentiation) [82-84]. During embryonic development, BMPs mediate apoptosis and accumulated evidence indicates that BMPs play an important role in regulation of stem cell properties [85-87]. There is also evidence of the role of BMPs in oncogenesis/tumor suppression [88, 89].

It is now clear that BMPs upregulate the expression of critical transcription factors, *Cbfa1*/runt-related transcription factor 2 (*Runx2*) [90, 91] and *Osx* [92, 93], and a number of matrix molecules genes such as type I collagen, alkaline phosphatase *(Alp),* osteocalcin and SLRPs, essential for osteoblast differentiation and matrix formation/mineralization [94-97]. Of BMP members, BMP-2, -4, -6 and -7 (the latter is also known as osteogenic protein-1) are known to be potent osteoinductive growth factors [98, 99] that induce osteogenic differentiation of pluripotent mesenchymal cell lines (such as C3H10T1/2) and promote the maturation of osteoblastic progenitor cells [100-102]. In the myogenic cell line C2C12, for instance, BMP-2 suppresses the expression of myogenic markers such as *Myo-D* and myogenin, and stimulate the expression of genes involved in osteogenesis, such as *Alp*, parathyroid-hormone/parathyroid-hormone-related protein receptor, osteocalcin *(Ocn),*

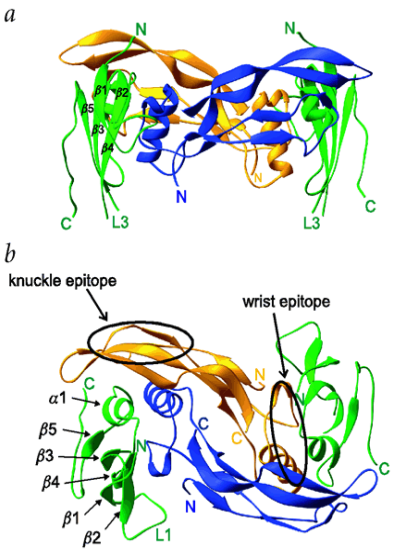

Fig 1.7. The structure of the BMP-2−BRIA ectodomain complex. *a*, Side view with the membrane proximal side on the bottom and ***b***, top view approximately along the twofold axis of the complex in a ribbon representation. The BMP monomers are colored gold and blue, the two BRIA ectodomain molecules are green. Secondary structure elements, chain termini and receptor loops 1 and 3 are labeled. The 'wrist' and the putative 'knuckle' epitopes on BMP-2 are highlighted. © *Figure and legend printed with permission from Nature. Kirsch et al., Crystal structure of the BMP-2-BRIA ectodomain complex. Nature Structural Biology 2000 7: 492-496.*

Cbfa1/Runx2 and *Osx*, thus transdifferentiating from myogenic to osteogenic cell lineage [91, 93, 103].

BMP-2 has mostly received attention and most of the *in vitro* as well as human *in vivo* studies involve BMP-2. Its approval for human use by the FDA occurred in 2002. Unfortunately, despite large amounts of BMP being used for human application especially for spine fusion procedures and more recently for maxillofacial grafting, a percentage of bone regeneration procedures is not completely successful. Clinical complications have been attributed to a hyper inflammatory response due to the high amount of BMP-2 delivered [104]. But little is known about the key players in BMP function and thus modulation rather than increasing its amount may be the answer to some of its clinical limitations.

1.4.1. BMP antagonists and agonists

The process of BMP signaling is highly controlled by numerous molecules at extracellular, cell surface and intracellular levels (Fig 1.8). A well orchestrated and tight control of BMPs by these molecules at various levels is crucial for the normal cell functions. At the cell surface, a pseudo type I receptor, BAMBI, antagonizes the effects of BMPs by preventing the formation of active receptor complexes [105], while a co-receptor, DRAGON, potentiates BMP signaling by interacting with BMPs and receptors [106].

At the intracellular level, BMP signaling is inhibited by several I (inhibitory)-Smads (Smad 6 and 7) that efficiently interact with activated type I receptors and compete with R (receptor-regulated)-Smads (Smads1, 5 and 8) for type I receptor interaction [107]. The signal is also inhibited by two closely related Smurf (Smad ubiquitination regulatory factors) 1 and 2 that selectively degrade the activated type I receptor and Smad proteins [108, 109].

In the extracellular space, antagonists are classified into three subgroups based on the size of the cystine-knot; Dan family (eight-membered ring), Tsg (nine-membered ring) and chordin/noggin (twelve-membered ring) [110-112]. These secreted polypeptides inhibit BMP

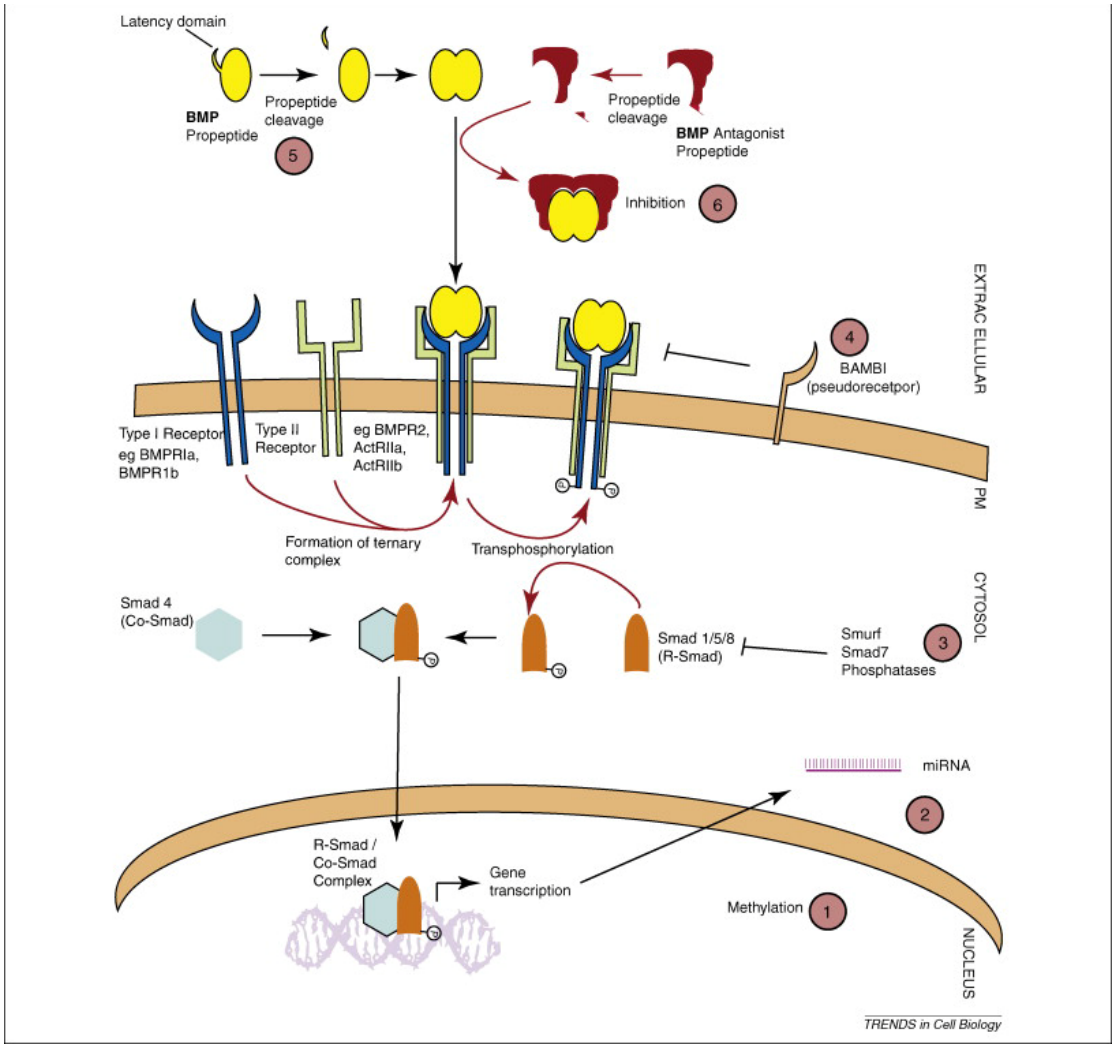

Fig 1.8. BMP Signal Transduction. Shown here is the canonical BMP–Smad signaling pathway. BMP agonists are post-transcriptionally cleaved and processed, and then form active dimers. Upon receptor binding, two type I and two type II receptors associate to form a hexameric receptor–agonist complex. On activation, type I receptors are trans-phosphorylated by type II receptors. Type I receptors, in turn, phosphorylate their R-Smads. Phosphorylated R-Smads form a complex with the co-Smad, Smad-4, translocating to the nucleus, and promoting transcription of target genes. In the presence of active BMP antagonists a ternary agonist–antagonist complex is formed in the extracellular space and receptor activation is prevented. Steps 1–6 mark both the intracellular and extracellular sites at which the signaling pathway can be modulated. Step 2 highlights the likelihood that regulation of BMP and BMP-antagonist expression by as yet undiscovered miRNA will probably be revealed in the near future. BMPR, BMP receptor; Smurf, Smad–ubiquitin regulatory factor . *© Figure and legend reprinted with authorization of Elsevier. Walsh et al. Extracellular BMP-antagonist regulation in development and disease: tied up the knots. Trends in Cell Biology 2010 March; 20(5): 244-256.*

activity by binding BMPs, thus preventing BMPs binding to their specific cell receptors. Interestingly, the expression of some of these antagonists is induced by BMPs indicating a local feedback mechanism to maintain the balance between BMPs and inhibitors.

BMP agonists have not been well defined. A recent attempt to agonize BMP function was through identification of a key residue on BMP-6 that conferred noggin resistance. Introduction of a Lysine (Lys) residue at the corresponding positions of BMP-2 and BMP-7 allowed for molecular engineering of recombinant BMPs with increased resistance to noggin antagonism [113].

1.4.2. BMP receptors and downstream signaling

BMPs bind to BMP receptors composed of two transmembrane serine/threonine (Thr) protein kinases, type-I and type-II (BMPR-I and II). They consist of a signal peptide, Cys-rich extracellular domain, transmembrane region and Ser/Thr kinase domain [114]. The affinity of BMPR-I for BMPs is higher than that of BMPR-II [115], thus, it is likely that BMPs bind BMPR-I initially and then recruit BMPR-II into the complex as demonstrated by Gilboa et al [63]. There have been also reports of pre-formed complexes of type I and II receptors prior to BMP binding [63]. Three type I receptors for BMPs have been characterized: activin receptor-like kinase-2 (ALK2), type IA and IB BMP receptors (BMPR-IA/ALK3 and BMPR-IB/ALK6) [116, 117]. The various assembly modes can also lead to different pathways activation. The type II receptors are constitutively active and phosphorylate the Gly-Ser (GS) box of type I receptors. Then the activation of type I receptor kinases initiate phosphorylation of specific downstream components including the nuclear effector proteins, Smads, in chondroblasts and osteoblasts. The Smad pathway is the

canonical downstream event upon BMP-2-receptor coupling. These R-Smads 1, 5 and 8 are released from the receptors to form a hetero-oligomeric complex with a common mediator Smad (Co-Smad; Smad 4), which is capable of migrating into the nucleus to function as transcription factors to regulate specific BMP target genes in concert with several co-factors [107, 118] (Fig 1.8).

The non-Smad pathways of ERK, p38 and Wnt have also been reported to be influenced by BMP [33, 53, 119, 120]. The activation of such pathways may occur via internal cellular cross-talks or different patterns of oligomerization mode of the receptors or interaction/stimulation of other molecules important for the activation of those pathways. Recently, Wnt signaling has been described as an important pathway in bone regeneration that is induced by BMP-2 and strongly present during fracture repair [121]. The mechanisms by which Wnt signaling is activated during repair are still largely unknown. Similarly, the mechanisms by which BMP-2 acts in *in vivo* bone regeneration are also largely unknown.

The pattern of expression of those receptors is different from each other with ALK3 being expressed throughout the tissues in the body during mouse development and in adult tissues, whereas ALK6 during mouse development is expressed in mesenchymal pre-cartilage condensations and in chondrocytes and osteoblasts at adult stage [122, 123]. In our laboratory, we have found that ALK6 expression in MC3T3-E1 cells peaks at 7 days and is significantly reduced from then on (unpublished data). ALK6 has been shown to be essential for osteoblast differentiation and matrix mineralization by using truncated dominant-negative and constitutively active forms of ALK3 and 6 in a clonal osteoblast precursor cell line, 2T3 [85]. When a truncated ALK6 targeted to osteoblasts using the type I collagen promoter was overexpressed in mice, the transgenic mice showed defective bone formation (bone mineral

density, bone volume, rate of bone formation) due to the blockage of BMP signaling [124]. These studies clearly demonstrate a critical role of ALK6-transduced BMP signaling in osteoblast differentiation and bone formation.

As far as the type II receptor, BMPRII, it is necessary to phosphorylate the GS box in type I receptors. Without it coupling with a type I receptor, it was thought that no BMP signaling would be transduced. However, with lack of BMPRII, smooth muscle cells tranduce signals through another type II receptor, ActRIIa [125]. This suggests net gain of ligands to other BMP receptors in case of absent or non-functional BMPRII.

Bibliography

[1] S. Gajjeraman, K. Narayanan, J. Hao, C. Qin, and A. George, Matrix macromolecules in hard tissues control the nucleation and hierarchical assembly of hydroxyapatite, J Biol Chem 282 (2007) 1193-1204.

[2] J. B. Lian, G. S. Stein, J. L. Stein, and A. J. van Wijnen, Regulated expression of the bone-specific osteocalcin gene by vitamins and hormones, Vitam Horm 55 (1999) 443-509.

[3] P. G. Robey, Vertebrate mineralized matrix proteins: structure and function, Connect Tissue Res 35 (1996) 131-136.

[4] R. V. Iozzo, Matrix proteoglycans: from molecular design to cellular function, Annu Rev Biochem 67 (1998) 609-652.

[5] L. W. Fisher, J. D. Termine, S. W. Dejter, Jr., S. W. Whitson, M. Yanagishita, J. H. Kimura, V. C. Hascall, H. K. Kleinman, J. R. Hassell, and B. Nilsson, Proteoglycans of developing bone, J Biol Chem 258 (1983) 6588-6594.

[6] P. A. McEwan, P. G. Scott, P. N. Bishop, and J. Bella, Structural correlations in the family of small leucine-rich repeat proteins and proteoglycans, J Struct Biol 155 (2006) 294-305.

[7] R. V. Iozzo, The biology of the small leucine-rich proteoglycans. Functional network of interactive proteins, J Biol Chem 274 (1999) 18843-18846.

[8] P. G. Scott, N. Winterbottom, C. M. Dodd, E. Edwards, and C. H. Pearson, A role for disulphide bridges in the protein core in the interaction of proteodermatan sulphate and collagen, Biochem Biophys Res Commun 138 (1986) 1348-1354.

[9] M. D. Ross, L. A. Bruggeman, B. Hanss, M. Sunamoto, D. Marras, M. E. Klotman, and P. E. Klotman, Podocan, a novel small leucine-rich repeat protein expressed in the sclerotic glomerular lesion of experimental HIV-associated nephropathy, J Biol Chem 278 (2003) 33248-33255.

[10] S. P. Henry, M. Takanosu, T. C. Boyd, P. M. Mayne, H. Eberspaecher, W. Zhou, B. de Crombrugghe, M. Hook, and R. Mayne, Expression pattern and gene characterization of asporin. a newly discovered member of the leucine-rich repeat protein family, J Biol Chem 276 (2001) 12212-12221.

[11] T. Xu, P. Bianco, L. W. Fisher, G. Longenecker, E. Smith, S. Goldstein, J. Bonadio, A. Boskey, A. M. Heegaard, B. Sommer, K. Satomura, P. Dominguez, C. Zhao, A. B. Kulkarni, P. G. Robey, and M. F. Young, Targeted disruption of the biglycan gene leads to an osteoporosis-like phenotype in mice, Nat Genet 20 (1998) 78-82.

[12] L. Ameye, and M. F. Young, Mice deficient in small leucine-rich proteoglycans: novel in vivo models for osteoporosis, osteoarthritis, Ehlers-Danlos syndrome, muscular dystrophy, and corneal diseases, Glycobiology 12 (2002) 107R-116R.

[13] Y. Bi, D. Ehirchiou, T. M. Kilts, C. A. Inkson, M. C. Embree, W. Sonoyama, L. Li, A. I. Leet, B. M. Seo, L. Zhang, S. Shi, and M. F. Young, Identification of tendon stem/progenitor cells and the role of the extracellular matrix in their niche, Nat Med 13 (2007) 1219-1227.

[14] K. G. Danielson, H. Baribault, D. F. Holmes, H. Graham, K. E. Kadler, and R. V. Iozzo, Targeted disruption of decorin leads to abnormal collagen fibril morphology and skin fragility, J Cell Biol 136 (1997) 729-743.

[15] S. Chakravarti, Functions of lumican and fibromodulin: lessons from knockout mice, Glycoconj J 19 (2002) 287-293.

[16] G. Pogany, D. J. Hernandez, and K. G. Vogel, The in vitro interaction of proteoglycans with type I collagen is modulated by phosphate, Arch Biochem Biophys 313 (1994) 102-111.

[17] A. M. Hocking, R. A. Strugnell, P. Ramamurthy, and D. J. McQuillan, Eukaryotic expression of recombinant biglycan. Post-translational processing and the importance of secondary structure for biological activity, J Biol Chem 271 (1996) 19571-19577.

[18] E. Schonherr, P. Witsch-Prehm, B. Harrach, H. Robenek, J. Rauterberg, and H. Kresse, Interaction of biglycan with type I collagen, J Biol Chem 270 (1995) 2776-2783.

[19] S. Kalamajski, A. Aspberg, K. Lindblom, D. Heinegard, and A. Oldberg, Asporin competes with decorin for collagen binding, binds calcium and promotes osteoblast collagen mineralization, Biochem J 423 (2009) 53-59.

[20] A. Hildebrand, M. Romaris, L. M. Rasmussen, D. Heinegard, D. R. Twardzik, W. A. Border, and E. Ruoslahti, Interaction of the small interstitial proteoglycans biglycan, decorin and fibromodulin with transforming growth factor beta, Biochem J 302 (Pt 2) (1994) 527-534.

[21] A. M. Hocking, T. Shinomura, and D. J. McQuillan, Leucine-rich repeat glycoproteins of the extracellular matrix, Matrix Biol 17 (1998) 1-19.

[22] H. Kresse, and E. Schonherr, Proteoglycans of the extracellular matrix and growth control, J Cell Physiol 189 (2001) 266-274.

[23] J. H. Yoon, and J. Halper, Tendon proteoglycans: biochemistry and function, J Musculoskelet Neuronal Interact 5 (2005) 22-34.

[24] F. Elefteriou, J. Y. Exposito, R. Garrone, and C. Lethias, Binding of tenascin-X to decorin, FEBS Lett 495 (2001) 44-47.

[25] R. Gendelman, N. I. Burton-Wurster, J. N. MacLeod, and G. Lust, The cartilage-specific fibronectin isoform has a high affinity binding site for the small proteoglycan decorin, J Biol Chem 278 (2003) 11175-11181.

[26] R. Krumdieck, M. Hook, L. C. Rosenberg, and J. E. Volanakis, The proteoglycan decorin binds C1q and inhibits the activity of the C1 complex, J Immunol 149 (1992) 3695-3701.

[27] J. Nadesalingam, A. L. Bernal, A. W. Dodds, A. C. Willis, D. J. Mahoney, A. J. Day, K. B. Reid, and N. Palaniyar, Identification and characterization of a novel interaction between pulmonary surfactant protein D and decorin, J Biol Chem 278 (2003) 25678-25687.

[28] Y. Mochida, D. Parisuthiman, and M. Yamauchi, Biglycan is a positive modulator of BMP-2 induced osteoblast differentiation, Adv Exp Med Biol 585 (2006) 101-113.

[29] A. Babelova, K. Moreth, W. Tsalastra-Greul, J. Zeng-Brouwers, O. Eickelberg, M. F. Young, P. Bruckner, J. Pfeilschifter, R. M. Schaefer, H. J. Grone, and L. Schaefer, Biglycan, a danger signal that activates the NLRP3 inflammasome via toll-like and P2X receptors, J Biol Chem 284 (2009) 24035-24048.

[30] L. Desnoyers, D. Arnott, and D. Pennica, WISP-1 binds to decorin and biglycan, J Biol Chem 276 (2001) 47599-47607.

[31] W. Yan, P. Wang, C. X. Zhao, J. Tang, X. Xiao, and D. W. Wang, Decorin gene delivery inhibits cardiac fibrosis in spontaneously hypertensive rats by modulation of transforming growth factor-beta/Smad and p38 mitogen-activated protein kinase signaling pathways, Hum Gene Ther 20 (2009) 1190-1200.

[32] L. Schaefer, A. Babelova, E. Kiss, H. J. Hausser, M. Baliova, M. Krzyzankova, G. Marsche, M. F. Young, D. Mihalik, M. Gotte, E. Malle, R. M. Schaefer, and H. J. Grone, The matrix component biglycan is proinflammatory and signals through Toll-like receptors 4 and 2 in macrophages, J Clin Invest 115 (2005) 2223-2233.

[33] X. Wang, K. Harimoto, S. Xie, H. Cheng, J. Liu, and Z. Wang, Matrix protein biglycan induces osteoblast differentiation through extracellular signal-regulated kinase and Smad pathways, Biol Pharm Bull 33 (2010) 1891-1897.

[34] L. W. Fisher, J. D. Termine, and M. F. Young, Deduced protein sequence of bone small proteoglycan I (biglycan) shows homology with proteoglycan II (decorin) and several nonconnective tissue proteins in a variety of species, J Biol Chem 264 (1989) 4571-4576.

[35] Y. Wegrowski, J. Pillarisetti, K. G. Danielson, S. Suzuki, and R. V. Iozzo, The murine biglycan: complete cDNA cloning, genomic organization, promoter function, and expression, Genomics 30 (1995) 8-17.

[36] I. C. Scott, Y. Imamura, W. N. Pappano, J. M. Troedel, A. D. Recklies, P. J. Roughley, and D. S. Greenspan, Bone morphogenetic protein-1 processes probiglycan, J Biol Chem 275 (2000) 30504-30511.

[37] B. Johnstone, M. Markopoulos, P. Neame, and B. Caterson, Identification and characterization of glycanated and non-glycanated forms of biglycan and decorin in the human intervertebral disc, Biochem J 292 (Pt 3) (1993) 661-666.

[38] L. W. Fisher, A. M. Heegaard, U. Vetter, W. Vogel, W. Just, J. D. Termine, and M. F. Young, Human biglycan gene. Putative promoter, intron-exon junctions, and chromosomal localization, J Biol Chem 266 (1991) 14371-14377.

[39] A. Chatterjee, C. J. Faust, and G. E. Herman, Genetic and physical mapping of the biglycan gene on the mouse X chromosome, Mamm Genome 4 (1993) 33-36.

[40] P. Bianco, L. W. Fisher, M. F. Young, J. D. Termine, and P. G. Robey, Expression and localization of the two small proteoglycans biglycan and decorin in developing human skeletal and non-skeletal tissues, J Histochem Cytochem 38 (1990) 1549-1563.

[41] A. L. Boskey, L. Spevak, S. B. Doty, and L. Rosenberg, Effects of bone CS-proteoglycans, DS-decorin, and DS-biglycan on hydroxyapatite formation in a gelatin gel, Calcif Tissue Int 61 (1997) 298-305.

[42] P. J. Neame, H. U. Choi, and L. C. Rosenberg, The primary structure of the core protein of the small, leucine-rich proteoglycan (PG I) from bovine articular cartilage, J Biol Chem 264 (1989) 8653-8661.

[43] L. W. Fisher, G. R. Hawkins, N. Tuross, and J. D. Termine, Purification and partial characterization of small proteoglycans I and II, bone sialoproteins I and II, and osteonectin from the mineral compartment of developing human bone, J Biol Chem 262 (1987) 9702-9708.

[44] P. J. Roughley, R. J. White, M. C. Magny, J. Liu, R. H. Pearce, and J. S. Mort, Non-proteoglycan forms of biglycan increase with age in human articular cartilage, Biochem J 295 (Pt 2) (1993) 421-426.

[45] H. Kresse, D. G. Seidler, M. Muller, E. Breuer, H. Hausser, P. J. Roughley, and E. Schonherr, Different usage of the glycosaminoglycan attachment sites of biglycan, J Biol Chem 276 (2001) 13411-13416.

[46] M. F. Young, Y. Bi, L. Ameye, and X. D. Chen, Biglycan knockout mice: new models for musculoskeletal diseases, Glycoconj J 19 (2002) 257-262.

[47] J. M. Wallace, R. M. Rajachar, X. D. Chen, S. Shi, M. R. Allen, S. A. Bloomfield, C. M. Les, P. G. Robey, M. F. Young, and D. H. Kohn, The mechanical phenotype of biglycan-deficient mice is bone- and gender-specific, Bone 39 (2006) 106-116.

[48] A. Corsi, T. Xu, X. D. Chen, A. Boyde, J. Liang, M. Mankani, B. Sommer, R. V. Iozzo, I. Eichstetter, P. G. Robey, P. Bianco, and M. F. Young, Phenotypic effects of biglycan deficiency are linked to collagen fibril abnormalities, are synergized by decorin deficiency, and mimic Ehlers-Danlos-like changes in bone and other connective tissues, J Bone Miner Res 17 (2002) 1180-1189.

[49] X. D. Chen, L. W. Fisher, P. G. Robey, and M. F. Young, The small leucine-rich proteoglycan biglycan modulates BMP-4-induced osteoblast differentiation, Faseb J 18 (2004) 948-958.

[50] Y. Bi, C. H. Stuelten, T. Kilts, S. Wadhwa, R. V. Iozzo, P. G. Robey, X. D. Chen, and M. F. Young, Extracellular matrix proteoglycans control the fate of bone marrow stromal cells, J Biol Chem 280 (2005) 30481-30489.

[51] M. Moreno, R. Munoz, F. Aroca, M. Labarca, E. Brandan, and J. Larrain, Biglycan is a new extracellular component of the Chordin-BMP4 signaling pathway, Embo J 24 (2005) 1397-1405.

[52] D. Parisuthiman, Y. Mochida, W. R. Duarte, and M. Yamauchi, Biglycan modulates osteoblast differentiation and matrix mineralization, J Bone Miner Res 20 (2005) 1878-1886.

[53] G. Xiao, R. Gopalakrishnan, D. Jiang, E. Reith, M. D. Benson, and R. T. Franceschi, Bone morphogenetic proteins, extracellular matrix, and mitogen-activated protein kinase signaling pathways are required for osteoblast-specific gene expression and differentiation in MC3T3-E1 cells, J Bone Miner Res 17 (2002) 101-110.

[54] L. Svensson, D. Heinegard, and A. Oldberg, Decorin-binding sites for collagen type I are mainly located in leucine-rich repeats 4-5, J Biol Chem 270 (1995) 20712-20716.

[55] R. V. Sugars, A. M. Milan, J. O. Brown, R. J. Waddington, R. C. Hall, and G. Embery, Molecular interaction of recombinant decorin and biglycan with type I collagen influences crystal growth, Connect Tissue Res 44 Suppl 1 (2003) 189-195.

[56] M. Raspanti, M. Viola, A. Forlino, R. Tenni, C. Gruppi, and M. E. Tira, Glycosaminoglycans show a specific periodic interaction with type I collagen fibrils, J Struct Biol 164 (2008) 134-139.

[57] C. Wiberg, D. Heinegard, C. Wenglen, R. Timpl, and M. Morgelin, Biglycan organizes collagen VI into hexagonal-like networks resembling tissue structures, J Biol Chem 277 (2002) 49120-49126.

[58] Y. Yamaguchi, and E. Ruoslahti, Expression of human proteoglycan in Chinese hamster ovary cells inhibits cell proliferation, Nature 336 (1988) 244-246.

[59] K. R. Taylor, J. A. Rudisill, and R. L. Gallo, Structural and sequence motifs in dermatan sulfate for promoting fibroblast growth factor-2 (FGF-2) and FGF-7 activity, J Biol Chem 280 (2005) 5300-5306.

[60] S. Hou, M. Maccarana, T. H. Min, I. Strate, and E. M. Pera, The secreted serine protease xHtrA1 stimulates long-range FGF signaling in the early Xenopus embryo, Dev Cell 13 (2007) 226-241.

[61] J. Tocharus, A. Tsuchiya, M. Kajikawa, Y. Ueta, C. Oka, and M. Kawaichi, Developmentally regulated expression of mouse HtrA3 and its role as an inhibitor of TGF-beta signaling, Dev Growth Differ 46 (2004) 257-274.

[62] J. Gallagher, Messages in the matrix: proteoglycans go the distance, Dev Cell 13 (2007) 166-167.

[63] L. Gilboa, A. Nohe, T. Geissendorfer, W. Sebald, Y. I. Henis, and P. Knaus, Bone morphogenetic protein receptor complexes on the surface of live cells: a new oligomerization mode for serine/threonine kinase receptors, Mol Biol Cell 11 (2000) 1023-1035.

[64] W. W. Kao, and C. Y. Liu, Roles of lumican and keratocan on corneal transparency, Glycoconj J 19 (2002) 275-285.

[65] P. J. Roughley, The structure and function of cartilage proteoglycans, Eur Cell Mater 12 (2006) 92-101.

[66] L. Schaefer, and R. V. Iozzo, Biological functions of the small leucine-rich proteoglycans: from genetics to signal transduction, J Biol Chem 283 (2008) 21305-21309.

[67] J. E. Silbert, and G. Sugumaran, A starting place for the road to function, Glycoconj J 19 (2002) 227-237.

[68] T. M. Handel, Z. Johnson, S. E. Crown, E. K. Lau, and A. E. Proudfoot, Regulation of protein function by glycosaminoglycans--as exemplified by chemokines, Annu Rev Biochem 74 (2005) 385-410.

[69] M. E. Herndon, C. S. Stipp, and A. D. Lander, Interactions of neural glycosaminoglycans and proteoglycans with protein ligands: assessment of

selectivity, heterogeneity and the participation of core proteins in binding, Glycobiology 9 (1999) 143-155.

[70] M. Bernfield, M. Gotte, P. W. Park, O. Reizes, M. L. Fitzgerald, J. Lincecum, and M. Zako, Functions of cell surface heparan sulfate proteoglycans, Annu Rev Biochem 68 (1999) 729-777.

[71] N. S. Fedarko, U. Vetter, and P. G. Robey, The bone cell biology of osteogenesis imperfecta, Connect Tissue Res 31 (1995) 269-273.

[72] W. J. Grzesik, C. R. Frazier, J. R. Shapiro, P. D. Sponseller, P. G. Robey, and N. S. Fedarko, Age-related changes in human bone proteoglycan structure. Impact of osteogenesis imperfecta, J Biol Chem 277 (2002) 43638-43647.

[73] J. D. Nuttall, L. K. Brumfield, N. L. Fazzalari, J. J. Hopwood, and S. Byers, Histomorphometric analysis of the tibial growth plate in a feline model of mucopolysaccharidosis type VI, Calcif Tissue Int 65 (1999) 47-52.

[74] H. Kresse, S. Rosthoj, E. Quentin, J. Hollmann, J. Glossl, S. Okada, and T. Tonnesen, Glycosaminoglycan-free small proteoglycan core protein is secreted by fibroblasts from a patient with a syndrome resembling progeroid, Am J Hum Genet 41 (1987) 436-453.

[75] M. Faiyaz-Ul-Haque, S. H. Zaidi, M. Al-Ali, M. S. Al-Mureikhi, S. Kennedy, G. Al-Thani, L. C. Tsui, and A. S. Teebi, A novel missense mutation in the galactosyltransferase-I (B4GALT7) gene in a family exhibiting facioskeletal anomalies and Ehlers-Danlos syndrome resembling the progeroid type, Am J Med Genet A 128 (2004) 39-45.

[76] P. G. Scott, P. A. McEwan, C. M. Dodd, E. M. Bergmann, P. N. Bishop, and J. Bella, Crystal structure of the dimeric protein core of decorin, the archetypal small leucine-rich repeat proteoglycan, Proc Natl Acad Sci U S A 101 (2004) 15633-15638.

[77] M. R. Urist, Bone: formation by autoinduction, Science 150 (1965) 893-899.

[78] J. M. Wozney, and V. Rosen, Bone morphogenetic protein and bone morphogenetic protein gene family in bone formation and repair, Clin Orthop Relat Res (1998) 26-37.

[79] E. Ozkaynak, D. C. Rueger, E. A. Drier, C. Corbett, R. J. Ridge, T. K. Sampath, and H. Oppermann, OP-1 cDNA encodes an osteogenic protein in the TGF-beta family, Embo J 9 (1990) 2085-2093.

[80] H. Chang, C. W. Brown, and M. M. Matzuk, Genetic analysis of the mammalian transforming growth factor-beta superfamily, Endocr Rev 23 (2002) 787-823.

[81] C. Scheufler, W. Sebald, and M. Hulsmeyer, Crystal structure of human bone morphogenetic protein-2 at 2.7 A resolution, J Mol Biol 287 (1999) 103-115.

[82] D. Chen, M. Zhao, S. E. Harris, and Z. Mi, Signal transduction and biological functions of bone morphogenetic proteins, Front Biosci 9 (2004) 349-358.

[83] A. K. Hall, and R. H. Miller, Emerging roles for bone morphogenetic proteins in central nervous system glial biology, J Neurosci Res 76 (2004) 1-8.

[84] M. Y. Hsu, S. Rovinsky, S. Penmatcha, M. Herlyn, and D. Muirhead, Bone morphogenetic proteins in melanoma: angel or devil? Cancer Metastasis Rev 24 (2005) 251-263.

[85] D. Chen, X. Ji, M. A. Harris, J. Q. Feng, G. Karsenty, A. J. Celeste, V. Rosen, G. R. Mundy, and S. E. Harris, Differential roles for bone morphogenetic protein (BMP) receptor type IB and IA in differentiation and specification of mesenchymal precursor cells to osteoblast and adipocyte lineages, J Cell Biol 142 (1998) 295-305.

[86] R. H. Xu, X. Chen, D. S. Li, R. Li, G. C. Addicks, C. Glennon, T. P. Zwaka, and J. A. Thomson, BMP4 initiates human embryonic stem cell differentiation to trophoblast, Nat Biotechnol 20 (2002) 1261-1264.

[87] J. Zhang, and L. Li, BMP signaling and stem cell regulation, Dev Biol 284 (2005) 1-11.

[88] H. Yoshikawa, T. Nakase, A. Myoui, and T. Ueda, Bone morphogenetic proteins in bone tumors, J Orthop Sci 9 (2004) 334-340.

[89] R. Montesano, Bone morphogenetic protein-4 abrogates lumen formation by mammary epithelial cells and promotes invasive growth, Biochem Biophys Res Commun 353 (2007) 817-822.

[90] E. Canalis, A. N. Economides, and E. Gazzerro, Bone morphogenetic proteins, their antagonists, and the skeleton, Endocr Rev 24 (2003) 218-235.

[91] K. S. Lee, H. J. Kim, Q. L. Li, X. Z. Chi, C. Ueta, T. Komori, J. M. Wozney, E. G. Kim, J. Y. Choi, H. M. Ryoo, and S. C. Bae, Runx2 is a common target of transforming growth factor beta1 and bone morphogenetic protein 2, and cooperation between Runx2 and Smad5 induces osteoblast-specific gene expression in the pluripotent mesenchymal precursor cell line C2C12, Mol Cell Biol 20 (2000) 8783-8792.

[92] Z. S. Ai-Aql, A. S. Alagl, D. T. Graves, L. C. Gerstenfeld, and T. A. Einhorn, Molecular mechanisms controlling bone formation during fracture healing and distraction osteogenesis, J Dent Res 87 (2008) 107-118.

[93] Y. Ohyama, A. Nifuji, Y. Maeda, T. Amagasa, and M. Noda, Spaciotemporal association and bone morphogenetic protein regulation of sclerostin and osterix expression during embryonic osteogenesis, Endocrinology 145 (2004) 4685-4692.

[94] T. Katagiri, and N. Takahashi, Regulatory mechanisms of osteoblast and osteoclast differentiation, Oral Dis 8 (2002) 147-159.

[95] E. Balint, D. Lapointe, H. Drissi, C. van der Meijden, D. W. Young, A. J. van Wijnen, J. L. Stein, G. S. Stein, and J. B. Lian, Phenotype discovery by gene expression profiling: mapping of biological processes linked to BMP-2-mediated osteoblast differentiation, J Cell Biochem 89 (2003) 401-426.

[96] T. Katagiri, A. Yamaguchi, M. Komaki, E. Abe, N. Takahashi, T. Ikeda, V. Rosen, J. M. Wozney, A. Fujisawa-Sehara, and T. Suda, Bone morphogenetic protein-2 converts the differentiation pathway of C2C12 myoblasts into the osteoblast lineage, J Cell Biol 127 (1994) 1755-1766.

[97] M. Suzawa, Y. Takeuchi, S. Fukumoto, S. Kato, N. Ueno, K. Miyazono, T. Matsumoto, and T. Fujita, Extracellular matrix-associated bone morphogenetic proteins are essential for differentiation of murine osteoblastic cells in vitro, Endocrinology 140 (1999) 2125-2133.

[98] I. Asahina, T. K. Sampath, and P. V. Hauschka, Human osteogenic protein-1 induces chondroblastic, osteoblastic, and/or adipocytic differentiation of clonal murine target cells, Exp Cell Res 222 (1996) 38-47.

[99] S. Ebara, and K. Nakayama, Mechanism for the action of bone morphogenetic proteins and regulation of their activity, Spine 27 (2002) S10-15.

[100] T. Katagiri, A. Yamaguchi, T. Ikeda, S. Yoshiki, J. M. Wozney, V. Rosen, E. A. Wang, H. Tanaka, S. Omura, and T. Suda, The non-osteogenic mouse pluripotent cell line, C3H10T1/2, is induced to differentiate into osteoblastic cells by recombinant human bone morphogenetic protein-2, Biochem Biophys Res Commun 172 (1990) 295-299.

[101] A. Yamaguchi, T. Katagiri, T. Ikeda, J. M. Wozney, V. Rosen, E. A. Wang, A. J. Kahn, T. Suda, and S. Yoshiki, Recombinant human bone morphogenetic protein-2 stimulates osteoblastic maturation and inhibits myogenic differentiation in vitro, J Cell Biol 113 (1991) 681-687.

[102] A. Yamaguchi, T. Komori, and T. Suda, Regulation of osteoblast differentiation mediated by bone morphogenetic proteins, hedgehogs, and Cbfa1, Endocr Rev 21 (2000) 393-411.

[103] K. Nakashima, X. Zhou, G. Kunkel, Z. Zhang, J. M. Deng, R. R. Behringer, and B. de Crombrugghe, The novel zinc finger-containing transcription factor osterix is required for osteoblast differentiation and bone formation, Cell 108 (2002) 17-29.

[104] R. Vaidya, J. Carp, A. Sethi, S. Bartol, J. Craig, and C. M. Les, Complications of anterior cervical discectomy and fusion using recombinant human bone morphogenetic protein-2, Eur Spine J 16 (2007) 1257-1265.

[105] D. Onichtchouk, Y. G. Chen, R. Dosch, V. Gawantka, H. Delius, J. Massague, and C. Niehrs, Silencing of TGF-beta signalling by the pseudoreceptor BAMBI, Nature 401 (1999) 480-485.

[106] T. A. Samad, A. Rebbapragada, E. Bell, Y. Zhang, Y. Sidis, S. J. Jeong, J. A. Campagna, S. Perusini, D. A. Fabrizio, A. L. Schneyer, H. Y. Lin, A. H. Brivanlou, L. Attisano, and C. J. Woolf, DRAGON, a bone morphogenetic protein co-receptor, J Biol Chem 280 (2005) 14122-14129.

[107] S. Itoh, F. Itoh, M. J. Goumans, and P. Ten Dijke, Signaling of transforming growth factor-beta family members through Smad proteins, Eur J Biochem 267 (2000) 6954-6967.

[108] T. Ebisawa, M. Fukuchi, G. Murakami, T. Chiba, K. Tanaka, T. Imamura, and K. Miyazono, Smurf1 interacts with transforming growth factor-beta type I receptor through Smad7 and induces receptor degradation, J Biol Chem 276 (2001) 12477-12480.

[109] P. Kavsak, R. K. Rasmussen, C. G. Causing, S. Bonni, H. Zhu, G. H. Thomsen, and J. L. Wrana, Smad7 binds to Smurf2 to form an E3 ubiquitin ligase that targets the TGF beta receptor for degradation, Mol Cell 6 (2000) 1365-1375.

[110] O. Avsian-Kretchmer, and A. J. Hsueh, Comparative genomic analysis of the eight-membered ring cystine knot-containing bone morphogenetic protein antagonists, Mol Endocrinol 18 (2004) 1-12.

[111] M. Yanagita, BMP antagonists: their roles in development and involvement in pathophysiology, Cytokine Growth Factor Rev 16 (2005) 309-317.

[112] J. Groppe, J. Greenwald, E. Wiater, J. Rodriguez-Leon, A. N. Economides, W. Kwiatkowski, K. Baban, M. Affolter, W. W. Vale, J. C. Izpisua Belmonte, and S. Choe, Structural basis of BMP signaling inhibition by Noggin, a novel twelve-membered cystine knot protein, J Bone Joint Surg Am 85-A Suppl 3 (2003) 52-58.

[113] K. Song, C. Krause, S. Shi, M. Patterson, R. Suto, L. Grgurevic, S. Vukicevic, M. van Dinther, D. Falb, P. Ten Dijke, and M. H. Alaoui-Ismaili, Identification of a key residue mediating bone morphogenetic protein (BMP)-6 resistance to noggin inhibition allows for engineered BMPs with superior agonist activity, J Biol Chem 285 12169-12180.

[114] P. ten Dijke, Bone morphogenetic protein signal transduction in bone, Curr Med Res Opin 22 Suppl 1 (2006) S7-11.

[115] B. L. Rosenzweig, T. Imamura, T. Okadome, G. N. Cox, H. Yamashita, P. ten Dijke, C. H. Heldin, and K. Miyazono, Cloning and characterization of a human type II

receptor for bone morphogenetic proteins, Proc Natl Acad Sci U S A 92 (1995) 7632-7636.

[116] B. B. Koenig, J. S. Cook, D. H. Wolsing, J. Ting, J. P. Tiesman, P. E. Correa, C. A. Olson, A. L. Pecquet, F. Ventura, R. A. Grant, and et al., Characterization and cloning of a receptor for BMP-2 and BMP-4 from NIH 3T3 cells, Mol Cell Biol 14 (1994) 5961-5974.

[117] P. ten Dijke, H. Yamashita, H. Ichijo, P. Franzen, M. Laiho, K. Miyazono, and C. H. Heldin, Characterization of type I receptors for transforming growth factor-beta and activin, Science 264 (1994) 101-104.

[118] K. Miyazono, S. Maeda, and T. Imamura, BMP receptor signaling: transcriptional targets, regulation of signals, and signaling cross-talk, Cytokine Growth Factor Rev 16 (2005) 251-263.

[119] M. Zhang, Y. Yan, Y. B. Lim, D. Tang, R. Xie, A. Chen, P. Tai, S. E. Harris, L. Xing, Y. X. Qin, and D. Chen, BMP-2 modulates beta-catenin signaling through stimulation of Lrp5 expression and inhibition of beta-TrCP expression in osteoblasts, J Cell Biochem 108 (2009) 896-905.

[120] N. Kamiya, L. Ye, T. Kobayashi, Y. Mochida, M. Yamauchi, H. M. Kronenberg, J. Q. Feng, and Y. Mishina, BMP signaling negatively regulates bone mass through sclerostin by inhibiting the canonical Wnt pathway, Development 135 (2008) 3801-3811.

[121] B. Chen, H. Lin, J. Wang, Y. Zhao, B. Wang, W. Zhao, W. Sun, and J. Dai, Homogeneous osteogenesis and bone regeneration by demineralized bone matrix loading with collagen-targeting bone morphogenetic protein-2, Biomaterials 28 (2007) 1027-1035.

[122] N. Dewulf, K. Verschueren, O. Lonnoy, A. Moren, S. Grimsby, K. Vande Spiegle, K. Miyazono, D. Huylebroeck, and P. Ten Dijke, Distinct spatial and temporal expression patterns of two type I receptors for bone morphogenetic proteins during mouse embryogenesis, Endocrinology 136 (1995) 2652-2663.

[123] Y. Ishidou, I. Kitajima, H. Obama, I. Maruyama, F. Murata, T. Imamura, N. Yamada, P. ten Dijke, K. Miyazono, and T. Sakou, Enhanced expression of type I receptors for bone morphogenetic proteins during bone formation, J Bone Miner Res 10 (1995) 1651-1659.

[124] M. Zhao, S. E. Harris, D. Horn, Z. Geng, R. Nishimura, G. R. Mundy, and D. Chen, Bone morphogenetic protein receptor signaling is necessary for normal murine postnatal bone formation, J Cell Biol 157 (2002) 1049-1060.

[125] P. B. Yu, H. Beppu, N. Kawai, E. Li, and K. D. Bloch, Bone morphogenetic protein (BMP) type II receptor deletion reveals BMP ligand-specific gain of signaling in pulmonary artery smooth muscle cells, J Biol Chem 280 (2005) 24443-24450.

Chapter 2

Specific aims

Autologous bone grafting has been the gold standard in repair of bone defects but the complications with donor sites have led to the use of alternatives as synthetic materials, xenogenic or allogeneic bone despite their inconsistent performance. Addition of growth factors like bone morphogenetic proteins (BMPs) to bone graft substitutes to improve bone formation has been extensively studied. However, there are still several problems for the clinical use of BMPs including high cost and inconsistent results. Despite the extensive research particularly with BMP-2, little is known about the extracellular regulators that promote BMP functions. Very recently, our laboratory has reported that biglycan (BGN) positively affects BMP-2 signaling through its binding to BMP-2 and its type I receptor, ALK6, resulting in enhanced osteoblast differentiation *in vitro*. The studies in this dissertation aim to elucidate more on the mechanisms by which BGN promote BMP function by analyzing the role of BGN GAGs vs. its core and by determining which domain is most promising as a future clinically useful BMP agonist. The following specific aims were pursued:

1. To determine the role of GAGs of BGN on BGN-assisted BMP-2 functions *in vitro* by utilizing a well recognized BMP-2 responsive cell system (i.e. C2C12 cells) and *in vivo* by utilizing a well established critical-sized rat mandible defect model.

2. To characterize the effect of BGN core protein on BMP-2 induced osteogenesis *in vivo* in a rat mandible model by μCT and histological analyses.

3. To determine the effect of BGN core protein domains on BMP-2 function *in vitro* and *in vivo*.

Chapter 3

Study I

Role of glycosaminoglycans of biglycan in bone morphogenetic protein-2 signaling

by Miguez PA, Terajima M, Nagaoka H, Mochida Y, Yamauchi M.

Abstract

Recently we have reported that biglycan (BGN) promotes osteoblast differentiation and that this function is due in part to its ability to positively modulate bone morphogenetic protein (BMP) functions. In this study we investigated the role of glycosaminoglycans (GAGs) of BGN in this function using *in vitro* and *in vivo* models. *Methods:* C2C12 myogenic cells were treated or untreated with BMP-2 alone or in combination with glycanated, partially glycanated or de-glycanated BGN, and the effects on BMP signaling and function were assessed by Smad1/5/8 phosphorylation and alkaline phosphatase (ALP) activity. Furthermore, the effect of de-glycanation of BGN on BMP-2 induced osteogenesis was investigated employing a rat mandible defect model. The defects were filled with collagen scaffolds loaded with glycanated, partially glycanated or de-glycanated BGN alone or in combination with a sub-optimal dose of BMP-2 (subBMP). *Results:* In *in vitro* experiments, BMP signaling and function were the greatest when BMP-2 was combined with de-glycanated BGN among the groups tested. In the rat mandible experiments, μCT analyses revealed that the newly formed bone was significantly increased only when subBMP was combined with de-glycanated BGN. *Conclusion:* The data indicate that the GAG component of BGN functions as a suppressor for the BGN-assisted BMP function.

Keywords: biglycan, BMP-2, C2C12 cells, Smad pathway, microcomputed tomography, osteogenesis

Introduction

Small leucine rich proteoglycans (SLRPs) are a large family of extracellular matrix proteins composed of a core protein that includes 10-20 leucine-rich repeats (LRRs) and covalently bound glycosaminoglycan chains (GAGs) [1, 2]. The latter are highly negative-charged polymers of repeating disaccharides. One of the key functions of SLRPs in the extracellular matrix is the modulation of growth factor functions through its core protein or GAG component. [3, 4]. Biglycan (BGN) is a multifunctional Class I SLRP member playing roles in collagen assembly [5, 6], regulation of inflammation by interacting with TLR 2 and 4 receptors [7, 8], binding and modulation of transforming growth factor (TGF)-β [3, 9] and bone morphogenetic protein (BMP)-2 and -4 functions [10, 11]. Previously, we have demonstrated that BGN promotes osteoblast differentiation, accelerates and increases matrix mineralization *in vitro*, and enhances the formation of a highly organized mineralized matrix *in vivo* [12]. These functions could be due to the capability of BGN to bind BMP-2/4 and their receptors [10, 11, 13]. However, the binding- and/or functional domains of BGN for its positive modulation of BMP functions are unknown. In this study, we investigated the role of GAGs of BGN in the BGN-assisted BMP-2 functions employing both *in vitro* and *in vivo* models.

Experimental procedures

Generation of partially glycanated, de-glycanated BGN and non-glycanated recombinant BGN

GAG containing BGN (glycanated) purified from bovine articular cartilage was commercially obtained (Sigma-Aldrich, St. Louis, MO), suspended in distilled water

(2μg/μl) and an aliquot (4μl) was treated with chondroitinase-ABC (C-ABC) (Seikagaku, Tokyo, Japan) overnight at 37°C [14]. Two concentrations of C-ABC, i.e. 0.3U and 0.1U/100μg of protein were used to generate de-glycanated or partially glycanated BGN. C-ABC alone, C-ABC treated and non-treated BGNs were subjected to 4-12% SDS-PAGE and stained with Coomassie brilliant blue R-250 (CBB, Bio-rad, Hercules, CA) to confirm the extent of de-glycanation of BGN.

Non-glycanated, glutathione S-transferase (GST)-fused BGN and GST-protein were generated in bacteria as previously described [11]. Briefly, the primer sequences of mouse *Bgn* cDNA corresponding to its mature core protein (amino acids 38-369; Asp38-Lys369) were designed as in Mochida *et al.,* 2006 [11]. The PCR products amplified were then ligated into pGEX4T-1 vector (GE Healthcare, Waukesha, WI), sequenced, and the plasmid harboring the mature *Bgn* cDNA (pGEX4T-1-*Bgn*) was obtained. The pGEX4T-1-*Bgn* or pGEX4T-1 empty vector was transformed into BL21-CodonPlus bacterial strain (Stratagene, La Jolla, CA), and GST-BGN or GST protein was synthesized. Supernatants of the bacterial lysates were incubated with glutathione-sepharose beads (Amersham Biosciences, Piscataway, NJ) and the eluted proteins were dialyzed against distilled water and lyophilized. The identity and purity of the proteins generated were confirmed on SDS-PAGE and Western blot (WB) analyses with anti-BGN polyclonal antibody LF-159 (generous gift from Dr. Larry W. Fisher at NIDCR, Bethesda, MD) and anti-GST antibody (Sigma)[11].

Alkaline phosphatase activity

The BMP function was assessed by the C2C12 cell assay system previously described [11, 15, 16]. The mouse C2C12 myoblastic cells were obtained from American Type Culture

Collection (ATCC, CRL-1772). Cells were maintained in Dulbecco's modified Eagle's medium (DMEM, Invitrogen, Carlsbad, CA) as described [11, 16]. C2C12 cells were untreated or treated with glycanated BGN (4μg), C-ABC alone, BMP-2 (R&D Systems, Minneapolis, MN) (150ng), BMP-2 + glycanated BGN or BMP-2 + C-ABC treated BGN (0.3U/100μg of protein) (de-glycanated). After 3 days of culture, the cell lysates were collected and subjected to Alkaline phosphatase (ALP) activity in the same manner as described [11, 16]. ALP assay was performed in triplicate and the values obtained were subjected to factorial analyses One-Way ANOVA and Tukey at 95% confidence interval using JMP 8.0 software (SAS, Charlotte, NC).

Smad phosphorylation assay

The effect of GAGs of BGN on BMP signaling was assessed by the extent of the Smad1/5/8 phosphorylation in C2C12 cells. BGN glycanated, partially glycanated and de-glycanated with BMP-2 (see above) were added to cell culture medium. Cell extracts were then applied to 4-12% SDS-PAGE followed by WB analyses with anti-phospho-Smad1/5/8 antibody (Cell Signaling, Danvers, MA) or anti-β actin antibody (Cell Signaling) for normalization.

To assess a possible effect of C-ABC on BMP signaling, two control groups were investigated for Smad phosphorylation: C-ABC + BMP-2 (150ng), and C-ABC + GST-BGN (non-glycanated) + BMP-2.

Effect of removal of GAGs of BGN in in vivo bone formation

The protocol of animal experiments was approved by the Institutional Animal Care and Use Committee (IACUC) at the University of North Carolina at Chapel Hill (IACUC ID: 09-

237.0). To investigate craniofacial bone regeneration using BGN and BMP, 5mm-critical-sized defects were generated in mandibles of sixteen Sprague-Dawley male breeder rats weighing ~525g [17-20]. According to Arosarena et al., 100ng of BMP-2 is considered as "sub-optimal" dose of BMP as defects exhibit minimal osteogenesis even after 8 weeks of healing [20]. Thus, this "sub-optimal" dose of BMP (subBMP) was used to evaluate the effect of BGN on BMP-induced bone formation. Briefly, all animals were given a pre-operative dose of antibiotic Cefazolin (10mg/kg). Anesthesia was achieved by Ketamine (80 mg/kg)/Xylazine (10 mg/kg). Two cm incisions were made along the inferior border of the hemi-mandibles and the masseter muscle and periosteum detached to expose the ramus. Using a 5mm-diameter trephine (Salvin Dental, Charlotte, NC), a critical-sized defect was placed at the ramus ~3mm above the lower border of the mandible and 2mm distal to the incisor root (Fig 3.3). The defects were unfilled or filled with a UV-cross-linked collagen sponge (Nitta Gelatin, Japan) as a scaffold. Each scaffold precut with a 5mm-diameter tissue punch (Miltex Incorporated, York, PA) was soaked uniformly in 10µl total solution of phosphate buffer saline containing the experimental protein groups. Control groups included: 1. unfilled, 2. collagen scaffold-filled with glycanated BGN, 3. collagen scaffold-filled with de-glycanated BGN [0.3U/100µg protein], and 4. C-ABC alone (a total of 4 control groups without any addition of subBMP). Treatment groups received the scaffold loaded with: 5. subBMP alone or combined with 6. glycanated BGN, 7. de-glycanated BGN, or 8. C-ABC (a total of 4 treatment groups). For each group, 2 rats were used. The muscle layer was tightly sutured with 5-0 chromic gut (Ethicon, Somerville, NJ) and the skin with 4-0 polypropylene suture (Ethicon) and the rats were maintained on a diet of soft rat chow (Harlan Taklad, Indianapolis, IN) and water for 4 days.

Microcomputed tomography

At 2 weeks post-surgery, all animals were euthanized, the mandibles were removed, fixed with 10% formalin for 3 days, and μCT scanning (Scanco Medical μCT 40, Bruttisellen, Switzerland) was performed. The X-ray parameters were 70kVp at 114uA with a 200ms integration time.

Image matrix size was 2048 x 2048 with acquired 2000 projections over a 360 degree rotation. A tube of 20.5mm diameter which allows a pixel size of 10μm was used. Acquisitions were made using a conebeam geometry and a Feldkamp filtered backprojection reconstruction algorithm used to create the reconstructions. All samples were positioned and scanned in a standard manner using an airtight cylindrical sample holder filled with PBS. For the analyses of the acquired images, the CTAn analyser software 1.9.1. (Skyscan, Kontich, Belgium) was used. The region of interest was selected in all images through a standardized drawing of the area within the defect borders. The region was first positioned in the middle of the surgical defect and it was then extended to all slices of the data set. A new drawing was done every 20 images. Quantitative morphometric analysis of the mineralized tissue inside the defects was carried out on voxels that corresponded to bone. After tomographic acquisitions, 3D images were reconstructed through direct volume rendering from the series of 2D projections.

Results

GAG removal enhances BGN-assisted BMP-2 function

For the removal of GAGs, glycanated BGN was treated with several concentrations of C-ABC and the release of the core protein was examined by SDS-PAGE. At the concentration

of 0.3U/100µg of protein (denoted as ++), the core protein (~45 kDa) was efficiently released (Fig 3.1A, lane 2) (also see below), which is consistent with the report by Matsuno et al., 2007[14]. The effects of glycanated and de-glycanated BGN on BMP-2 function were evaluated by ALP activity (Fig 3.1B). No treatment (lane 1) or treatment with BGN (lane 2) or C-ABC alone (lane 3) did not exert significant ALP activity. The BMP-2 induced ALP

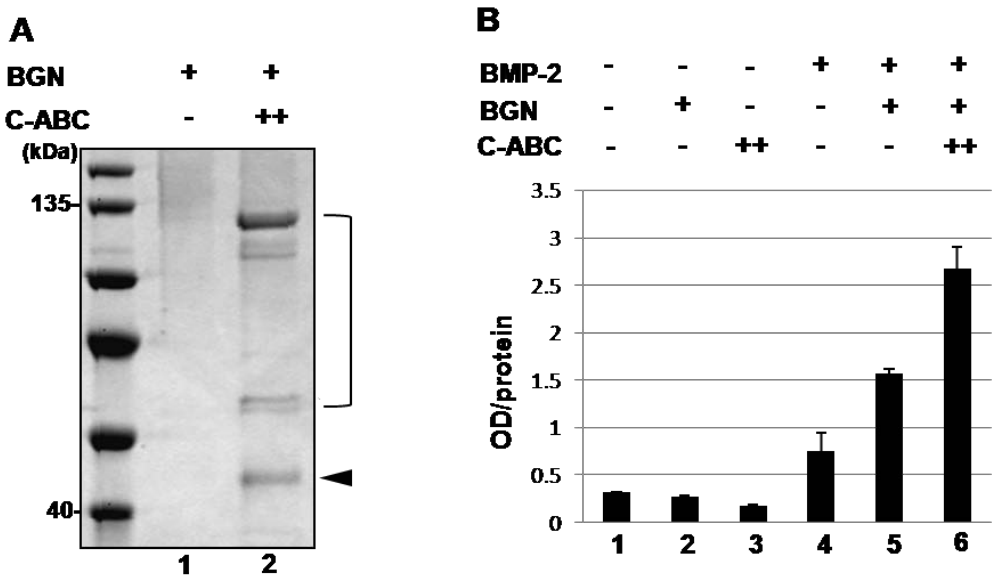

Figure 3.1. Generation of de-glycanated BGN and its effect on BMP-2 function. (A) SDS-PAGE of BGN without (lane 1) and with (lane 2) chondroitinase ABC (C-ABC) treatment. A bracket indicates C-ABC. An arrow head indicates the core protein of BGN. (B) ALP activity in C2C12 cells. Note that BMP-2 induced ALP activity is significantly increased by the addition of glycanated BGN (lane 5) but the effect is further enhanced by de-glycanation of BGN by C-ABC treatment (lane 6) ($p<0.05$). ++ of C-ABC: 0.3U/100µg, + for BGN and BMP-2 are 4µg and 150ng, respectively. *© Printed with permission from Elsevier. Miguez et al., Role of glycosaminoglycans of BGN in BMP-2 signaling. BBRC 2011; 405(2): 262-6.*

activity (lane 4) was significantly increased with the addition of glycanated BGN (lane 5), but the increase was further enhanced with de-glycanated BGN (lane 6) ($p<0.05$).

The levels of GAGs of BGN affect the enhancement of BGN-assisted BMP-2 signaling

Figure 3.2A shows BGN core protein band when it was untreated (lane 1) or treated with 0.3U/100 µg (++) (lane 2) or 0.1U/100 µg of C-ABC (+) (lane 3). As demonstrated, C-ABC treatment at a concentration of 0.3U/100 µg (++) was sufficient to generate a distinct BGN

core band at ~45kDa (lane 2) (de-glycanated). Use of higher concentrations of C-ABC did not change the level of core protein indicating that the BGN is likely fully de-glycanated with this concentration of C-ABC (data not shown). With a concentration of 0.1U/100 μg (+) the BGN core appeared as a smear band with a slightly higher molecular weight indicating that the GAGs were not fully removed (i.e. partially glycanated).

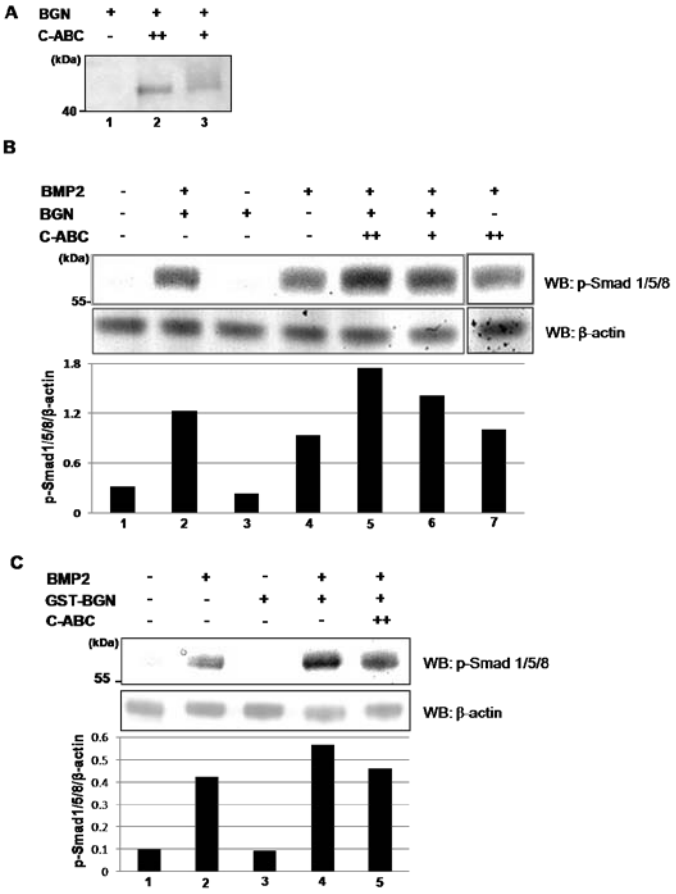

Figure 3.2. Effects of partially- and fully de-glycanated BGN on BMP-2 signaling. + of C-ABC: 0.1U/100μg of protein and ++: 0.3U/100μg of protein. + for BGN and BMP-2 are 4μg and 150ng, respectively. (A) BGN (glycanated) (lane 1), BGN treated with chondroitinase-ABC (C-ABC) at a concentration of ++ (lane 2) or + (lane 3). Note that only partial de-glycanation was achieved with the latter treatment. (B) Effects of glycanated, partially- (C-ABC +) and fully (++) de-glycanated BGN on BMP-2 signaling measured by Smad1/5/8 phosphorylation. BMP-2 induced signaling (lane 4) was increased by glycanated BGN (lane 2), and it was further enhanced by de-glycanation of BGN with C-ABC (lanes 5-6). Note that the fully de-glycanated BGN (lane 5) shows higher signaling compared to that of partially glycanated (lane 6). C-ABC alone with BMP (no BGN) did not enhance BMP signaling (lane 7). (C) Effect of C-ABC treatment on GST-BGN-enhanced BMP-2 signaling. C-ABC did not increase the effect of GST-BGN (lane 5). GST-BGN: glutathione S-transferase fused BGN.

Fig 3.2B shows the effects of de-glycanation of BGN on BMP-2 signaling assessed by Smad1/5/8 phosphorylation. Without treatment (lane 1) or treated with BGN alone (lane 3) C2C12 cells did not induce Smad phosphorylation. When glycanated BGN was added to BMP-2 (lane 2), the signaling level was increased when compared to that of BMP-2 alone (lane 4). This positive effect was further enhanced with de-glycanated BGN (lane 5), but the enhancement was decreased with partially glycanated BGN (lane 6). C-ABC alone did not affect the BMP-2 signaling (lane 7). The results indicate that though all BGN species exerted positive effects on BMP-2 signaling, the enhancement levels were inversely correlated with the level of GAGs. The positive effect of non-glycanated BGN was further confirmed by the use of recombinant GST-BGN (Fig 3.2C). The GST-BGN alone did not induce the BMP-2 signaling (lanes 1 and 3). The BMP-2 induced signaling (lane 2) was enhanced with the addition of GST-BGN (lane 4). Addition of C-ABC to (GST-BGN + BMP-2) did not increase the (GST-BGN + BMP-2) induced signaling (lane 5) confirming the lack of C-ABC effect on BMP-2 signaling (also see Fig 3.2B, lane 7). GST protein alone showed no effect as we previously reported [11].

De-glycanated BGN enhances BMP-2 induced osteogenesis

Figure 3.3 shows the representative 3D and 2D μCT images obtained from similar anatomical areas including the defects (indicated by dotted line) at the 2 week post-surgery. The graph at the bottom shows the bone volume (BV) of newly formed bone (NFB) in the defects. The NFB in the subBMP group (lane 1) was similar to those of control groups (i.e. empty, collagen scaffold alone or filled with glycanated or de-glycanated BGN, or C-ABC alone) (data not shown). When subBMP was combined with glycanated BGN (lane 2) or C-

ABC (lane 3), the newly formed bone was unchanged or slightly lower when compared to the group of subBMP alone. However, when de-glycanated BGN was combined with subBMP, the NFB volume was markedly increased (lane 4).

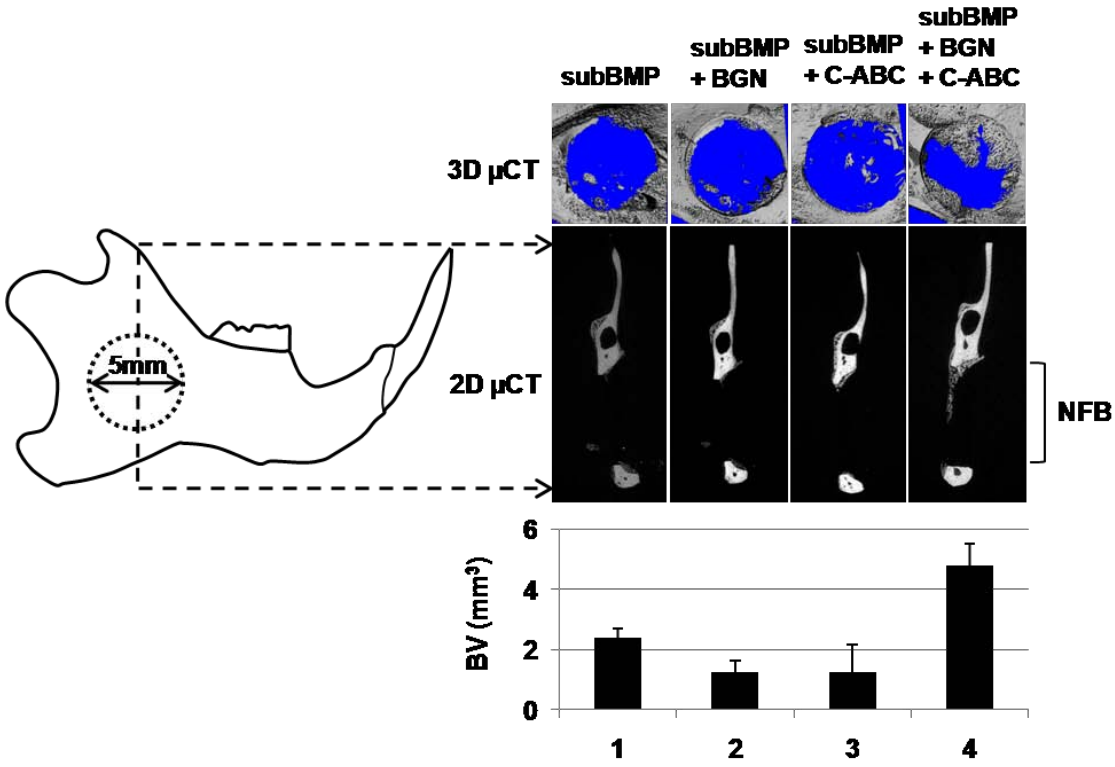

Figure 3.3. µCT images corresponding to the rat mandible 5mm-surgical defects at 2 weeks post-surgery. subBMP: sub-optimal BMP-2 (100ng), BGN:4µg. (A) Schematic representation of rat mandible and defect location on the left. On the right, top panel shows 3D µCT and lower panel 2D µCT views of the defects treated with subBMP dose without (lane 1) or in combination with BGN (glycanated) (lane 2), C-ABC (lane 3) or BGN/C-ABC (de-glycanated)(lane 4). Below, the median (represented by columns) and range (error bars) of bone volume (BV) of the newly formed bone (NFB) of 2 defects per group of treatment 2 weeks post-surgery. *© Printed with permission from Elsevier. Miguez et al., Role of glycosaminoglycans of BGN in BMP-2 signaling. BBRC 2011 405(2): 262-6.*

Discussion

BGN was originally found in the mineral-associated compartment of bone suggestive of its role in mineralization [21]. In addition, it has been reported that BGN is highly present in the areas of growth of skeletal tissues and the cell surface of both chondroblasts and osteoblasts,

suggesting its role in modulating the cellular activity [22]. The study reported by Chen et al., 2004 [10] was the first to propose a mechanism by which BGN could facilitate osteoblast functions. Independent of these studies, we have reported that BGN levels were "positively" correlated with the timing, extent and quality of matrix mineralization [12]. Also, Chen et al. and we further reported that BGN suppression resulted in poor response of osteoblastic cells to BMP [10, 12]. Furthermore, we demonstrated that BMP-induced ALP activity in C2C12 cells was synergistically increased with the exogenous addition of GST-BGN and that BGN bound to BMP-2 and its type I receptor, ALK6, and possibly other receptors [11].

In the present study, we explored the potential role of GAG component of BGN on the BGN-assisted BMP function. Our study demonstrated that de-glycanation of BGN with C-ABC treatment significantly enhances the BGN-assisted BMP-2 signaling and function. The partial removal of GAGs obtained with a low concentration of C-ABC (0.1U/100µg) showed that the enhancement was indeed less potent compared to that of fully de-glycanated BGN.

C-ABC alone did not potentiate BMP-2 signaling. In fact, an addition of C-ABC to GST-BGN rather tended to decrease the BMP-2 signaling (Fig 3.2C). C-ABC could cleave the GAGs of other proteoglycans present at the myoblastic cell surface and/or in the extracellular matrix in the cultures, which may affect BMP-2 signaling. Indeed, myoblasts are known to synthesize chondroitin sulfate (CS)/dermatan sulfate (DS) proteoglycans such as decorin and versican [23, 24]. Thus, higher doses of C-ABC (up to 4.0U/100µg) were also tested in combination with BMP-2, however, this caused even a further decrease in BMP-2 signaling (data not shown). This suggests that the positive effect of de-glycanation on BMP function is specific to BGN.

The mechanism by which the GAG component suppresses the BGN assisted BMP-2 function is not clear at this point. However, it is conceivable that the highly negative charged GAGs can sequester the basic protein, BMP-2, leading to reduced interaction between BGN core protein and BMP-2. During the preparation of this manuscript, a study was published on the effect of BGN on BMP-2 canonical and non-canonical pathways in MC3T3-E1 cells [25]. The authors found that glycanated BGN is able to increase the phosphorylation of ERK in addition to Smad 1/5/8. We have also investigated the effect of glycanated and de-glycanated BGN on ERK phosphorylation and found no effect in C2C12 cells (data not shown).

The *in vitro* ALP and Smad phosphorylation data (Fig 3.1B and 3.2B, respectively) unequivocally demonstrated that de-glycanation of BGN greatly increases the BGN-assisted BMP-2 function and signaling. A positive effect of de-glycanation of BGN on BMP-induced osteogenesis was also observed in the *in vivo* study, while glycanated BGN had no effect. For the results from *in vivo* study, a few possibilities should be considered. First, the glycanated BGN used in this study was purified from articular cartilage resulting as a protein with a mixture of CS and DS-GAGs (Sigma). The presence of those GAGs and the ratio of CS to DS in this sample could influence significantly BGN function as these disaccharides possess different affinity to calcium and hydroxyapatite (HAP)[26, 27]. Also, due to the increased structural flexibility, DS could function as an inhibitor of mineralization [28]. Second, is that BGN with GAGs may favor alternative interactions rather than with BMPs and/or its receptors. It has been reported that BGN highly interacts with macrophages stimulating secretion of pro-inflammatory molecules [7, 8], which could impair proper osteogenesis. Third, the release kinetics of glycanated vs. de-glycanated BGN from the collagen scaffold could be different. BGN has been found to weakly interact with collagen type I via both core

and GAGs [29]. However, if GAGs are present, the interaction is mainly through the disaccharides with a lower dissociation constant (K_d), i.e., stronger binding, than through core [30-32]. Thus, longer retention of glycanated BGN in the scaffold could have negatively affected the release of BGN to assist on BMP function. Further studies investigating the kinetics of (glycanated, de-glycanated) BGN release are warranted. However, it is clear that the removal of GAGs from BGN facilitates the BMP-2 induced osteogenesis *in vivo*, which is consistent with the *in vitro* data.

In conclusion, these *in vitro* and *in vivo* results strongly indicate that the BGN core protein is responsible for its function in promoting the BMP-2 functions and that the GAG component could function as a suppressor in this process. BGN core protein could be used in clinical settings to enhance BMP-2 induced bone formation after the optimal conditions *in vivo* are established. The rat mandible defect model described is feasible and appears to be appropriate for these future studies.

Bibliography

[1] L. W. Fisher, J. D. Termine, and M. F. Young, Deduced protein sequence of bone small proteoglycan I (biglycan) shows homology with proteoglycan II (decorin) and several nonconnective tissue proteins in a variety of species, J Biol Chem 264 (1989) 4571-4576.

[2] G. Stocker, H. E. Meyer, C. Wagener, and H. Greiling, Purification and N-terminal amino acid sequence of a chondroitin sulphate/dermatan sulphate proteoglycan isolated from intima/media preparations of human aorta, Biochem J 274 (Pt 2) (1991) 415-420.

[3] A. Hildebrand, M. Romaris, L. M. Rasmussen, D. Heinegard, D. R. Twardzik, W. A. Border, and E. Ruoslahti, Interaction of the small interstitial proteoglycans biglycan, decorin and fibromodulin with transforming growth factor beta, Biochem J 302 (Pt 2) (1994) 527-534.

[4] H. Kresse, H. Hausser, E. Schonherr, and K. Bittner, Biosynthesis and interactions of small chondroitin/dermatan sulphate proteoglycans, Eur J Clin Chem Clin Biochem 32 (1994) 259-264.

[5] R. L. Karvonen, F. Fernandez-Madrid, M. A. Lande, L. Hazlett, R. Barrett, T. An, and C. J. Huebner, Proteoglycans from osteoarthritic human articular cartilage influence type II collagen in vitro fibrillogenesis, Connect Tissue Res 27 (1992) 235-250.

[6] C. Wiberg, D. Heinegard, C. Wenglen, R. Timpl, and M. Morgelin, Biglycan organizes collagen VI into hexagonal-like networks resembling tissue structures, J Biol Chem 277 (2002) 49120-49126.

[7] A. Babelova, K. Moreth, W. Tsalastra-Greul, J. Zeng-Brouwers, O. Eickelberg, M. F. Young, P. Bruckner, J. Pfeilschifter, R. M. Schaefer, H. J. Grone, and L. Schaefer, Biglycan, a danger signal that activates the NLRP3 inflammasome via toll-like and P2X receptors, J Biol Chem 284 (2009) 24035-24048.

[8] L. Schaefer, A. Babelova, E. Kiss, H. J. Hausser, M. Baliova, M. Krzyzankova, G. Marsche, M. F. Young, D. Mihalik, M. Gotte, E. Malle, R. M. Schaefer, and H. J. Grone, The matrix component biglycan is proinflammatory and signals through Toll-like receptors 4 and 2 in macrophages, J Clin Invest 115 (2005) 2223-2233.

[9] Y. Bi, C. H. Stuelten, T. Kilts, S. Wadhwa, R. V. Iozzo, P. G. Robey, X. D. Chen, and M. F. Young, Extracellular matrix proteoglycans control the fate of bone marrow stromal cells, J Biol Chem 280 (2005) 30481-30489.

[10] X. D. Chen, L. W. Fisher, P. G. Robey, and M. F. Young, The small leucine-rich proteoglycan biglycan modulates BMP-4-induced osteoblast differentiation, Faseb J 18 (2004) 948-958.

[11] Y. Mochida, D. Parisuthiman, and M. Yamauchi, Biglycan is a positive modulator of BMP-2 induced osteoblast differentiation, Adv Exp Med Biol 585 (2006) 101-113.

[12] D. Parisuthiman, Y. Mochida, W. R. Duarte, and M. Yamauchi, Biglycan modulates osteoblast differentiation and matrix mineralization, J Bone Miner Res 20 (2005) 1878-1886.

[13] M. Moreno, R. Munoz, F. Aroca, M. Labarca, E. Brandan, and J. Larrain, Biglycan is a new extracellular component of the Chordin-BMP4 signaling pathway, Embo J 24 (2005) 1397-1405.

[14] Y. K. Matsuno, K. Yamada, A. Tanabe, M. Kinoshita, S. Z. Maruyama, Y. S. Osaka, T. Masuko, and K. Kakehi, Development of an apparatus for rapid release of oligosaccharides at the glycosaminoglycan-protein linkage region in chondroitin sulfate-type proteoglycans, Anal Biochem 362 (2007) 245-257.

[15] T. Katagiri, A. Yamaguchi, M. Komaki, E. Abe, N. Takahashi, T. Ikeda, V. Rosen, J. M. Wozney, A. Fujisawa-Sehara, and T. Suda, Bone morphogenetic protein-2 converts the differentiation pathway of C2C12 myoblasts into the osteoblast lineage, J Cell Biol 127 (1994) 1755-1766.

[16] M. Kaku, Y. Mochida, P. Atsawasuwan, D. Parisuthiman, and M. Yamauchi, Post-translational modifications of collagen upon BMP-induced osteoblast differentiation, Biochem Biophys Res Commun 359 (2007) 463-468.

[17] G. Zellin, and A. Linde, Importance of delivery systems for growth-stimulatory factors in combination with osteopromotive membranes. An experimental study using rhBMP-2 in rat mandibular defects, J Biomed Mater Res 35 (1997) 181-190.

[18] O. A. Arosarena, A. Falk, L. Malmgren, L. Bookman, M. J. Allen, J. Schoonmaker, S. Tatum, and R. Kellman, Defect repair in the rat mandible with bone morphogenic proteins and marrow cells, Arch Facial Plast Surg 5 (2003) 103-108.

[19] O. A. Arosarena, and W. L. Collins, Bone regeneration in the rat mandible with bone morphogenetic protein-2: a comparison of two carriers, Otolaryngol Head Neck Surg 132 (2005) 592-597.

[20] O. Arosarena, and W. Collins, Comparison of BMP-2 and -4 for rat mandibular bone regeneration at various doses, Orthod Craniofac Res 8 (2005) 267-276.

[21] L. W. Fisher, G. R. Hawkins, N. Tuross, and J. D. Termine, Purification and partial characterization of small proteoglycans I and II, bone sialoproteins I and II, and osteonectin from the mineral compartment of developing human bone, J Biol Chem 262 (1987) 9702-9708.

[22] P. Bianco, L. W. Fisher, M. F. Young, J. D. Termine, and P. G. Robey, Expression and localization of the two small proteoglycans biglycan and decorin in developing human skeletal and non-skeletal tissues, J Histochem Cytochem 38 (1990) 1549-1563.

[23] E. Balint, D. Lapointe, H. Drissi, C. van der Meijden, D. W. Young, A. J. van Wijnen, J. L. Stein, G. S. Stein, and J. B. Lian, Phenotype discovery by gene expression profiling: mapping of biological processes linked to BMP-2-mediated osteoblast differentiation, J Cell Biochem 89 (2003) 401-426.

[24] J. C. Casar, B. A. McKechnie, J. R. Fallon, M. F. Young, and E. Brandan, Transient up-regulation of biglycan during skeletal muscle regeneration: delayed fiber growth along with decorin increase in biglycan-deficient mice, Dev Biol 268 (2004) 358-371.

[25] X. Wang, K. Harimoto, S. Xie, H. Cheng, J. Liu, and Z. Wang, Matrix protein biglycan induces osteoblast differentiation through extracellular signal-regulated kinase and Smad pathways, Biol Pharm Bull 33 1891-1897.

[26] C. C. Chen, and A. L. Boskey, Mechanisms of proteoglycan inhibition of hydroxyapatite growth, Calcif Tissue Int 37 (1985) 395-400.

[27] A. L. Boskey, L. Spevak, S. B. Doty, and L. Rosenberg, Effects of bone CS-proteoglycans, DS-decorin, and DS-biglycan on hydroxyapatite formation in a gelatin gel, Calcif Tissue Int 61 (1997) 298-305.

[28] B. Casu, M. Petitou, M. Provasoli, and P. Sinay, Conformational flexibility: a new concept for explaining binding and biological properties of iduronic acid-containing glycosaminoglycans, Trends Biochem Sci 13 (1988) 221-225.

[29] E. Schonherr, P. Witsch-Prehm, B. Harrach, H. Robenek, J. Rauterberg, and H. Kresse, Interaction of biglycan with type I collagen, J Biol Chem 270 (1995) 2776-2783.

[30] M. Raspanti, M. Viola, A. Forlino, R. Tenni, C. Gruppi, and M. E. Tira, Glycosaminoglycans show a specific periodic interaction with type I collagen fibrils, J Struct Biol 164 (2008) 134-139.

[31] R. V. Sugars, A. M. Milan, J. O. Brown, R. J. Waddington, R. C. Hall, and G. Embery, Molecular interaction of recombinant decorin and biglycan with type I collagen influences crystal growth, Connect Tissue Res 44 Suppl 1 (2003) 189-195.

[32] G. Pogany, D. J. Hernandez, and K. G. Vogel, The in vitro interaction of proteoglycans with type I collagen is modulated by phosphate, Arch Biochem Biophys 313 (1994) 102-111.

Chapter 4

Study II

Characterization of biglycan-assisted bone morphogenetic protein-2 induced osteogenesis *in vivo*

by Miguez PA, Terajima M, Nagaoka H, Ferreira J, Ko CC, Yamauchi M.

Abstract

In the previous study, we established that the positive effect of biglycan (BGN) on bone morphogenetic protein-2 (BMP-2) function was due to the core protein and that the glycosaminoglycan (GAG) component functions as a negative regulator (Study I). Thus, in this study, we generated glutathione-S-transferase (GST)-fused recombinant BGN (GST-BGN) that lacks GAGs and tested its effect on BMP-2 function *in vitro* and *in vivo*. *Methods:* The effects of GST-BGN on BMP-2 function *in vitro* were evaluated using the myogenic C2C12 cells. After incubation with BMP-2 with and without GST-BGN, the cell lysates were analyzed for Smad1/5/8, β-catenin and ERK 1/2 phosphorylation and alkaline phosphatase (ALP) activity. *In vivo*, five-mm critical-size defects were generated in the hemimandibles of mature Sprague-Dawley rats. Control groups were unfilled or filled with a cross-linked collagen sponge alone or with GST or GST-BGN alone. Treatment groups received the collagen sponge with: suboptimal (subBMP/0.1μg) and optimal (optBMP/1μg) concentrations of BMP-2; and various doses of GST-BGN with subBMP. At 2 weeks post-surgery, the newly formed bone (NFB) in the defects was evaluated by μCT and histological analyses. *Results:* By C2C12 cell system assay, BMP-2 induced *p*-Smad 1/5/8 and ALP activity were enhanced by GST-BGN. *In vivo*, μCT and histological analyses showed little NFB in the controls, subBMP and (subBMP + 2μg of GST-BGN) groups. The optBMP group showed significant amounts of NFB that was ectopically formed. The greatest amounts of NFB that was associated with the collagen sponge were seen with subBMP + 4 and 8 μg of GST-BGN. The analyses employing μCT, Masson's trichrome and picrosirius red (PSR) staining suggested that the (subBMP + GST-BGN) groups may exhibit less porous, more compact and organized bone matrix when compared to optBMP. Wnt signaling was

significantly upregulated in BGN-treated rats at 2 weeks. OptBMP NFB seemed to have the highest turnover as per presence of TRAP positive cells and green/orange PSR pattern. *Conclusion:* These data indicate that GST-BGN predictably promotes the BMP osteogenic function *in vitro* and *in vivo* without compromising the matrix quality.

Keywords: biglycan, BMP-2, Smad 1/5/8, osteogenesis, β-catenin, Wnt

Introduction

Craniofacial bone defects of congenital and/or acquired origin, e.g. age-associated bone loss, cleft palate and lip, periodontal disease, odontogenic tumors, etc, are a major health threat to our society directly affecting the quality and length of life. Today, more than 500,000 bone grafting operations are performed annually in the US in an attempt to regenerate bone in the orofacial area alone [1]. Autograft has been the gold standard, but the morbidity and the requirements of a large quantity of bone and the second surgical sites are of significant problems. Allografts may provoke immune rejection and alloplastic bone substitutes generally exhibit poor (or no) bone integration and bone induction [2, 3]. To resolve these problems, an approach of "tissue engineering" consisting of a biocompatible scaffold, osteogenic growth factors such as bone morphogenetic proteins (BMPs) and stem cells, has been developed [4-6]. The clinical use of BMPs combined with various scaffolds is promising but still faces serious limitations, e.g. high cost, requirement of high quantities of BMP, difficulties to retain BMP in situ, etc.

Recently, we have shown that BGN is a potent positive modulator of BMP function and increases osteoblast differentiation and mineralization [7]. Most recently, we also have established that this function is exerted primarily through BGN core protein and that the glycosaminoglycan (GAG) component of BGN functions as a suppressor (see Chapter 3, study I and Miguez *et al.*, 2011[8]). In this study we further investigated the effect of recombinant BGN (devoid of GAGs), i.e. glutathione-S-transferase (GST)-fused BGN (GST-BGN), on BMP signaling and functions by C2C12 cell assay system. In addition, we investigated the efficacy of several doses of GST-BGN on BMP-2 function *in vitro* and *in*

vivo by using several doses of BGN. For *in vivo*, we tomographically and histologically characterized the newly formed bone (NFB) in a rat mandible model by means of bone volume, collagen organization, osteoclastic activity and BMP signaling.

Experimental Procedures

Cell line and culture conditions

C2C12 cells were cultured as previously described by Mochida *et al*., 2006 [9]. Briefly, cells were purchased from American Type Culture Collection (ATCC, cat# CRL1772). Cells were grown in DMEM (Invitrogen, Carlsbad, CA) with high glucose (4.5g/l) containing 15% FBS (Invitrogen) and supplemented with 100 U/ml of penicillin G sodium and 100 µg/ml streptomycin sulfate. Cells were cultured at 5% CO_2 atmosphere at 37˚C and the medium was changed twice a week.

Generation of recombinant BGN and verification of effect on BMP-2 function

The generation and purification of recombinant BGN in E. coli system fused with glutathione-S-transferase tag (GST-BGN) has been previously published by Mochida *et al*., 2006 [9] and briefly described in Chapter 3, Study I [8] . After purification, the purity of GST-BGN was assessed by SDS-PAGE stained with Coomassie Brilliant Blue (CBB, Bio-rad, Hercules, CA) and Western blot (WB) with anti-GST (Sigma) antibody. The effect of GST-BGN on BMP-2 function was confirmed by ALP activity as described [9]. The dose-effect of GST-BGN on BMP-2 signaling was evaluated by adding 2, 4 or 8 µg of GST-BGN

combined with BMP-2 to C2C12 cells followed by the measurement of phosphorylation of Smad 1/5/8.

Smad 1/5/8, β-catenin and ERK 1/2 phosphorylation

The effect of GST-BGN on canonical (Smad) and non-Smad BMP-2 signaling pathways was assessed by the phosphorylation of Smad1/5/8, β-catenin and ERK 1/2 in C2C12 cells. Briefly, 4 μg of GST-BGN and 150 ng of BMP-2 (R&D, Minneapolis, MN) were added to the cell culture medium. Cell extracts were then applied to 4-12% SDS-PAGE followed by WB analyses with anti-phospho (*p*)-Smad1/5/8 (Cell Signaling, Danvers, MA), anti-*p*-β-catenin antibody (Cell Signaling) or anti-*p*-ERK 1/2 (Cell Signaling). The levels of *p*Smad1/5/8 and *p*Erk1/2 were normalized to β actin (Cell Signaling), and *p*-β-catenin to total β-catenin (Cell Signaling). These experiments were performed in duplicate.

Surgical procedure and euthanasia

The surgical procedures were carried out in the same manner as described in Chapter 3, Study I [8]. For this study, 18 rats were used (2/group). As stated above, according to Arosarena *et al*. [10], 100ng of BMP-2 is considered a "sub-optimal" dose of BMP as defects exhibit minimal osteogenesis even after 8 weeks of healing. In this same study, the authors concluded that 1 μg was an "optimal" dose to promote accelerated and increased bone regeneration of the mandible, completely closing the defect in as early as 2 weeks. Thus, this "sub-optimal" dose of BMP (subBMP) was used to evaluate the effect of GST-BGN doses on BMP-induced bone formation. The "optimal" dose of BMP (optBMP) was used as a means of comparison of the amount and quality of bone formed with and without BGN assistance. Control groups included: 1. unfilled defect, 2. collagen scaffold alone, 3. collagen scaffold-

filled with GST-BGN or GST-protein alone (a total of 4 control groups without any addition of subBMP). Treatment groups received the scaffold loaded with: 4. subBMP alone or combined with 5. 2 μg of GST-BGN, 6. 4μg of GST-BGN, or 7. 8 μg of GST-BGN and 9. optBMP (a total of 5 treatment groups). For each group, 2 rats were used. Rats were euthanized after 2 weeks of surgery.

Microcomputed tomography

The handling of the mandibles after euthanasia and μCT specifications and procedures were described in Chapter 3, Study I [8].

Measurement of bone volume and porosity

Bone volume (BV) and porosity were measured by selecting the region of interest in all images through a standardized drawing of the area within the defect borders as described above. The region was first positioned in the middle of the surgical defect and it was then extended to all slices of the data set. A new drawing was done every 20 images. The scans were converted into a binary image and bone volume was determined by dividing BV/ total area (TA). Results are reported as the median (columns) and the range (error bars) of the NFB in two defects per group. For the calculation of bone volume and porosity, a threshold of 850mg/cm3 was considered optimal for the distinction of the NFB. The percentage of porosity was computed by dividing the bone area (recognized by the computer/software based on the threshold established) by section area x 100 [11].

Histological preparations and analyses

The rats mandibles were harvested 2 weeks after the surgery, and after μCT measurements they were fixed in 10% buffered formalin (Sigma-Aldrich, St. Louis, MO), part of the soft tissues were removed and they were demineralized in 0.5 M EDTA (Fisher Scientific, Waltham, MA), pH 7.4 for 8 weeks. The samples were dehydrated in several ascending gradations of ethanol (50-100%), soaked in xylene and embedded in paraffin. Several sections from each mandible paraffin block were cut by using a microtome Leica Jung RM2045. Several sections were cut from each mandible within the middle of the 5mm defect and three sections were chosen for staining by each of several histological protocols. Sections were stained by Masson's trichrome [12] for histomorphometry, by Picrosirius red staining (PSR) [13, 14] for collagen organization, by immunohistochemistry (IHC) for bone sialoprotein (BSP) (Cell Signaling), *p*-Smad 1/5/8 (Cell Signaling), *p*-*β*-catenin (Cell Signaling), and *p*-ERK 1/2 (Cell Signaling) and by TRAP [15]. Sections were observed with a light microscope Olympus BX40 (with polarized light for PSR) at 4x to 40x magnification. High magnification images were taken from NFB immediately adjacent to the native bone for PSR and Smad, representative areas for TRAP and adjacent to the NFB and middle of the defect for BSP and β-Catenin. For histomorphometric analyses, the total area (TA) of the defect was outlined in two representative mid sections of Masson's trichrome staining from each rat within each group of treatment (n=4). The areas of interest (NFB) within the defects (TA) were outlined by using Image J software drawing tools. The histological bone area (BA) of NFB was calculated as NFB/TA. Image J is an image measurement software freely available from NIH.

Results

Effect of GST-BGN on BMP signaling and function in vitro

As shown in Fig 4.1A, both SDS-PAGE and WB analyses for the newly generated GST-BGN and GST showed the single bands at the expected migration positions at ~70 (45 kDa

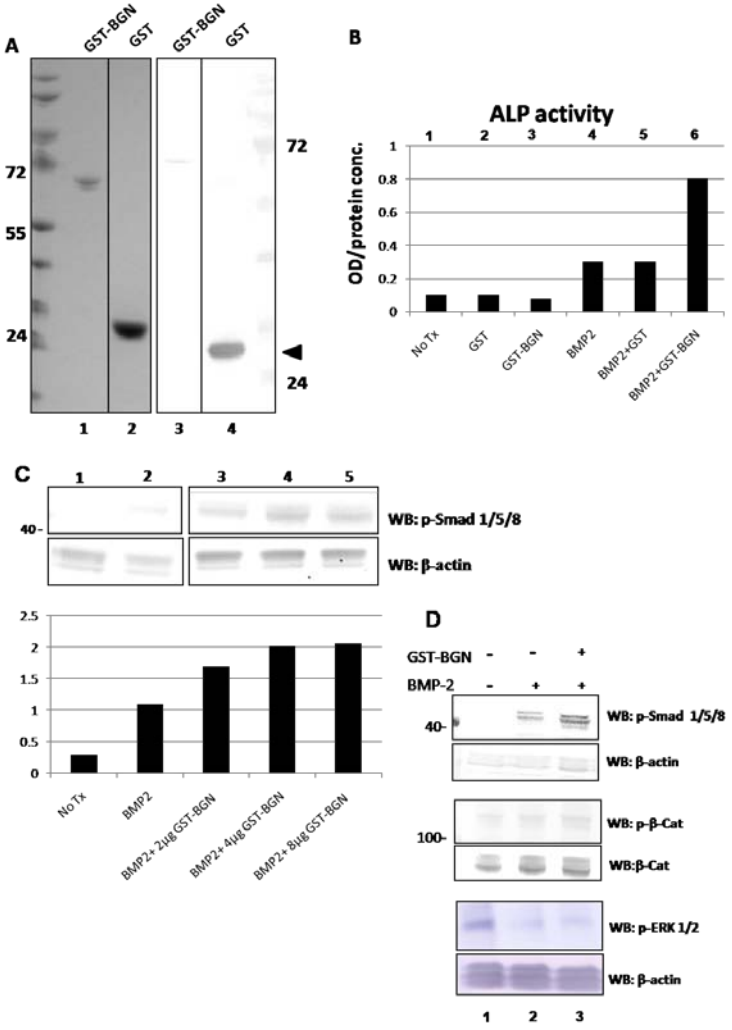

Fig 4.1. A. Purity of GST-BGN and GST-protein by SDS-PAGE and WB (anti-GST). B. GST-BGN shows about 70kDA and GST about 25kDA. B. ALP activity demonstrating that BMP-2 (lane 4) has increased ALP compared to controls (no treatment (Tx) (lane1), GST (lane 2) and GST-BGN (lane 3). BMP2 + GST (lane 5) has similar ALP to BMP-2 alone. GST-BGN significantly increased BMP-2 induced ALP activity in C2C12 cells (lane 6). C. Dose dependent effect of GST-BGN on BMP-2 signaling. 2μg of GST-BGN significantly increased phosphorylation of Smad 1/5/8 (lane 3). 4μg of GST-BGN further increased signaling (lane 4) but 8μg did not further enhanced the effect. D. Signaling pathways upon BMP-2 and BMP-2 + 4 μg GST-BGN. Upper panel shows GST-BGN significantly enhanced BMP-2 induced Smad phosphorylation (lane 3). Middle panel shows no significant increase in phosphorylated β-catenin with any of the treatments. Lower panel shows that BMP-2 reduced *p*-Erk 1/2 (lane 2) and addition of GST-BGN did not alter that signaling pattern (lane 3).

BGN core + 25 kDa GST) (lanes 1, 3) and 25 kDa (lanes 2 and 4), respectively, thus, confirming the purity. The positive effect of GST-BGN addition on BMP-2 induced ALP activity was also confirmed (Fig 4.1B). The effect on BMP-2 signaling was analyzed by Smad 1/5/8 phosphorylation and shown in Fig 4.1C. The phosphorylation was induced with BMP-2 (lane 1, 2) and it was enhanced with the addition of 2 μg of GST-BGN (lane 3). The signaling was further intensified with 4 μg of GST-BGN (lane 4) and stayed that level with 8 μg (lane 5).

Figure 4.1D shows the comparison of Smad and non-Smad signaling in C2C12 cells induced by BMP-2 with and without 4 μg of GST-BGN. Smad 1/5/8 phosphorylation was enhanced by GST-BGN in BMP-2 treated C2C12 cells (upper panel). However, β-catenin phosphorylation did not significantly change with BMP-2 with or without GST-BGN (middle panel, lane 2). Erk 1/2 phosphorylation was clearly reduced with BMP-2 (lane 2) and the addition of GST-BGN (lane 3) had no significant effect.

Tomographic bone volume (BV) and porosity of the newly formed bone (NFB) in the rat mandibles treated with BMP-2 or BMP-2 combined with GST-BGN

Figure 4.2 shows the representative 3D (upper panel) and 2D (middle panel) μCT images obtained at 2 weeks post-surgery. Lower panel shows quantification of bone volume (BV). The BV values of control groups, i.e. unfilled, scaffold alone, scaffold + GST, scaffold + GST-BGN (not shown) were all slightly lower than that of subBMP (lane 1). Compared to these groups, the levels of NFB were significantly higher in the optBMP (lane 2). However, the bone formed by optBMP appeared to be mainly ectopic in nature, not filling the defect area and quantification of BV showed that NFB occupied less than 80% of the defect area.

Incorporation of 2µg of GST-BGN into the scaffold in combination with subBMP-2 (lane 3) did not significantly enhance bone formation compared to subBMP-2 alone. When subBMP was combined with 4 and 8µg of GST-BGN, a significant increase in bone formation was

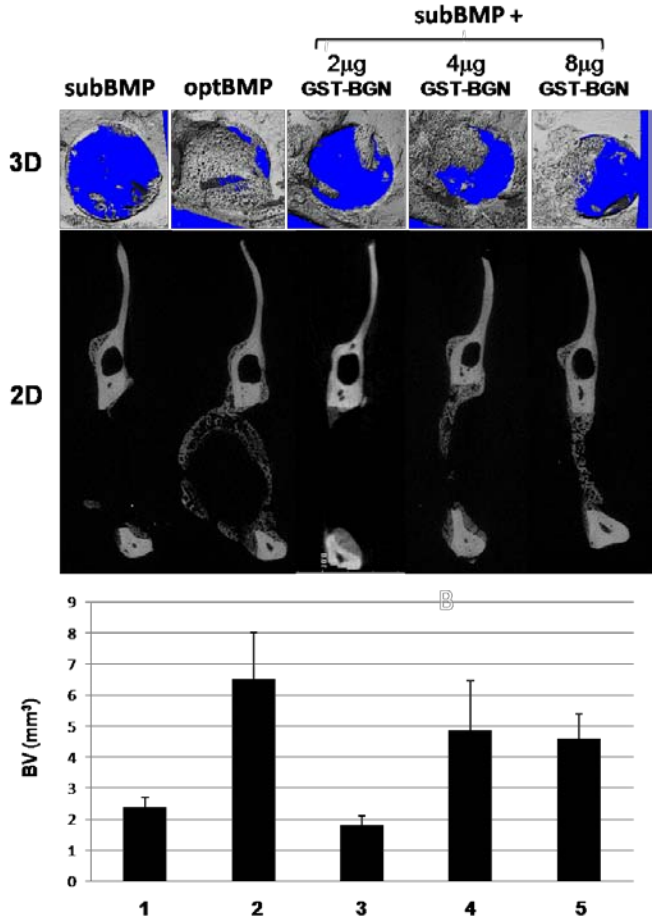

Fig 4.2. µCT analyses of the rat mandibles showing 3D (upper panel) and 2D (middle panel) views of the mandibles. Lower panel shows the bone volume (BV) quantitated by CT. Note that optBMP (lane 2) shows tendency of greater BV, however, it is of ectopic nature. SubBMP + GST-BGN show defects filled with newly formed bone (NFB) within the boundaries of the defect (lane 4 and 5).

achieved (lane 4 and 5, respectively).

Porosity calculated by the µCT software CTan Analyzer (Skyscan, Kontich, Belgium) within the NFB in the defect boundaries showed that subBMP and optBMP groups had 30% and 53% porosity, respectively. The subBMP + GST-BGN groups showed similar porosity for all three groups averaging 25% [11].

Histological evaluation

Masson's trichrome staining

Trichrome staining shows in blue color the collagen rich tissues either represented by native or newly formed bone or by fibrous tissue present between the defect borders. Fibrotic tissue shows loose fibers lightly stained in blue with no recognizable bony architecture (i.e. lamellar or trabecular structure). Muscle is stained in red. In figure 4.3, for easy of identification the edge of NFB is delineated by dotted yellow line and the native bone by

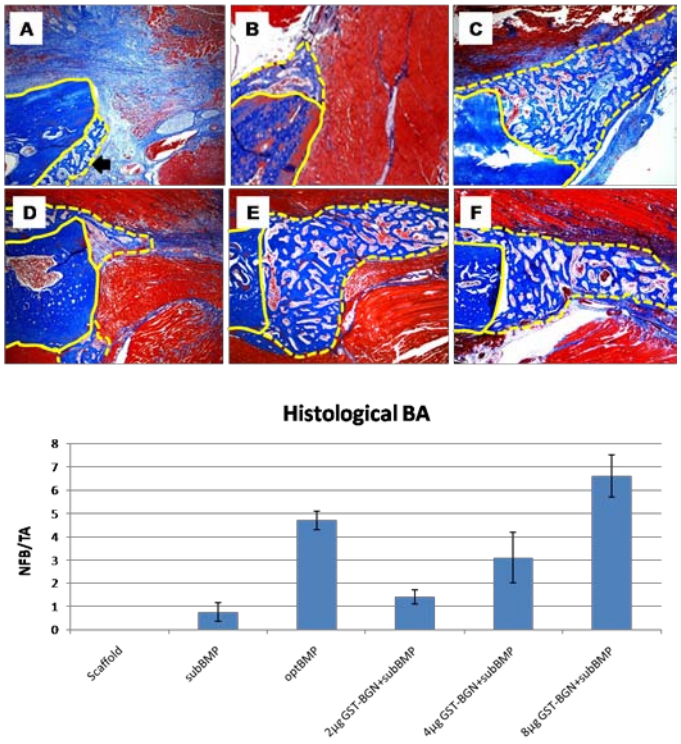

Fig 4.3. Masson's trichrome staining and histological calculation of bone area (BA). A. scaffold alone. Arrow: newly formed bone (NFB) due to periosteum release, B. subBMP, C. optBMP. D. subBMP + 2µg GST-BGN, E. subBMP + 4µg of GST-BGN, F. subBMP + 8µg of GST-BGN. Yellow solid line around native bone. Yellow dotted line around NFB. Lower graph shows quantification of BA (NFB/TA) by Image J within the defect area of 2 rats per group. Bars are medians and error bars are variations. subBMP: suboptimal dose of BMP-2/100 ng, optBMP: optimal dose: BMP-2/ 1µg.

solid line. The presence of NFB as a result of periosteum release around native bone was evident in all samples as shown by an arrow in the scaffold alone group (Fig 4.3A). The other

control groups showed minimal bone formed at the edge of the defect (not shown). SubBMP group showed a small and compact NFB (Fig 4.3B). OptBMP group showed a much greater amount of NFB compared to subBMP (Fig 4.3C). However, in both rats of this group, the pattern of osteogenesis was ectopic with bone formed outside of the defect area, i.e. (within muscle). Fig 4.3D, E and F show the images obtained from the subBMP groups combined with 2, 4 and 8 μg of GST-BGN, respectively. While NFB did not change with the addition of 2μg of GST-BGN (Fig 4.3D), it was significantly increased with 4μg of GST-BGN (Fig 4.3E) and further enhanced with 8 μg of GST-BGN (Fig 4.3F). These changes were confirmed by histomorphometric analyses (lower panel of Fig 4.3). No cartilage-like tissues (based on morphology) were found in any of the samples.

BSP

Among the non-collagenous proteins investigated as markers of osteoblast differentiation some are also involved in calcification of bones (i.e. osteonectin, osteopontin, BSP and osteocalcin). BSP has been mostly attributed to deposit of calcium and regulation of HAP crystal growth just before mineralization (see review [16]. BSP is involved in upregulation of Cbfa1 and ALP activity in osteoblasts *in vitro* as well as in critical-sized defects in calvaria, thus, its presence may indicate continuous stimulation of osteoblast differentiation in *in vivo* models [17-19]. Immunohistochemical staining for BSP showed no significant immunostaining within the defect area in the control groups (data not shown). The subBMP group had some immunoreactivity around the NFB bone (dotted line) but mostly undetectable in the middle of the defect (between continuous lines) (Fig 4 A, B). The optBMP groups showed significant immunoreactivity around the NFB (dotted lines, Fig

4.4C) as well as in the mid-area where mineralization was still not evident (Fig 4.4D). The (2 µg of recombinant BGN + subBMP) group showed more immunoreactivity compared to subBMP alone (Fig 4.4E, F). With increasing doses of GST-BGN, the immunoreactivity for BSP was proportionally stronger (Fig 4.4G, H, I, J). The highest dose of BGN with subBMP showed intense, patch-like staining for BSP in the non-mineralized areas (Fig 4.4I, J)

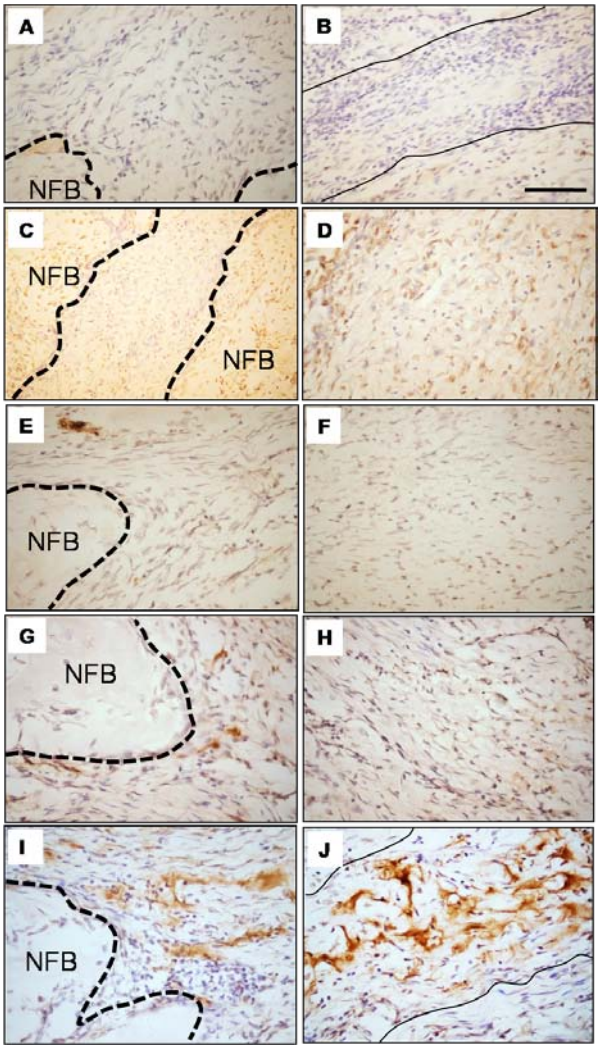

Figure 4.4. Bone sialoprotein (BSP) in the rat mandibles. A. subBMP group showing minor amounts of BSP adjacent to newly formed bone (NFB) (dotted line). B. No significant reactivity in the middle of the defect (main stream of the defect is delineated with solid line). C. optBMP group with BSP present within and adjacent to NFB. D. Significant immunoreactivity for BSP present within non mineralized areas. E. subBMP + 2 µg of GST-BGN group with BSP adjacent to NFB (dotted line). F. Immunoreactivity also present in the middle of the defect. G. subBMP + 4µg GST-BGN group with stronger BSP expression compared to subBMP alone (A), adjacent to NFB. H. Immunoreactivity strongly present in the middle of the defect. I. subBMP + 8µg group with BSP found adjacent to NFB (dotted line). J. BSP is found highly present in the middle of the defect. Scale bar is 200µm on B.

possibly indicative of concentrated deposition of BSP which could indicate faster mineralization compared to other groups. This was present for both sections in both rats for this group.

Picrosirius red (PSR) staining

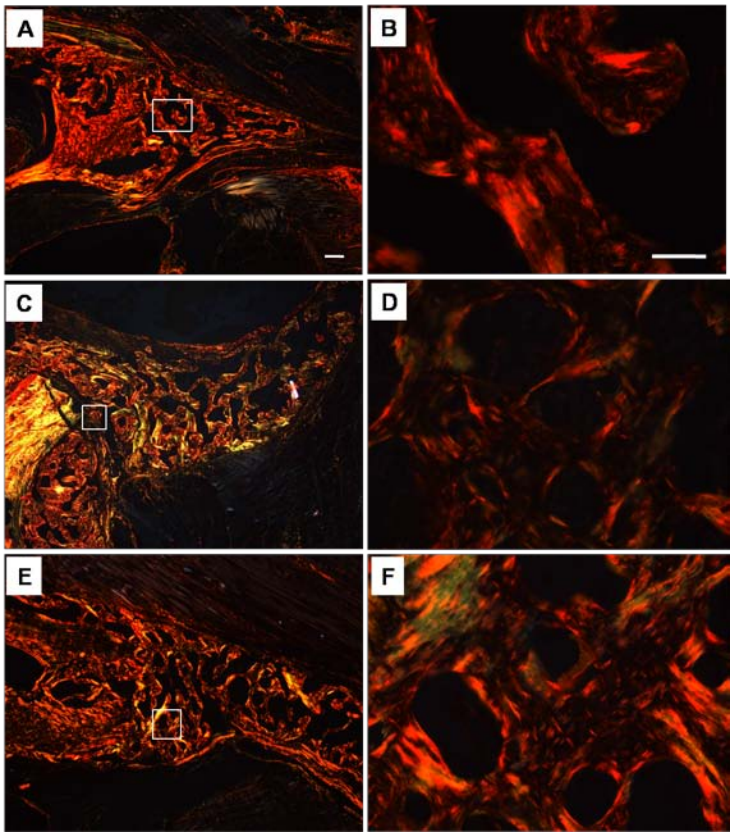

Fig 4.5. Picrosirius red (PSR) staining of rat mandibles. SubBMP group appears with red collagen fibers. B. High magnification of boxed area. C. optBMP group appears with green/yellow to orange collagen fibers. D. High magnification of boxed area. E. subBMP + 8µg GST-BGN group showing yellow to red collagen fibers in the NFB area. F. High magnification of the boxed area. Scale bar on A is 500µm and on B is 200µm.

The organization and maturation of fibrillar collagen matrices in the controls and treatment groups were assessed by PSR staining and shown in Fig 4.5. The collagen matrix in the defects in controls, thus non-mineralized, were thin and not visible under polarized light (data not shown). As shown in Figure 4.5A and B, the collagen matrix of the NFB in the

subBMP group was organized, mature and thick, as indicated by the intense red staining of the collagen fibers. On the other hand, the NFB of optBMP group showed faint orange to red color with patches of green color indicating that the collagen matrix is less mature and less organized (4.5C, D). The subBMP + 2µg group showed similar appearance to controls with very faint collagen staining except for the periosteum-induced NFB (not shown). SubBMP + 4µg GST-BGN appeared similar to optBMP in organization (not shown) but higher dose of GST-BGN seemed to have slightly more red and compact collagen fibers (4.5E, F). The major difference between 4 and 8 µg was the presence of patches of collagen fibers in the latter but not in the former. Nonetheless, the use of GST-BGN did not seem to disturb collagen organization as did optBMP.

TRAP

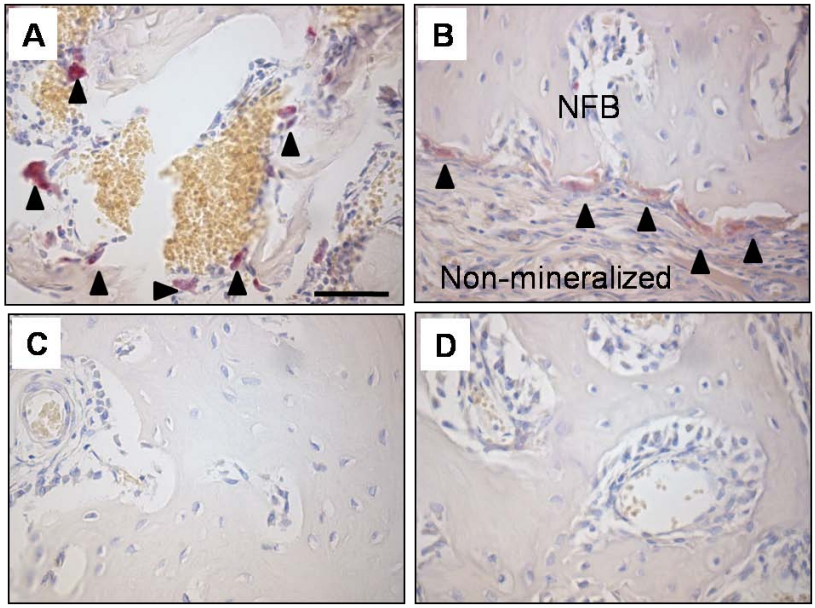

Fig 4.6. TRAP staining for osteoclastic activity in the rat mandibles. Trap positive sections were found for both rats treated with optBMP dose (A,B). Arrows indicate positive cells. Negative TRAP activity in subBMP + 4µg (C) and 8µg (D) GST-BGN treated groups. Scale bar on A is 200um.

When sections were subjected to TRAP-staining to identify osteoclasts, the positive staining was observed only in the optBMP group (Fig 4.6A, B). In these sections, the TRAP-positive cells were found distributed throughout the NFB in one rat (4.6A) and around the borders of the NFB in another (4.6B). All other groups including controls (data not shown), did not show any TRAP-positive cells in the observed sections of the NFB area at 2 weeks. Figures 4.6C and 4.6D show the images of the subBMP+ 4 and 8 µg of GST-BGN groups, respectively, showing no TRAP-positive cells.

Signaling pathways

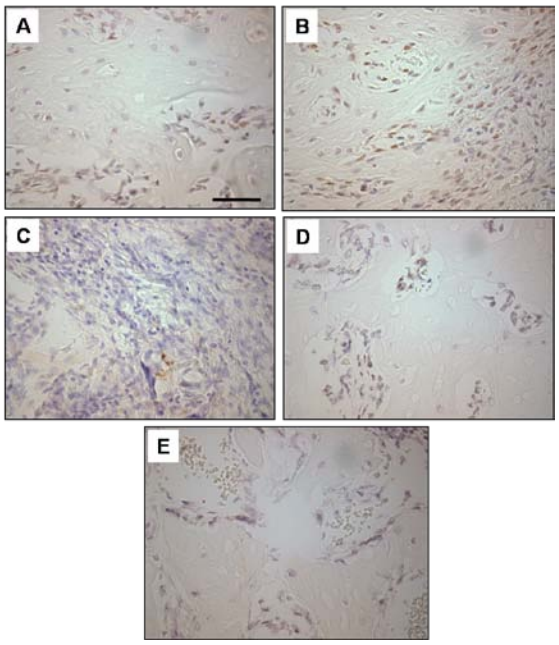

Fig 4.7. Immunohistochemistry for phosphorylated Smad 1/5/8 in the rat mandibles. SubBMP (A) and optBMP (B) groups show mild to moderate staining for Smad 1/5/8. SubBMP group + 2µg (C), 4µg (D) and 8 µg of GST-BGN (E) show modest immunoreactivity. Scale bar on A is 200µm.

p-Smad 1/5/8 signaling was negative for all control groups (not shown). subBMP group showed modest staining for *p*-Smad 1/5/8 (Fig 4.7A) and optBMP group seemed to have slightly stronger immunoreactivity (Fig 4,7B). Surprisingly, subBMP + GST-BGN treated

groups showed even less immunoreactivity to *p*-Smad 1/5/8 compared to subBMP alone (Fig 4.7C, D and E).

p-β-catenin showed strong staining in subBMP group (Fig 4.8C, D) compared to

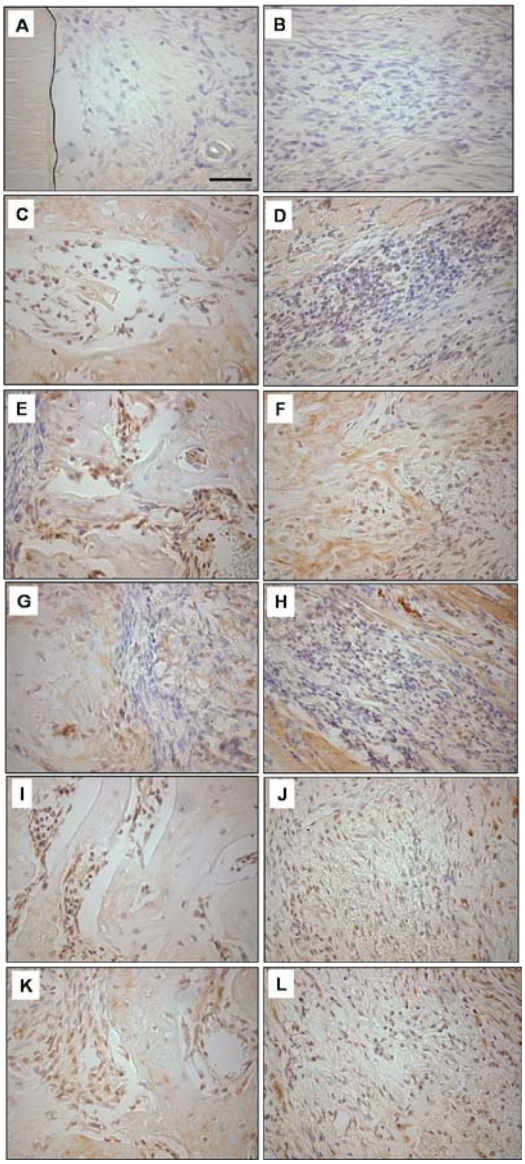

Fig 4.8. Immunohistochemistry for phosphorylated (*p*)-β catenin in the rat mandibles. Absense of immunoreactivity in scaffold alone group (A and B). A. Continuous line indicates native bone. B. Middle of defect. C. Moderate immunoreactivity for p-β catenin was found within the NFB area of subBMP group. D. Mild to moderate staining of cells in the middle region of the defect of subBMP group. E, F. Strong immunoreactivity for p-β catenin in optBMP. G. Moderate immunoreactivity present on subBMP group + 2μg GST-BGN within and around the area of newly formed bone (NFB). H. Moderate staining also present in the middle of the defect. Strong immunostaining for p-β catenin in subBMP group + 4 and 8 μg GST-BGN within the NFB (I and K, respectively) as well as in the non mineralized middle of the defects (J and L). Scale bar on A is 200um.

controls (represented by scaffold alone, Fig 4.8A, B). The staining was evident around NFB (Fig 4.8C) and in the non mineralized area (middle of defect) (Fig 4.8D). OptBMP showed much greater intensity of staining for *p*-β-catenin throughout the NFB (Fig 8E, F). SubBMP + GST-BGN groups all showed strong immunoreactivity (Fig 4.8G-L) but at 4 (4.8I, J) and 8 μg (4.8K, L) the intensity was more significant within the cells cytoplasm, similar to optBMP (4.8E, F). Erk 1/2 did not show positive staining in any of the samples (data not shown).

Discussion

The generated GST-BGN enhanced BMP-2 signaling and function *in vitro* as demonstrated by Smad 1/5/8 phosphorylation and ALP activity in this study, thus, confirming our previous study [9]. The dose effect was observed up to 4 μg of GST-BGN/150 ng of BMP-2. Potential saturation of the ratio of GST-BGN to BMP and/or to receptors may have limited further positive effect of GST-BGN on BMP function. Though GST alone did not affect BMP function (Fig 1B), with high doses, it could potentially limit the BGN effect by sterically impeding the interaction between BMP-2 and its receptors.

Other pathways besides Smad 1/5/8 as Wnt and Erk 1/2 were not shown to be positively influenced by addition of BMP-2 or BMP-2 + GST-BGN after 1h of incubation in cell medium. Previously, Wnt/β-catenin pathway has been shown to be activated by BMP-2 in C2C12, C3H10T1/2 and MC3T3-E1. The increase in ALP activity in those cells were found to be due to increases in Wnt proteins like Wnt 3a [20, 21]. The insignificant effect of BMP-2 on Wnt signaling in the current study could be due to the passage effect on cells

making them produce small amounts of BMPs which would already saturate the Wnt protein production.

In the *in vivo* study, microcomputed tomography showed that the BV of subBMP + 4 and 8 μg GST-BGN were similar to that of optBMP (Fig 4.2, lower panel). The optBMP group showed a significant amount of bone within the muscle area with limited amount of bone bridging the defect. This could be due to the potent osteoinducer effect of this molecule on non osteogenic cells (i.e. mesenchymal stem cells). None of the GST-BGN treated groups showed this ectopic bone formation. BMP binds to collagen as well as BGN [22-24]. With excessive amounts of BMP-2 (optBMP), i.e. 1 μg, it could have led to extravasation of BMP to the surrounding tissues leading them to osteoblastic differentiation outside the defect. Based on our amino acid analysis, the collagen scaffold used is highly purified collagen (hydroxyproline represents ~10% of the total amino acids and glycine ~33% of the total amino acids) carrying about 300 μg of collagen in 5mm diameter X 0.5mm thick (Nitta Gelatin, Japan). Potentially, a greater amount of collagen per scaffold would have to be used to maintain such large amount of BMP-2 in the scaffold, thus, preventing extravasation. Nonetheless, GST-BGN in combination with subBMP was a more predictable means of bone regeneration than optBMP as the NFB was confined to the defect boundaries.

OptBMP-treated rats showed bone with higher μCT porosity (53%) than subBMP groups treated with 4 and 8 μg of GST-BGN (~25%) and without (30%). Higher porosity may be explained by rapid turnover due to increased remodeling spaces and endosteal resorption [25, 26]. This notion of high turnover is supported by our finding that osteoclasts were identified only in the optBMP groups. It has been reported that BMP-2 causes a dose-

and time-dependent increase in bone resorption pits excavated by highly purified rabbit osteoclasts. In this system, it also elevated the mRNA expressions of cathepsin K and carbonic anhydrase II, which are key enzymes for the degradation of organic and inorganic bone matrices, respectively [27]. Another independent study also showed that in culturing osteoblasts in the presence of BMP-2 and inflammatory markers like IL-1, osteoclast-like multinucleated cells were formed [28]. Itoh *et al*., [29] also reported that in mouse bone marrow macrophage cultures, BMP-2 also enhanced osteoclast formation in the concomitant presence of RANKL.

The rapid bone turnover seen in the optBMP group is also supported by the pattern of PSR staining. Compared to the subBMP treated groups with or without GST-BGN, this group exhibited less red and more orange with patches of green color (Fig 4.5C and D). When collagen is resorbed and laid down rapidly, the formation of well-aligned, mature collagen fibrils could be compromised. In rapid-remodeling tissues, at the molecular level, the maturation from divalent to trivalent collagen cross-links is impaired, thus, accumulating less stable cross-links [30, 31]. This can lead to more loosely packed, less stable collagen conferring the collagen matrices with orange to greenish color as seen in the optBMP histological sections. Rapid turnover of extracellular matrix by BMP-2 has also been documented in cartilage. In this study, BMP-2 was overexpressed in healthy murine knee joints and proteoglycans synthesis and degradation as well as collagen type I and II mRNA expression were investigated. It was found that BMP-2 boosted matrix turnover in intact and damaged (IL-1 injected intra-articularly) cartilage [32].

Masson's trichrome staining permitted distinction between the NFB and surrounding muscle tissues. The easy distinction between the lamellar native bone and the newly formed trabecular bone facilitated quantification of the NFB. The BV measurements by μCT and BA by histology were consistent with each other exhibiting that the subBMP + 8 μg of GST-BGN group showed the greatest BV volume with smaller variation. Previously, it has been demonstrated that μCT scans have a high predictive value of the porosity calculated by histology. μCT porosity calculations also have showed better estimation of porous structures than bone mineral density [11].

Presence and distribution of BSP was evident in optBMP and all subBMP + GST-BGN groups. The intense immunoreactivities were found for the optBMP and subBMP + 8 μg of GST-BGN groups although the distribution was more uniform in the former compared to that of the latter. The expression of bone sialoprotein (*BSP*) is normally restricted to mineralizing connective tissues of bones and teeth [33, 34] where it has been associated with mineral crystal formation [35]. The fact that BSP was deposited in a location distant from mineralized areas within the defect could indicate those areas would be mineralized soon.

Smad signaling has been well recognized as the canonical pathway upon BMP-2 transduction through BMP receptors [36, 37]. With high dose of BMP-2 (optBMP), some increase in immunoreactivity for phosphorylated Smad 1/5/8 was noticed compared to the subBMP group. However, although our *in vitro* studies and others [8, 9, 38] have shown that BGN significantly increases Smad 1/5/8 signaling, this was not observed *in vivo*. It is important to note that this signaling is representative of the mechanism of *in vivo* osteogenesis at 2 weeks post surgery. Early signaling *in vivo* of the BGN assisted BMP-

induced osteogenesis has not been investigated. It is clear that at 2 weeks though, phosphorylation of β-catenin was occurring very strongly within the NFB in subBMP, optBMP and subBMP + GST-BGN treated samples. Except for subBMP, the degree of phosphorylation was similar and indicates that at least in part the osteogenesis is occurring through activation of Wnt signaling. In the non-mineralized areas GST-BGN treated groups, *p*-β-catenin was also highly stained compared to control or subBMP. Wnt signaling has been associated with *in vivo* bone regeneration in rats and mice. BMP-2 up-regulates expression of several Wnt ligands and their receptors. Mice expressing conditional β-catenin null alleles displayed an inhibition of BMP-induced osteogenesis [39]. It has also been suggested that at later stages of repair, when cells have already been committed to mesenchymal lineage, β-catenin is specifically upregulated and the main pathway in bone regeneration [40]. The data suggest that the BGN-assisted osteogenesis could be due in part to this pathway. Through upregulation of BMP-2 signaling, GST-BGN positively affects Wnt signaling leading to increased osteogenesis. Like *in vitro*, there was no activation of ERK 1/2 pathways found for BMP-2 or BGN-assisted BMP-2 function *in vivo*.

In summary, this study demonstrated that: 1. BGN core protein specifically and predictably enhances BMP-2 function *in vitro* and *in vivo*, 2. The bone formed by a favorable ratio of a low dose of BMP-2 to GST-BGN have similar volume, less porosity and more organization and maturity than those formed by a high dose of BMP-2 at 2 weeks post-surgery, and 3. Wnt signaling is strongly activated by BMP-2 and BGN-assisted BMP-2 osteogenesis *in vivo* at 2 weeks post-surgery. This study provides additional evidence that BGN core protein could be predictably used in clinical settings to enhance BMP-2 induced bone formation.

Bibliography

[1] K. U. Lewandrowski, J. D. Gresser, D. L. Wise, and D. J. Trantol, Bioresorbable bone graft substitutes of different osteoconductivities: a histologic evaluation of osteointegration of poly(propylene glycol-co-fumaric acid)-based cement implants in rats, Biomaterials 21 (2000) 757-764.

[2] A. Sculean, P. Windisch, T. Keglevich, and I. Gera, Clinical and histologic evaluation of an enamel matrix protein derivative combined with a bioactive glass for the treatment of intrabony periodontal defects in humans, Int J Periodontics Restorative Dent 25 (2005) 139-147.

[3] A. Moreira-Gonzalez, C. Lobocki, K. Barakat, L. Andrus, M. Bradford, M. Gilsdorf, and I. T. Jackson, Evaluation of 45S5 bioactive glass combined as a bone substitute in the reconstruction of critical size calvarial defects in rabbits, J Craniofac Surg 16 (2005) 63-70.

[4] N. Saito, T. Okada, H. Horiuchi, H. Ota, J. Takahashi, N. Murakami, M. Nawata, S. Kojima, K. Nozaki, and K. Takaoka, Local bone formation by injection of recombinant human bone morphogenetic protein-2 contained in polymer carriers, Bone 32 (2003) 381-386.

[5] X. L. Xu, J. Lou, T. Tang, K. W. Ng, J. Zhang, C. Yu, and K. Dai, Evaluation of different scaffolds for BMP-2 genetic orthopedic tissue engineering, J Biomed Mater Res B Appl Biomater 75 (2005) 289-303.

[6] T. P. Richardson, M. C. Peters, A. B. Ennett, and D. J. Mooney, Polymeric system for dual growth factor delivery, Nat Biotechnol 19 (2001) 1029-1034.

[7] D. Parisuthiman, Y. Mochida, W. R. Duarte, and M. Yamauchi, Biglycan modulates osteoblast differentiation and matrix mineralization, J Bone Miner Res 20 (2005) 1878-1886.

[8] P. A. Miguez, M. Terajima, H. Nagaoka, Y. Mochida, and M. Yamauchi, Role of glycosaminoglycans of biglycan in BMP-2 signaling, Biochem Biophys Res Commun 405 262-266.

[9] Y. Mochida, D. Parisuthiman, and M. Yamauchi, Biglycan is a positive modulator of BMP-2 induced osteoblast differentiation, Adv Exp Med Biol 585 (2006) 101-113.

[10] O. Arosarena, and W. Collins, Comparison of BMP-2 and -4 for rat mandibular bone regeneration at various doses, Orthod Craniofac Res 8 (2005) 267-276.

[11] N. J. Wachter, P. Augat, G. D. Krischak, M. Mentzel, L. Kinzl, and L. Claes, Prediction of cortical bone porosity in vitro by microcomputed tomography, Calcif Tissue Int 68 (2001) 38-42.

[12] S. S. Lu, X. Zhang, C. Soo, T. Hsu, A. Napoli, T. Aghaloo, B. M. Wu, P. Tsou, K. Ting, and J. C. Wang, The osteoinductive properties of Nell-1 in a rat spinal fusion model, Spine J 7 (2007) 50-60.

[13] D. Dayan, Y. Hiss, A. Hirshberg, J. J. Bubis, and M. Wolman, Are the polarization colors of picrosirius red-stained collagen determined only by the diameter of the fibers? Histochemistry 93 (1989) 27-29.

[14] L. C. Junqueira, G. Bignolas, and R. R. Brentani, Picrosirius staining plus polarization microscopy, a specific method for collagen detection in tissue sections, Histochem J 11 (1979) 447-455.

[15] T. A. Linkhart, S. G. Linkhart, Y. Kodama, J. R. Farley, H. P. Dimai, K. R. Wright, J. E. Wergedal, M. Sheng, W. G. Beamer, L. R. Donahue, C. J. Rosen, and D. J. Baylink, Osteoclast formation in bone marrow cultures from two inbred strains of mice with different bone densities, J Bone Miner Res 14 (1999) 39-46.

[16] J. Zhang, Q. Tu, and J. Chen, Applications of transgenics in studies of bone sialoprotein, J Cell Physiol 220 (2009) 30-34.

[17] J. Wang, H. Y. Zhou, E. Salih, L. Xu, L. Wunderlich, X. Gu, J. G. Hofstaetter, M. Torres, and M. J. Glimcher, Site-specific in vivo calcification and osteogenesis stimulated by bone sialoprotein, Calcif Tissue Int 79 (2006) 179-189.

[18] J. A. Gordon, C. E. Tye, A. V. Sampaio, T. M. Underhill, G. K. Hunter, and H. A. Goldberg, Bone sialoprotein expression enhances osteoblast differentiation and matrix mineralization in vitro, Bone 41 (2007) 462-473.

[19] Y. Sasano, J. X. Zhu, S. Kamakura, S. Kusunoki, I. Mizoguchi, and M. Kagayama, Expression of major bone extracellular matrix proteins during embryonic osteogenesis in rat mandibles, Anat Embryol (Berl) 202 (2000) 31-37.

[20] G. Rawadi, B. Vayssiere, F. Dunn, R. Baron, and S. Roman-Roman, BMP-2 controls alkaline phosphatase expression and osteoblast mineralization by a Wnt autocrine loop, J Bone Miner Res 18 (2003) 1842-1853.

[21] M. Zhang, Y. Yan, Y. B. Lim, D. Tang, R. Xie, A. Chen, P. Tai, S. E. Harris, L. Xing, Y. X. Qin, and D. Chen, BMP-2 modulates beta-catenin signaling through stimulation of Lrp5 expression and inhibition of beta-TrCP expression in osteoblasts, J Cell Biochem 108 (2009) 896-905.

[22] W. Friess, H. Uludag, S. Foskett, R. Biron, and C. Sargeant, Characterization of absorbable collagen sponges as recombinant human bone morphogenetic protein-2 carriers, Int J Pharm 185 (1999) 51-60.

[23] B. Chen, H. Lin, J. Wang, Y. Zhao, B. Wang, W. Zhao, W. Sun, and J. Dai, Homogeneous osteogenesis and bone regeneration by demineralized bone matrix loading with collagen-targeting bone morphogenetic protein-2, Biomaterials 28 (2007) 1027-1035.

[24] E. Schonherr, P. Witsch-Prehm, B. Harrach, H. Robenek, J. Rauterberg, and H. Kresse, Interaction of biglycan with type I collagen, J Biol Chem 270 (1995) 2776-2783.

[25] S. A. Lloyd, Y. Y. Yuan, P. J. Kostenuik, M. S. Ominsky, A. G. Lau, S. Morony, M. Stolina, F. J. Asuncion, and T. A. Bateman, Soluble RANKL induces high bone turnover and decreases bone volume, density, and strength in mice, Calcif Tissue Int 82 (2008) 361-372.

[26] O. D. Kennedy, O. Brennan, S. M. Rackard, A. Staines, F. J. O'Brien, D. Taylor, and T. C. Lee, Effects of ovariectomy on bone turnover, porosity, and biomechanical properties in ovine compact bone 12 months postsurgery, J Orthop Res 27 (2009) 303-309.

[27] H. Kaneko, T. Arakawa, H. Mano, T. Kaneda, A. Ogasawara, M. Nakagawa, Y. Toyama, Y. Yabe, M. Kumegawa, and Y. Hakeda, Direct stimulation of osteoclastic bone resorption by bone morphogenetic protein (BMP)-2 and expression of BMP receptors in mature osteoclasts, Bone 27 (2000) 479-486.

[28] M. Koide, Y. Murase, K. Yamato, T. Noguchi, N. Okahashi, and T. Nishihara, Bone morphogenetic protein-2 enhances osteoclast formation mediated by interleukin-1alpha through upregulation of osteoclast differentiation factor and cyclooxygenase-2, Biochem Biophys Res Commun 259 (1999) 97-102.

[29] K. Itoh, N. Udagawa, T. Katagiri, S. Iemura, N. Ueno, H. Yasuda, K. Higashio, J. M. Quinn, M. T. Gillespie, T. J. Martin, T. Suda, and N. Takahashi, Bone morphogenetic protein 2 stimulates osteoclast differentiation and survival supported by receptor activator of nuclear factor-kappaB ligand, Endocrinology 142 (2001) 3656-3662.

[30] M. Yamauchi, E. P. Katz, and G. L. Mechanic, Intermolecular cross-linking and stereospecific molecular packing in type I collagen fibrils of the periodontal ligament, Biochemistry 25 (1986) 4907-4913.

[31] M. Yamauchi, D. T. Woodley, and G. L. Mechanic, Aging and cross-linking of skin collagen, Biochem Biophys Res Commun 152 (1988) 898-903.

[32] E. N. Blaney Davidson, E. L. Vitters, P. L. van Lent, F. A. van de Loo, W. B. van den Berg, and P. M. van der Kraan, Elevated extracellular matrix production and

degradation upon bone morphogenetic protein-2 (BMP-2) stimulation point toward a role for BMP-2 in cartilage repair and remodeling, Arthritis Res Ther 9 (2007) R102.

[33] L. W. Fisher, O. W. McBride, J. D. Termine, and M. F. Young, Human bone sialoprotein. Deduced protein sequence and chromosomal localization, J Biol Chem 265 (1990) 2347-2351.

[34] A. Oldberg, A. Franzen, and D. Heinegard, The primary structure of a cell-binding bone sialoprotein, J Biol Chem 263 (1988) 19430-19432.

[35] G. K. Hunter, and H. A. Goldberg, Nucleation of hydroxyapatite by bone sialoprotein, Proc Natl Acad Sci U S A 90 (1993) 8562-8565.

[36] K. Miyazono, S. Maeda, and T. Imamura, BMP receptor signaling: transcriptional targets, regulation of signals, and signaling cross-talk, Cytokine Growth Factor Rev 16 (2005) 251-263.

[37] S. Itoh, F. Itoh, M. J. Goumans, and P. Ten Dijke, Signaling of transforming growth factor-beta family members through Smad proteins, Eur J Biochem 267 (2000) 6954-6967.

[38] X. Wang, K. Harimoto, S. Xie, H. Cheng, J. Liu, and Z. Wang, Matrix protein biglycan induces osteoblast differentiation through extracellular signal-regulated kinase and Smad pathways, Biol Pharm Bull 33 (2010) 1891-1897.

[39] Y. Chen, H. C. Whetstone, A. Youn, P. Nadesan, E. C. Chow, A. C. Lin, and B. A. Alman, Beta-catenin signaling pathway is crucial for bone morphogenetic protein 2 to induce new bone formation, J Biol Chem 282 (2007) 526-533.

[40] Y. Chen, H. C. Whetstone, A. C. Lin, P. Nadesan, Q. Wei, R. Poon, and B. A. Alman, Beta-catenin signaling plays a disparate role in different phases of fracture repair: implications for therapy to improve bone healing, PLoS Med 4 (2007) e249.

Chapter 5

Study III

Evaluation of biglycan core domains on BMP-2 function

by Miguez PA, Sricholpech M, Terajima M, Nagaoka N, M. Yamauchi

Abstract

We have found that BGN core is responsible for the positive effect on BMP-2 function while the glycosaminoglycan component rather functions as a suppressor for this effect. In this study, we explored the effects of various domains of BGN core protein [central leucine-rich repeat (LRR) domains with deleted N and C terminal cysteine loops (ΔNC), N terminal to LRR) 6 (N~LRR6), LRR7 to C terminal (LRR7~C) and LRRs 1 to 3 (LRR1~3), 4 to 6 (LRR4~6) and 7 to 10 (LRR7~10)] on BMP-2 function. Methods: The glutathione-S-transferase (GST) tagged deletion constructs were generated in E. coli system by deletion of the specific BGN core domains as described above. After purification, 4 μg of each construct was added to C2C12 cells in combination with 150 ng of BMP-2. After cell lysis, lysates were subjected to p-Smad 1/5/8 Western Blot and ALP activity assay. The construct found most effective for BMP-2 function was further tested on the rat mandible model (see Study I and II) with a suboptimal dose of BMP-2 (subBMP/100 ng). Results: Smad 1/5/8 phosphorylation was the greatest with N~LRR6 and ALP activity was significantly enhanced with the constructs ΔNC, N~LRR6 and LRR1~3. Thus, LRR1~3 was further tested *in vivo*. In the animal experiments, LRR1~3 showed significant bone regeneration capacity when combined with subBMP and the enhancement was comparable to that of (subBMP + GST-BGN). Conclusion: The positive modulation of BMP-2 function by BGN or its functional domains occurs through Smad 1/5/8 leading to an increase in ALP activity in C2C12 cells. The effector domain appears to reside between the N terminus and LRR6, possibly in the LRR1~3, and it is effective in promoting BMP-2 induced osteogenesis *in vivo*.

Keywords: biglycan, BMP-2, C2C12, Smad 1/5/8, leucine-rich repeats, microcomputed tomography.

Introduction

BGN has been increasingly investigated in the past decade for its function in modulation of BMP functions [1-5]. The BGN knock out study was the first to show the effect of this proteoglycan on bone homeostasis demonstrating that the null mice had age-dependent osteoporosis [6]. The same group later reported that without BGN, calvaria cells responded poorly to BMP-4 [1, 7]. Independent of this study, our laboratory has also reported that BGN is a positive modulator of osteoblastic function and it promotes matrix mineralization [2]. *In vivo*, we have shown that BGN facilitates bone formation without compromising matrix organization [2] (also see Chapter 4, Study II). One of our recent findings was that the core protein of BGN, not its glycosaminoglycans, is responsible for this positive effect on BMP functions [5] (also see Chapter 3, Study I). BGN is composed of 10 leucine rich repeats (LRR) flanked by two cysteine-rich domains, a characteristic that has been known to promote protein-protein interactions [8, 9]. Among the core polypeptide sequence in BGN, there is no peculiarity in the LRRs described in the literature that would seem to favor more protein-protein interactions. However, the key may reside in the position of certain amino acid(s) in the peptide sequence turns or pockets (i.e. secondary structure) that could favor interaction with BMP-2 and/or its receptors. For example, it has been reported that while phenylalanine 85 in a pocket of the BMP type I receptor (ALK3) is essentical for the interaction between BMP-2 and this receptor, for more efficient interaction, the conformation involving non consecutive 27 residues from ALK3 and 26 from BMP-2 are required [10].

In this study, we attempted to establish which domain of the BGN core protein is responsible for the positive effect on BMP function. For this purpose, we generated several

BGN deletion constructs and evaluated the effects of these domains on BMP-2 function in a C2C12 cell assay system [11]. In addition, we selected the smallest functional domain and applied to a rat mandible model [12] and investigated early bone regeneration.

Experimental Procedures

Generation of recombinant full BGN and BGN deletion constructs

Primers / GST-construct	Forward	Reverse
BGN	see Mochida et al., 2006	see Mochida et al., 2006
ΔNC	5'GCGGATCCACACTGCTAGACCTG3'	5'GCCTCGAGGGTGATGTTGTT3'
N~LRR6	same as BGN, see Mochida et al., 2006	5'GCCTCGAGAGTGTGGCCTCTGA-3'
LRR7~C	5'GCGGATCCACCCTGAACGAACTT3'	same as BGN, see Mochida et al., 2006
LRR1~3	5'GCGGATCCACACTGCTAGACCTG3'	5'GCCTCGAGCACCAGCAGGGCTAG3'
LRR4~6	5'GCGGATCCTCCCTGGTAGAACTA3'	5'GCCTCGAGAGTGTGGCCTCTGA3'
LRR7~10	5'GCGGATCCACCCTGAACGAACTT3'	5'GCCTCGAGGGTGATGTTGTT3'

Table 1. Primers for generation of GST-BGN and GST-deletion constructs.

Generation of full glutathione-S-transferase (GST) tagged BGN was described earlier in Mochida *et al*., 2006 [3]. To investigate the effects of the N, C termini (i.e. cysteine rich domains) and LRR domains of BGN on BMP-2 function *in vitro* we generated the following BGN-derived constructs: LRRs with deleted N and C termini (ΔNC), N-terminus to LRR 6, (N~LRR6), LRR7 to C-terminus (LRR7~C), and several LRR domains: LRR1~3, LRR4~6 and LRR7~10 (Fig 5.1). A total of 6 deletion constructs were generated with described primers (Table 1).

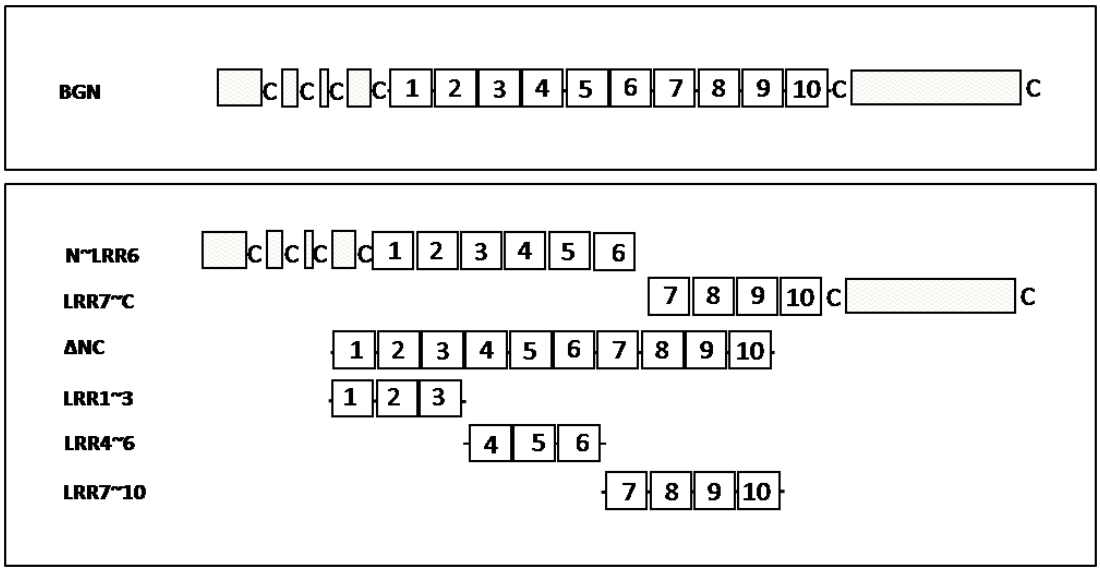

Fig 5.1.Drawing scheme of BGN core protein (upper panel) and deletion constructs (lower panel). BGN: biglycan, LRR: leucine rich repeat, ΔNC: LRR one to ten without N and C terminal, N~LRR6: N terminal to LRR6, LRR7~C: LRR7 to C terminal, LRR1-3: LRR one to three, LRR4-6: four to six, LRR7-10: seven to ten. C: cysteine. Wavy boxes: random amino acids between cysteine clusters. Numbered boxes: LRRs.

The amplified PCR products were then digested by restriction enzymes, ligated into pGEX4T-1 vectors (Amersham Biosciences, Piscataway, NJ), sequenced and the plasmids harboring the mutant *Bgn* cDNAs (pGEX4T-1-*Bgn* constructs) were obtained. The plasmids were transformed into BL21-CodonPlus bacterial strain, the synthesis of GST-BGN fusion protein was induced by isopropyl -D-1-thiogalactopyranoside (IPTG, Fisher Scientific, Waltham, MA) and the GST-deletion constructs/proteins were purified in the same manner as described [3]. Additionally, purification was carried out by molecular sieve chromatography using a Superdex 200 (HiLoad 16/60, GE Healthcare, Waukesha, WI) column in 2M guanidine-HCl, pH 7.5, for ΔNC, N~LRR6 and LRR7~C. The purified fractions were dialyzed against distilled water for 3 days to remove the salt and lyophilized. Then GST-fused BGN-derived constructs were subjected to SDS-PAGE and WB analysis with anti-GST antibody (Sigma-Aldrich, St. Louis, MO). Quantification of proteins after

purification was carried out by the Lowry method [13] with the DC protein assay kit (Bio-rad).

Cell line and culture conditions

C2C12 cells were cultured as previously described [3], and in Chapter 3, Study I and Chapter 4, Study II.

Effect of BGN and BGN-derived constructs on BMP-2 function in vitro

The effect of recombinant BGN and deletion constructs on canonical BMP-2 pathway was assessed by Smad1/5/8 phosphorylation in C2C12 cells as described in Chapter 3, Study I [5] and Chapter 4, Study II. Four μg of BGN or BGN deletion constructs were added in combination with 150 ng of BMP-2 to the cell medium. Cell extracts were then applied to 4-12% SDS-PAGE followed by WB analyses with anti-phospho (p)-Smad1/5/8 (Cell Signaling, Danvers, MA) and anti-β actin antibody (Cell Signaling). These experiments were repeated in duplicates.

For ALP activity, after 3 days of culture in the above conditions, the cell lysates were collected and subjected to microplate reading at an absorbance of 405nm after 15 minutes as reported [3]. ALP assay was performed in duplicate.

Effect of short most beneficial BGN domain on BMP-2 function in vitro on in vivo osteogenesis

After the *in vitro* investigations described above, the LRR1~3 construct that revealed the greatest effect on BMP-2 function among the three short LRR constructs (i.e. LRR1~3, 4~6

and 7~10) was tested *in vivo*. The effect and specificity were tested by applying three doses in combination with a suboptimal dose of BMP-2 (subBMP/100ng) (see Chapter 4, Study II). The rat mandible model and the surgical procedures have been described in Chapter 3, Study I [5]. The rats (2 per group) included in this study were as reported for Chapter 4, Study II for controls (i.e. unfilled, scaffold, scaffold + GST, scaffold + GST-BGN) and for treatment groups (scaffold + subBMP or subBMP + GST-BGN). In addition, the following treatment groups were investigated: subBMP + 4, 8 and 16 µg GST-LRR1~3. At 2 weeks post-surgery, hemimandibles were placed in neutral buffered formalin and after three days they were evaluated by µCT. The procedures were described in Chapter 3, Study I [5] and the BV and porosity calculated as in Chapter 4, Study II.

Results

Generation of constructs and verification of signaling pathways and ALP activity

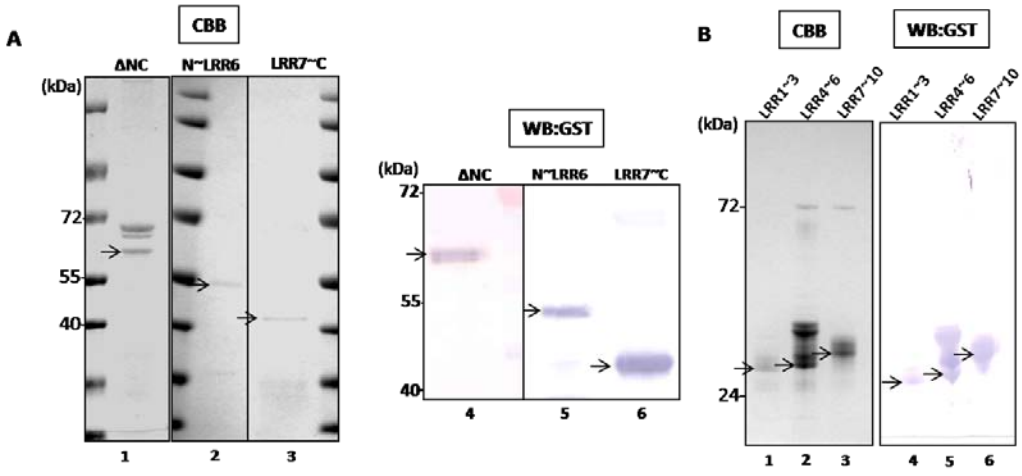

Fig 5.2. Generation of GST-tagged BGN deletion constructs and verification of purification by SDS-PAGE and WB (anti-GST). A. Commassie brilliant blue staining (CBB) of 4-12% gel showing ΔNC (63 kDa)(lane 1), N~LRR6 (46 kDa) (lane 2), LRR7~C (42 kDa)(lane 3). WB for ΔNC (lane 4), N~LRR6 (lane 5) and LRR7~C (lane 6). B. Purified LRR1~3 (33 kDa)(lanes 1 and 4), LRR4~6 (33.4 kDa)(lanes 2 and 5), LRR7~10 (36.5 kDa)(lanes 3 and 6) shown in SDS-PAGE by CBB and WB by anti-GST. Note that purity of LRR4~6 is the most compromised with several bands other than the band of interest. Arrows indicate bands of interest.

Constructs were generated successfully with various levels of purity. The larger constructs ΔNC, N~LRR6 and LRR7~C (Fig 5.2A lane 1, 2 and 3 respectively) were further purified by molecular sieve chromatography but ΔNC still contained some other peptides that could not be separated (Fig 5.2A, lane 1). The WB analysis with anti-GST antibody indicated that the other peptides did not contain GST (Fig 5.2A, lane 4). LRR constructs were relatively pure (Fig 5.2B) with exception of LRR1~4 (lanes 2 and 5). In Fig 5.3, Smad 1/5/8 phosphorylation was significantly enhanced when GST-BGN was added to BMP-2 (Fig 5.3A, lane 3). ΔNC and LRR7~C also enhanced BMP-2 induced Smad phosphorylation (lanes 5 and 6, respectively) but when N~LRR6 was added to BMP-2, the signaling was the greatest (lane 4). Fig 5.3B shows a representative graph of ALP activity where the deletion

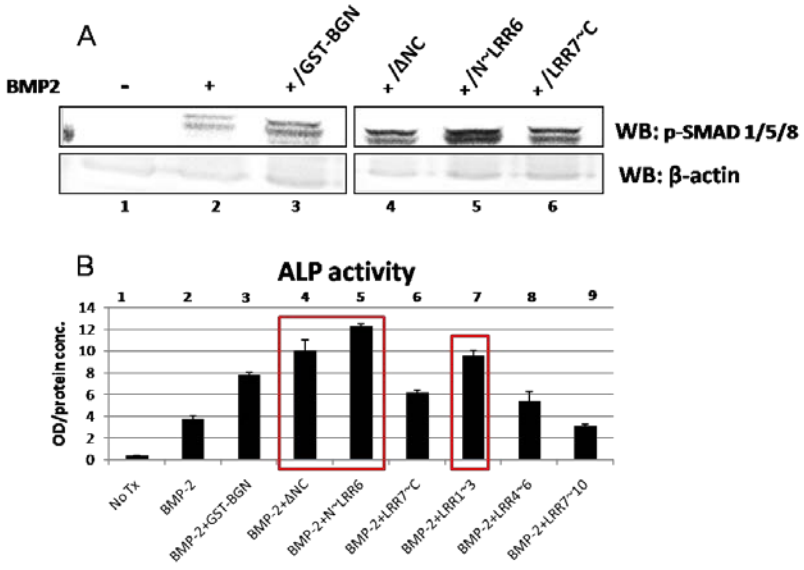

Fig 5.3. Effect of BGN deletion constructs on BMP-2 function in C2C12 cells A. Smad 1/5/8 phosphorylation in C2C12 cells treated with BMP-2 alone (lane 2) or with addition of GST-BGN (lane 3) and BGN deletion constructs (lanes 4-6). Note that GST-BGN significantly increases phosphorylation (lane 3) but the effect is much greater for N~LRR6 (lane 5). B. ALP activity of cells treated with BMP-2 (lane 2) is significantly increased by the addition of GST-BGN (lane 3) but the effect is further enhanced by ΔNC (lane 4), N~LRR6 (lane 5) and LRR1~3 (lane 7). Greatest ALP values highlighted by red boxes. Figures are representatives of duplicate experiments.

constructs ΔNC (lane 4), N~LRR6 (lane 5) and LRR1~3 (lane 7) were the most effective constructs to enhance the BMP-2 function (all highlighted by red boxes). N~LRR6 exhibited

~3.5 fold increase in ALP compared to BMP-2 alone. ΔNC and LRR1~3 were more than 2 fold increased than BMP-2 alone. Other groups a LRR7~C and LRR4~6 (lanes 5 and 7, respectively) showed some increases in ALP compared to that of BMP-2 alone but still lower than (BMP-2 + GST-BGN) (lane 3).

μCT analyses

Figure 5.4 shows the representative 3D and 2D μCT images obtained after euthanasia at 2 weeks post-surgery. Right graph shows quantification of bone volume (BV). In Study I and II we described the findings for empty, scaffold alone, scaffold + GST, scaffold + GST-BGN alone control groups and for subBMP and (subBMP + GST-BGN) treatment group. The BV

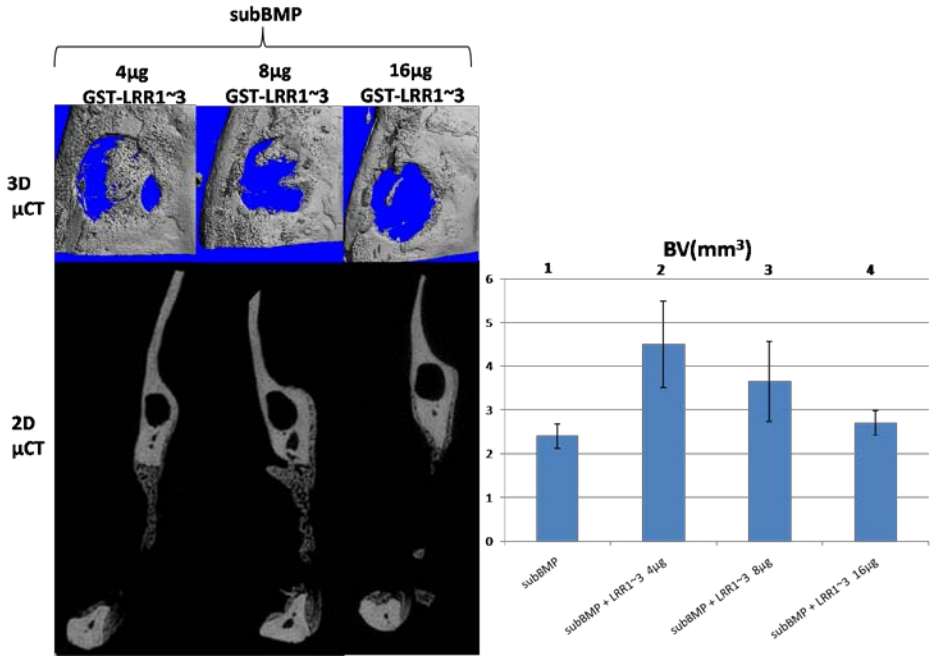

Fig. 5.4. μCT 2D and 3D views and BV quantification of NFB in the rat mandibles treated with BMP-2 and BGN deletion construct LRR1~3. Refer to Chapter 4, study II for data on controls (unfilled, scaffold alone, scaffold + GST, scaffold + GST-BGN) and treatment groups for comparison (subBMP and subBMP+ GST-BGN). Upper panel on the left shows 3D view and lower panel 2D view. On the right, bone volume (BV) was quantified as previously described (see Chapters 3 and 4). Graph shows the median (represented by columns) and the range (error bars) of BV of the newly formed bone (NFB) of 2 defects per group of treatment. Total defect is 9.8 mm^3Note that the lowest dose of LRR1~3 enhances BMP-2-induced osteogenesis the most (lane 2). subBMP: suboptimal dose of BMP-2 (100 ng), LRR1~3: leucine rich repeat one to three.

of the treatment group subBMP is shown again as a reference (lane 1). When subBMP was combined with 4 and 8μg of GST-LRR1~3, a remarkable increase in bone formation was achieved compared to subBMP alone (lane 2 and 3, respectively). Like previously demonstrated for GST-BGN (see Study II), the bone was confined to the defect area and not ectopic (see optBMP/1μg in Study II). The amount of bone regenerated diminished with increasing doses of GST-LRR1~3 (lanes 2, 3 and 4). Porosity calculated by the μCT software CTan Analyzer (Skyscan, Kontich, Belgium) within the newly formed bone (NFB) boundaries showed that subBMP and optBMP groups had 30% and 53% porosity (reported in Study II), respectively. The (subBMP + GST-BGN) groups showed similar porosity for all groups averaging 25% and for GST-LRR1~3 was about 30%.

Discussion

In this study we explored the effectiveness of BGN-derived domains on BMP-2 function. The results indicated that the central LRR domain (i.e. no N and C-terminal cysteine rich domains) alone can facilitate BMP-2 function as evidenced by the positive effect on Smad phosphorylation and ALP activity. When the shorter LRR sequences were tested separately, LRR1~3 showed the greatest effect followed by LRR4~6 (Fig 5.3). The LRR7~10 exerted no significant effect. However, due to the presence of other peptides in the LRR4~6 construct (Fig 5.2), the effect of this construct could have been affected. This construct had many non-determined, GST-tagged contaminants. Further purification was attempted by molecular sieve chromatography without success. It is possible that since contaminants were GST-tagged, aggregation occurred even in the presence of chaotropic agent such as guanidine-

HCl. Also, the close molecular weight of the contaminants to the protein of interest could make separation difficult.

The effect of LRR1~3 addition to subBMP on osteogenesis *in vivo* was remarkable as was seen for GST-BGN (see Chapter 3, Study II). However, the higher the dose of LRR1~3 the smaller the positive effect on BMP-2-induced osteogenesis. Before drawing conclusions from this negative effect with increasing doses of GST-LRR1~3 it would be ideal to test tag-free LRR1~3. This leucine rich amino acid stretch is only 68 amino acids long while its tag, GST, contains 226 amino acids. Though GST alone did not affect the BMP-2 function *in vivo* (Chapter 4, Study II) with higher concentrations, it may hinder the interaction of such a small domain with BMP-2 or receptors. In addition, the use of GST-tag significantly changes the isoelectric point (pI) of LRR1~3 from 7.6 to 10 but in case of BGN the pI only changes from 7.8 to 8. This could also change protein-protein interactions. In the future, we will generate small LRR sequences free of tags by using chemically synthesized peptides.

The newly formed bone of (subBMP + LRR1~3) treated hemimandibles had similar porosity to that of the (subBMP + GST-BGN) which was lower than the mandibles treated with an optimal dose of BMP-2 (optBMP) (see Chapter 4, study II). Reduced porosity is usually associated with lower bone turnover and high bone density. Lower bone turnover has been shown to confer bone better mechanical properties [14, 15]. It will be interesting to investigate how the bone remodels and ultimately fills the defect by the treatments with (subBMP + BGN), (subBMP + BGN domain) or optBMP after a longer period of time.

There may be more than one mechanism by which BGN assists BMP function. Not only through LRRs but possibly through the C terminal cysteine rich domain as well since

there is still some enhancement of BMP function with LRR7~C but not with LRR7~10. Previously, we have found that the cysteine cluster of the C terminus in BGN is necessary for BGN binding to ALK6 receptor (not published). Thus, the C terminus of LRR7~C may help BMP-2 function through ALK6 while LRRs (i.e. 1~3 and possibly 4~6) alone may utilize BMP-2 or other receptor(s) interaction. Nonetheless, use of the most effective domain combined with low concentrations of BMP-2 appears to be a more predictable, controllable and cost effective approach than the current marketed high dose BMP-2 delivery.

Bibliography

[1] X. D. Chen, L. W. Fisher, P. G. Robey, and M. F. Young, The small leucine-rich proteoglycan biglycan modulates BMP-4-induced osteoblast differentiation, Faseb J 18 (2004) 948-958.

[2] D. Parisuthiman, Y. Mochida, W. R. Duarte, and M. Yamauchi, Biglycan modulates osteoblast differentiation and matrix mineralization, J Bone Miner Res 20 (2005) 1878-1886.

[3] Y. Mochida, D. Parisuthiman, and M. Yamauchi, Biglycan is a positive modulator of BMP-2 induced osteoblast differentiation, Adv Exp Med Biol 585 (2006) 101-113.

[4] X. Wang, K. Harimoto, S. Xie, H. Cheng, J. Liu, and Z. Wang, Matrix protein biglycan induces osteoblast differentiation through extracellular signal-regulated kinase and Smad pathways, Biol Pharm Bull 33 (2010) 1891-1897.

[5] P. A. Miguez, M. Terajima, H. Nagaoka, Y. Mochida, and M. Yamauchi, Role of glycosaminoglycans of biglycan in BMP-2 signaling, Biochem Biophys Res Commun 405 262-266.

[6] T. Xu, P. Bianco, L. W. Fisher, G. Longenecker, E. Smith, S. Goldstein, J. Bonadio, A. Boskey, A. M. Heegaard, B. Sommer, K. Satomura, P. Dominguez, C. Zhao, A. B. Kulkarni, P. G. Robey, and M. F. Young, Targeted disruption of the biglycan gene leads to an osteoporosis-like phenotype in mice, Nat Genet 20 (1998) 78-82.

[7] Y. Bi, C. H. Stuelten, T. Kilts, S. Wadhwa, R. V. Iozzo, P. G. Robey, X. D. Chen, and M. F. Young, Extracellular matrix proteoglycans control the fate of bone marrow stromal cells, J Biol Chem 280 (2005) 30481-30489.

[8] L. W. Fisher, J. D. Termine, S. W. Dejter, Jr., S. W. Whitson, M. Yanagishita, J. H. Kimura, V. C. Hascall, H. K. Kleinman, J. R. Hassell, and B. Nilsson, Proteoglycans of developing bone, J Biol Chem 258 (1983) 6588-6594.

[9] R. V. Iozzo, Matrix proteoglycans: from molecular design to cellular function, Annu Rev Biochem 67 (1998) 609-652.

[10] T. Kirsch, W. Sebald, and M. K. Dreyer, Crystal structure of the BMP-2-BRIA ectodomain complex, Nat Struct Biol 7 (2000) 492-496.

[11] T. Katagiri, A. Yamaguchi, M. Komaki, E. Abe, N. Takahashi, T. Ikeda, V. Rosen, J. M. Wozney, A. Fujisawa-Sehara, and T. Suda, Bone morphogenetic protein-2 converts the differentiation pathway of C2C12 myoblasts into the osteoblast lineage, J Cell Biol 127 (1994) 1755-1766.

[12] O. Arosarena, and W. Collins, Comparison of BMP-2 and -4 for rat mandibular bone regeneration at various doses, Orthod Craniofac Res 8 (2005) 267-276.

[13] O. H. Lowry, N. J. Rosebrough, A. L. Farr, and R. J. Randall, Protein measurement with the Folin phenol reagent, J Biol Chem 193 (1951) 265-275.

[14] S. A. Lloyd, Y. Y. Yuan, P. J. Kostenuik, M. S. Ominsky, A. G. Lau, S. Morony, M. Stolina, F. J. Asuncion, and T. A. Bateman, Soluble RANKL induces high bone turnover and decreases bone volume, density, and strength in mice, Calcif Tissue Int 82 (2008) 361-372.

[15] O. D. Kennedy, O. Brennan, S. M. Rackard, A. Staines, F. J. O'Brien, D. Taylor, and T. C. Lee, Effects of ovariectomy on bone turnover, porosity, and biomechanical properties in ovine compact bone 12 months postsurgery, J Orthop Res 27 (2009) 303-309.

Chapter 6

Conclusions

1. BGN is a positive modulator of BMP-2 function *in vitro* in C2C12 cells and removal of GAGs further enhances BGN assistance of BMP function
2. Tissue extracted BGN (glycanated BGN, with GAGs) is not able to positively modulate BMP function *in vivo* in a critical-sized rat mandible defect model
3. Recombinant BGN core protein (without GAGs) is efficient in positively modulating BMP-2 function *in vitro* and *in vivo* as determined by the C2C12 system and the rat mandible model
4. Smad 1/5/8 is the main pathway of BGN-assisted BMP-2 function in C2C12 cells
5. The BGN core + a suboptimal dose of BMP-2 induced newly formed bone (NFB) that was similar in bone volume but less porous, more compact and organized than the NFB by an optimal dose of BMP-2
6. The NFB of BGN core + a suboptimal dose of BMP showed a strong β-catenin immunostaining, similar to optimal dose of BMP-2.

7. The effector domain of the core of BGN may reside in the N-terminal through leucine rich repeat (LRR)~6 based on Smad signaling and ALP activity. LRR1~3 is likely the effector domain.